10-28-2016

Cardiovascular regulation by Kvβ1.1 subunit

Jared Tur
University of South Florida, jtur@mail.usf.edu

Cardiovascular regulation by Kvβ1.1 subunit

by

Jared Tur

A dissertation submitted in partial fulfillment
of the requirements of the degree of
Doctor of Philosophy
Department of Molecular Medicine
Morsani College of Medicine
University of South Florida

Major Professor: Srinivas Tipparaju, Ph.D.
Eric Bennett, Ph.D.
Denise Cooper, Ph.D.
Javier Cuevas, Ph.D.
Andreas Seyfang, Ph.D.
Vladimir Uversky, Ph.D.

Date of Approval:
September 21, 2016

Keywords: Kvβ, redox regulation, Kv channel, heart, NADH, NAD, ECG

ACKNOWLEDGEMENTS

First and foremost I would like to thank my family for all of their support, inspiration, and inquisition into my work. While often perplexed by the work they never stopped being fascinated which provided great inspiration. A special thank you to my mother for always believing this would be a reality and for her unwavering support. I would like to sincerely thank my mentor, Dr. Srinivas Tipparaju who for the past four years has been a constant driving force for me offering me his knowledge, time, and guidance. I am truly grateful for the many opportunities he has shared with me to enhance my scientific and professional career.

I would like to extend my gratitude to my committee members Dr. Eric Bennett, Dr. Denise Cooper, Dr. Javier Cuevas, Dr. Andreas Seyfang and Dr. Vladimir Uversky for their years of support and guidance. I would like to thank my external chair, Dr. Rakesh Kukreja for offering his time and expertise. I would like to thank Dr. Chris Katnik for his guidance and assistance. I would also like to thank the current and former members of Dr. Srinivas Tipparaju's laboratory including Dr. Sachin Badole, Rohini Nimbalkar, Helena Marihel, Ana Groshev, and Timothy Padawer for their knowledge, support and friendship. I would like to extend a special thank you to Dr. Kalyan Chapalamadagu whose tireless determination towards science provided me with a greater knowledge, motivation, and dedication along with a few laughs. I would like to acknowledge the many friendships I have formed with such bright young scientists with whom made this journey so much more enjoyable. Thank you to Dr. Matlathi Thomas, Dr. Lisa Kirouac, Seol-Hee Kim, Prerna Malaney, Viviana Sampayo, and Krishna Reddy. I would also

like to acknowledge my friends outside of the scientific world who often kept me humble in particular Meredith Roberts who has been an amazing friend these past years. Finally I would like to thank the department of Molecular Medicine along with the College of Pharmacy for providing an outstanding research environment and for their dedication towards their students.

TABLE OF CONTENTS

LIST OF TABLES

LIST OF FIGURES

LIST OF ABBREVIATIONS

Kv	Voltage-Gated Potassium Channel
S4	Fourth Transmembrane Segment
AP	Action Potential
$I_{to,f}$	Rapidly Inactivating Transient Outward Current
$I_{to,s}$	Slowly Inactivating Transient Outward Current
IKslow	Rapidly Activating Slowly Inactivating Voltage-gated Potassium Current
ISS	Non-Inactivating Potassium Current
AV	Atrioventricular
ECG	Electrocardiogram
EAD	Early After Depolarization
DAD	Delayed After Depolarization
LQT	Long QT
mV	Millivolt
Ca^{+2}	Calcium Ion
Va	Voltage of Half-Activation
SSI	Voltage-Dependent Steady-State Inactivation
Vi	Voltage of Half-Inactivation
G-V	Conductance-Voltage
KO	Transgenic “Knock Out” Mouse
APD	Action Potential Duration
PCR	Polymerase Chain Reaction

LVA	Left Ventricular Myocyte
WT	Wild Type
mM	Millimoles Per Liter
kHz	Kilohertz
ms	milliseconds
MΩ	Megaohm
Gmax	Theoretical Maximum Conductance
τ inact	Time Constant of Inactivation
pA	Picoamps
I	Current
ml	milliliter
AU	Arbitrary Unit
kD	Kilodalton
μM	Micromoles Per Liter
4AP	4-Aminopyridine
APD20	Action Potential at 20% Repolarization
APD50	Action Potential at 50% Repolarization
APD70	Action Potential at 70% Repolarization
APD90	Action Potential at 90% Repolarization
U/ml	Unit per Milliliter
mU/ml	Milliunit Per Milliliter
NAD	Nicotinamide adenine dinucleotide
NADH	Nictotinamide adenine dinucleotide (hydrogen-reduced form)

ABSTRACT

Heterologous expression systems such as COS-7 cells have demonstrated the profound effects of KCNAB1-3 or Kvβ1-3 proteins on voltage gated potassium channels (Kv) channels. Indeed, in the presence of these β-subunits transiently expressed Kv channels are often modulated in multiple ways. Kv channel membrane expression is often increased in the presence of β-subunits. In addition, non-inactivating Kv currents suddenly become fast-inactivating and fast-inactivating channels become even faster. While much research has demonstrated the profound effects the β-subunits in particular the Kvβ1 subunit have on transiently expressed Kv currents little to date is known of the physiological role it may play. One study demonstrated that by "knocking out" Kvβ1 cardiomyocyte current changes were noted including a decrease in the $I_{to,f}$ current. While this novel finding demonstrated a key cardiac physiological role of the Kvβ1 subunit it left many unanswered questions as to determine the cardiovascular regulation the Kvβ1 subunit provides. Indeed, cardiac arrhythmias and other electrical abnormalities within the heart such as long QT present patients with many unfortunate unknowns. Many of these incidences occur often abruptly with cardiac electrical abnormalities. Genetic research has begun to shine light on key cardiovascular genes in particular those coding for ion channels and auxiliary subunits or β-subunits. Kv channels and their β-subunits have gained particular notoriety in their key responsibility in restoring the resting membrane potential known as the repolarization phase. Indeed genetic manipulation and physiological examination of Kv channels and recently their β-subunits has demonstrated profound physiological results including prolonged QT durations within mice altered functional activity during physiological cycles such as estrus. While initial

findings of Kvβ1 have demonstrated profound cellular and cardiomyocyte current alterations much still remains unknown. Therefore, this work hypothesizes that the Kvβ1 subunit provides a profound cardiovascular role in regulation and redox sensing at the physiological and pathophysiological level in both males and females. This work identifies a sex-based difference in cardiovascular regulation by Kvβ1 as well as demonstrated a profound redox sensing ability during altered metabolic states seen in pathophysiological conditions.

CHAPTER ONE:

Introduction

Significance

Many cardiovascular diseases including cardiac arrhythmias can often manifest from abnormal electrical activity within the heart, however a large portion of how these abnormalities arise often remain unknown. Atrial fibrillation one of the more common types of heart arrhythmias affects an estimated 3-6 million people within the United States (CDC). Both atrial and ventricular arrhythmias can arise from mutations in numerous genes from those that code specific membrane ion channels such as sodium or potassium to smaller proteins such as channel auxiliary subunits. While sodium channels as well as select potassium channels have been investigated for many years leading to the discovery of mutations in the SCN5A channel and the development of Brugada syndrome, less is known about mutations and alterations within the potassium channels and their auxiliary subunits (55, 160). Cardiac potassium channels play a key role in the repolarization phase of cardiac action potentials and are often the key targets affected in action potential prolongation as well as QT prolongation seen in ECG waveforms. Because of the recent advances in genetic manipulation many "knockout" mice have been created in the area of cardiac K^+ channels. Mutations conducted on the Kv4.2 (murine) channel the molecular determinate of the cardiac $I_{to,f}$ current demonstrates significant consequences including QT prolongation, cardiac hypertrophy and, heart failure (5, 95, 119). Similar deleterious effects have been noted in mutations in other Kv channels such as Kv2.1, 1.5 and, 1.4 demonstrating alterations including QT prolongation but demonstrate little to no effect on cardiac remodeling

(93, 97, 158). Recently modulation of the Kv channel auxiliary subunits have demonstrated profound effects sometimes even greater than mutations and or deletions of the potassium channel that they modulate in murine models. The Kv channel chaperone protein KCHIP2 for example when knocked out was demonstrated to induce QT prolongation, as well as incite arrhythmic events within the mice (59, 136). Cardiac hypertrophy in rats was blunted when overexpression of KCHIP2 by adenovirus was given rescuing the prolonged action potential as well as the Kv4.2 channel expression (100, 101). Similar effects were noted in other modulator proteins including DPPX proteins as well a MINK and MiRP2 (78, 92, 144, 152). The auxiliary subunits or otherwise known β subunits Kvβ (Shaker potassium channel subunit) include Kvβ1 (with splice variants Kvβ1.1, Kvβ1.2, and Kvβ1.3) and Kvβ2 are of particular interest to the cardiovascular system as research has demonstrated they are highly expressed within the heart and vascular system including the aorta in addition to sympathoadrenal and autonomic system (2, 26, 28, 31, 42, 122). While much in vitro work has demonstrated the profound effect the Kvβ subunit can have on Kv channel activity little is known of the *in vivo* effects of the Kvβ subunit alterations. Indeed, Kvβ1 subunits have been demonstrated to modulate key Kv channels including Kv1.5, 1.4 and most recently 4.2 all of which play a vital role in the repolarization of cardiac action potentials (30, 148). A 2005 report of Kvβ1 knockout mice demonstrated a significant decrease in $I_{to'f}$ current as well as the $I_{to's}$ current (2). More recently genetic testing has begun to demonstrate that Kvβ's absence is present in numerous disease conditions including schizophrenia, high blood pressure, and sudden cardiac death (4, 14, 62, 80, 161). Therefore a greater understanding of the cardiovascular physiological impact of Kvβ1 is needed.

Background

Voltage-Gated Potassium Channels

The voltage-gated potassium channels play a significant role throughout the body from maintaining the resting membrane potential in excitable cells, to the modulation of the waveform and frequency of the action potential (53, 54). Kv channels in non-excitable cells can also regulate cell volume, proliferation, and apoptosis (48, 53, 133). Because of this Kv channel activity and disruption has been associated with cardiac arrhythmias, pulmonary hypertension and, epilepsy (9, 35, 84, 143). Within the human genome, forty different genes encoding Kv channels was presented and subdivided into twelve sub-families (Kv1-Kv12) (41). Mammalian Kv channels are tetramers made up of 4 α-subunits composed of six α-helical transmembrane domains (S1-S6) with a cytosolic N and C-termini along with a membrane-reentering P loop between S5 and S6 (143). The S5-P-S6 segments make up the ion conducting pore, while S1-S4 segments are responsible for the voltage-sensing and gating. The Kv channel operates by sensing the voltage changes or membrane potential occurring within the cell and activates/inactivates or closes dependent upon the individual channels properties. Many Kv channels open (activate) at different voltages, become inactivate followed by closed as the voltage or membrane potential changes. This synchrony of opening, inactivating and, closing often works in a harmonious fashion in order to properly propagate action potentials.

Action potential prolongation is a result of concerted distortion of channel itself or along with its regulatory subunits. The activation or open state of the Kv channel is caused by the S4 segment known as the voltage sensor, this segment is able to sense the cellular voltage (potential) and thus modify the channel pore by conformational change. The kinetics of the activation of the Kv channel can be measured and is often represented as $V_{1/2}$ of activation which describes the

membrane voltage (potential) at which half of the channel(s) are open. This is often a critical measurement when analyzing pharmaceutical kinetics such a drug binding and interaction which can affect channel activation. If $V_{1/2}$ of activation is shifted towards the left a more negative potential or mV, in the Kv channel to a more negative potential then activation has increased or accelerated and hyperpolarization has occurred. If the $V_{1/2}$ of activation is shifted towards the right, in the Kv channel to a more positive potential than activation has decreased and hypopolarization has occurred.

The Kv channels have two distinct forms of inactivation which include the N-type and C-type. The N-type inactivation is dependent upon the N-terminus region (the first 20 amino acids) commonly known as the "ball" in which the "ball" occludes the channel pore by interacting with the S4-S5 linker region of the Kv channel blocking the channel pore (115). Fast inactivating channels such as Kv4.2 and 4.3 for example rely on the N-type inactivation which often occurs in milliseconds to tens of milliseconds. The C-type inactivation does not involve a "tethered ball" type on the C-terminus but the closure of the extracellular mouth of the pore (115). Similar to activation, inactivation can also be an important measurement in determining pharmaceutical kinetics as well as auxiliary subunit (such as Kvβ1) alterations. If the $V_{1/2}$ of inactivation is shifted towards the left, in the Kv channel to a more negative potential then inactivation has increased while a shift to the right would signal a possible rate in reduction in inactivation.

Kvβ Subunits

The initial identification of the Kvβ subunits came from the purification of Kv channels based on their binding affinity with α-dendrotoxin in bovine brain tissue, which demonstrated a tight association between Kvα and Kvβ subunits (105, 116). One of the first reports on the function of the Kvβ1 subunit came in a Nature publication in 1994 demonstrating the ability of

rat Kvβ1 to associate with A-type Kv channels and impart greater inactivation (117). Further human characterization demonstrated that Kvβ3 equivalent in sequence to Kvβ1 (mouse) was present in the left atrium as well as the left ventricle (26). More recent reports have demonstrated that the Kvβ subunits are abundantly expressed throughout the body including the brain, heart, and the vascular system including the aorta as well as the autonomic system (16, 28, 37, 42, 122).

The sequences of the Kvβ subunits were identified and found to share significant similarities with an extended protein superfamily, the oxidoreductases particularly the aldo-keto reductases (AKR) (40, 81). The AKR's catalyze the reduction or the oxidation of a broad range of carbonyl substrates including aldehydes, ketones, and steroids (107, 112). The Kvβ subunits were found most closely related to the AKR7 the aflatoxin reductase and AKR5 the morphine dehydrogenase therefore the Kvβ subunits were assigned to the AKR6 family (49). This sequence analysis was subsequently followed with the crystal structure of Kvβ2 demonstrating an $NADP^+$ molecule bound to the structure even in the harsh crystallography process (40). Similar to the oxidoreducatases, the Kvβ subunit contains multiple active sites which are composed of a substrate binding sites, NADP(H) cofactor binding pockets, as well as catalytic residues for hydride transfer (40, 112).

The Kvβ subunits is encoded by three separate genes for Kvβ1, Kvβ2, and Kvβ3 of which Kvβ1 and 2 undergo alternative splicing to give rise to Kvβ1.1, 1.2, 1.3 and Kvβ2.1 and 2.2 (53), whereas less is known in regards to Kvβ3 and its gene regulation, some reports suggest the existence of Kvβ4 in which the sequence overlaps with Kvβ3 except the breakaway region of Kvβ3 c-terminus (29, 44). Genomic DNA sequence analysis and genome mapping demonstrated that Kvβ1 resides on the telomere of chromosome arm 3q to a band 3q25 (50, 65). Initial

research demonstrated that Kvβ1 presented with 17 exons in which exons 2a, 2b, and 2c correspond with Kvβ1.1, 1.2, 1.3 isoforms (64). While the splice variants have many conserved domains the NH_2-terminal region varies which contains the N-type inactivation domain this accounts for the altered molecular weight as well as how the splice variants modulate Kv channels differently (112). Indeed, initial research has demonstrated that different isoforms have confirmed unique gating and sensing abilities to multiple Kv channels. Wang et al demonstrated that hKvβ1.2 and 1.3 bound to multiple Kv channels because of the identical C-terminal region however, gating and sensing abilities differed between the two likely due to the difference in N-terminal sequences. The hKvβ1.2 demonstrated as a more potent modulator and was the only subunit to confer redox sensing abilities in the presence of H_2O_2 which abolished the hKvβ1.2 inactivation (146). While splice variants demonstrate significantly similar traits so to do Kvβ1 and Kvβ2 sharing roughly 85% amino acid identity within their core region corresponding to their aldo-keto reductases background. The N-terminal regions are significantly different, Kvβ2 N-terminal region being almost non-existent which helps to explain why the subunit offers less in inactivation modulation in many Kv channel interactions (112, 117).

While initial structure findings found that NADP(H) molecules preferentially bind to the Kvβ subunit, little was demonstrated on how this binding alters Kv channel kinetics. Indeed, many of these initial findings demonstrated the unique Kv channel kinetics in the presence of Kvβ1 however often lacked any information on the pyridine nucleotide status in each model. Campomanes et al demonstrated that when Kvβ1.1 cofactor sites (NADP(H) and NADH) are mutated Kv1.2 surface expression is significantly decreased (11). The identification and importance of pyridine nucleotide binding to Kvβ subunits and modulation of Kv channel activity has only been identified within the past 10 years. Indeed, Tipparaju et al demonstrated

that Kv1.5 with Kvβ1.3 was modulated differently in the presence of varying concentrations of pyridine nucleotides; where reduced nucleotides NADH and NADPH when added demonstrated increased inactivation and oxidized nucleotides such as NAD and NADP presented with reduced inactivation (139). Further publications would highlight the importance of the Kvβ subunit in conferring pyridine nucleotide Kv channel alterations providing Kv channels with a "redox" sensor (99, 137, 138).

The Kvβ subunits when purified demonstrated greater affinity for pyridine nucleotide binding in vitro such as NADP(H) compared with NAD(H) interestingly in vivo NAD(H) levels are almost 2-7 fold higher compared with NADP(H). Therefore this may allow Kvβ to sense and respond to a wide range of metabolic alterations that change the overall pyridine nucleotide environment within a cell. Many cardiovascular diseases including cardiac hypertrophy often demonstrate a significant increase in NADH and or accompanying decrease in NAD levels compared to normal cardiac tissue (111, 155). Indeed, during low-flow reperfusion of ischemic myocardium which led to persistent arrhythmias ectopic beats were often generated in areas demonstrating the highest spatial gradient for NADH (52). While low-flow ischemic injury and inducing cardiac hypertrophy have been utilized models of studying cardiovascular disease so too has the manipulation of lactate and pyruvate within the heart to alter NAD/NADH levels. Indeed, multiple papers have demonstrated that increasing lactate concentrations up to 10:1 ratios of pyruvate not only significantly increase intracellular NADH levels but often mimic pathologic conditions observed within the heart and cardiomyocytes (71). This biochemical manipulation is currently one strategy being utilized in understanding human cardiovascular disease.

Trafficking and Assembly of Kv Channels and the Kvβ Subunits

The α-subunit, an integral membrane protein expresses tetrameric Kv channels and the auxiliary β-subunits found on the cytoplasmic side associate with the Kvα-subunits and can modulate Kv channel properties. The initial α-β interaction occurs within the endoplasmic reticulum in which the Kv-α and β subunit are packaged together and shipped from the Golgi apparatus to be delivered to the membrane (87). In the absence of the Kvβ subunit the Kv channel was still efficiently transferred to the Golgi apparatus. While seemingly unnecessary for transfer to the Golgi apparatus, Kvβ1 does demonstrate an effect on current kinetics as well as altering Kv channel expression (1, 11, 156). Indeed, in vitro studies demonstrated that co-expression of Kvβ subunits with Kvα channels significantly increased surface expression (11, 156). However, current in vivo work has shown little to no change in Kv channel expression in Kvβ knockout mice (2). While seemingly unaltered during the Golgi apparatus the Kvβ's may affect Kv channel expression by their interaction with the cytoskeleton as well as membrane bound proteins. The N-terminal domain of Kvβ1 and to some extent Kvβ2 was determined to have a cytoskeleton binding domain interacting with the actin cytoskeleton and in particular the F-actin and α-actinin (88). Kvβ2 subunit was recently demonstrated to bind with ProSAP2/Shank3 which are components of signaling cascades at the postsynaptic membrane and actin-based cytoskeleton of the dendritic spine (114). Kvβ1 and 2 were demonstrated to bind with Kv4.3 as well as increase its current density (pA/pF) (156). The Kv4.3 (Kv4.2 in mice) plays a profound effect on the cardiac action potential and make up one of the key repolarizing currents.

The Kvβ subunit binds with the α-unit in a one-to-one ratio per meric structure, thus there are four Kvβ subunits bound to one Kv channel (153). In 2005 the Kvβ2 was crystalized with the

Kv1.2 channel and for the first time demonstrated the unique interaction between the β-subunit and the α-subunit. The association was centered on a small area of the tetramerization domain in the NH_2 terminus of the α-subunit (74). The general binding of the α-β occurs on the N-terminus of the Kv channel the NAB region (N-terminal A and B box), in particular what is known as the T1 domain (159). The interaction occurs by a contact loop between the Kvα and Kvβ subunit allowing for the docking and surface engagement of only a few amino acids from both the Kvα and Kvβ subunit (112). Yu et al demonstrated that not only was the N-terminal region of the Kvα and core region of the Kvβ subunit responsible for N-type inactivation but in addition the inactivation gate of Kvβ1 with the compatible receptor on Kvα units (159). The lack of multiple amino acid binding interactions allows both the Kvα and Kvβ subunits to bind with other proteins along the membrane as well as cytoplasmic proteins. The binding of the N-terminus allows the Kvβ subunit to have direct binding access with the inactivation domain of the α-channel itself thus enhancing or hindering Kv channel gating properties.

The Kvβ1 subunit presents with a long N-terminus "tail" and with this actually binds and plugs the pore of the Kv channel thus acting to inactivate the channel or in specific α-channels accelerate inactivation. The same "tail" also interacts with the Kv channel N-terminus and cause self-inactivation to occur at a much faster rate compared in the absence of the Kvβ1 subunit (75, 98, 99). Kvβ subunits are not the only subunits bound at one time; there may also be other subunits such as KCHIP2 or even other β subunits bound to the Kv channel. Kuryshev et al demonstrated that Kv channels (rat Kv4.3, 1.4, 2.1, 1.5) bound not only Kvβ1 and 2 but also simultaneously KChAP protein which had significant alterations in the current amplitude (60). The Kvβ1 subunit when bound to many non-inactivation Kv channels actually converts them to A-type or fast inactivation currents (61, 64, 98, 117). In addition, when Kvβ1 is bound to A-type

or fast inactivating Kv channels they tend to foster faster inactivation rates evident by hyperpolarizing shifts in $V_{1/2}$ of inactivation rates (3, 75).

Kvβ1 and β2 demonstrate multiple alterations to many Kv channels; however these alterations are often in response to the Kvβ subunits unique functional attributes such as the binding of pyridine nucleotides as discussed earlier. Indeed, Liu et al demonstrated the high affinity for which isolated Kvβ2 bound to multiple nucleotides (72). The Kvβ1 also imparts unique sensing abilities to the Kv channels which provide a possible mechanism of Kv channel modulation in activity and expression during metabolic alterations within the cell. Perez Garcia et al et al demonstrated that when Kvβ1.2 was bound it provided oxygen sensitivity to Kv4.2 channel, as well as previously demonstrating that the Kvβ subunits provide a mechanism for redox alterations including sulfhydryl groups (108). Oxidizing agent (DTDP) which may increase intracellular NAD demonstrated decreased rate of inactivation while DTT a reducing agent fostered inactivation. Further that a hypoxic environment fostered a decrease in Kv4.2 amplitude but only in the presence of Kvβ. Further it was later demonstrated that Kvβ1 provided redox sensitivity towards H_2O_2 and direct injections of NADP resulting in reduced inactivation with Kv1.1 and Kv1.2 an otherwise non responsive channel towards redox alterations (98, 146). Therefore the Kvβ1 may be acting as an intracellular redox-sensing device modulating the activity of multiple Kv channels (Fig 1). While there are different Kvβ subunits in the heart, the relative affinities and the abundances may be useful for different physiological functions. For example: The Kvβ2 which lacks the ball has highest affinity for NADPH (0.14μM)>NADP>NADH>NAD (72). Similarly, Kvβ1 follows this affinity pattern, however, consists of long ball-and-chain capable of inactivation or accelerating the self-inactivating Kv channels. On the other hand Kvβ3, has the least affinity for NADPH (0.6μM)

>NADP>NADH>NAD, and consists of the longest ball and chain which originates from the available N-terminus region (137). Therefore overall, the Kvβ subunits are somewhat redundant in their features but differ in many biochemical features as well as affinities towards Kv channel assembly. While Kvβ subunits and pyridine nucleotide interactions demonstrate no effect on their ability to bind with Kv channels, their interaction does have the ability to significantly alter electrical and physiological channel function.

Cardiac Action Potential

The normal cardiac action potential within the myocardium begins in phase 4 also known as the resting membrane potential typically around -90mV for cardiac myocytes. Phase 0 is the rapid depolarization phase in which the membrane potential is sent to a positive voltage by the opening or activating of the cardiac sodium channels and the influx of sodium ions. The myocardium quickly enters phase 1 the rapid repolarization phase which sets the potential for the next phase. Phase 1 is initiated by the fast inactivating voltage-gated potassium channels or the I_{to} current which open and close rapidly. Phase 2 is the longest and is known as the plateau phase in which calcium channels are opened or activated. While calcium channels continue to allow Ca^{2+} to enter the cell potassium channels are working simultaneously with an efflux of K^+ ions. This continually release of potassium ions by multiple potassium channels eventually leads to phase 3, the rapid repolarization that returns the membrane potential to its resting state and thus return to phase 4 (38).

Cardiac K^+ channels exist in three categories including the Voltage-gated (I_{to}, $I_{Kur,}$ $I_{Kr,}$ I_{Ks}), inward rectifiers (I_{K1}, $I_{KAch,}$ I_{KATP}), and background K^+ currents (TASK-1, TWIK-1/2). The Kv channels activity play key roles in cardiac action potential including setting the membrane

potential, shaping the action potential waveform, and determining action potential frequencies (54). Interestingly the voltage-gated potassium channels can form heteromultimers with similar Kv channels (Kv4.2 and 4.3 for example) in which many of these channels as homomultimers (in heterologous expression models) can demonstrate unique electrical properties that may in fact be significantly altered from their heteromultimer form in native cells. In addition, not only can α-subunits form heteromultimers but Kvβ-subunits can also form heteromultimers within the Golgi while binding with Kvα channels demonstrating again unique electrical properties within native cells. The I_{to} current or the transient outward current is a Ca^{2+} -independent current playing a significant role in the repolarization composed of a fast and slow component, $I_{to'f}$ and $I_{to's}$ respectively with molecular correlates of Kv4.2/4.3 and Kv1.4 respectively (20, 43). The rate of activation for the I_{to} is fast generally <10 ms while inactivation is variable and voltage-dependent (38). While I_{to} plays a profound physiological role in establishing the AP, recent research has highlighted its importance during pathological conditions demonstrating a density reduction in failing hearts (86, 149). Indeed, recently I_{to} reduction in heart failure may act as a mediator or promoter of heart failure rather than a secondary change (100, 101, 123, 151). While current density and overall expression levels may be altered during these pathological conditions a better understanding of how the Kvβ1 subunit a known binding partner of Kv4.2/4.3 regulates theses pathological changes.

Kvβ1 in Cardiovascular System

To date little is known of the role Kvβ1 plays during cardiac pathology including cardiac hypertrophy and heart failure. However, Kv channel dysregulation and altered metabolic pathways including the NAD/NADH ratios occur during these pathophysiological conditions thus it stands to reason that the role of Kvβ1 may provide vital information in cardiac pathology.

Cardiac hypertrophy taken as one example often presents with an overall enlargement of the heart either demonstrating eccentric or concentric hypertrophy often dependent upon the stimulus. Eccentric hypertrophy often presents with an overall enlargement of the heart including an increase in ventricular diameters. Typically eccentric hypertrophy is demonstrated in physiological hypertrophy such as in constant exercise. Concentric hypertrophy presents with an enlargement of the heart with increased wall thickening such as the left ventricular free wall. This form of hypertrophy is often demonstrated during pathological conditions such as increased pressure overload (observed in those with hypertension and obesity). The heart is often challenged to pump harder to ensure proper blood flow thus increasing the amount of strain on the walls. Concentric hypertrophy is often an adaptive phenotype during pathological conditions and if continued often leads to heart failure in which the adaptations (increased wall thickening) can no longer manage the demand and can begin to cause chamber dilation ultimately leading to heart failure.

While physical alterations are occurring within in the heart during forms of hypertrophy, electrical changes are also occurring often demonstrating decreases in current density, prolonged QT durations as well as, prolonged action potential durations. These changes are well documented and are often the result of channel modulation including the decrease in Kv4.2 expression and I_{to} current density during cardiac hypertrophy (121, 140). The decrease in key Kv channels is often the start to electrical abnormalities as the repolarization phase prolongs allowing for greater risk of delayed after depolarization leading to arrhythmic events. Further studies have also hinted at the role Kv channel subunits play during these pathophysiological conditions as a possible area of rescue. Backx et al demonstrated that during banded aortic constriction a decrease in Kv4.2 and prolongation of action potential was noted in 14-week old

rats, however when injected with adeno-viral KCHIP2 resulting in an overproduction of KCHIP2 the prolonged action potential was reduced to pre-aortic constriction level (101). In addition, as discussed earlier these pathological conditions not only result in Kv channel changes but also result in metabolic alterations as well. In many cardiac pathological states the increased cytosolic levels of NADH have been noted in hypertension, ischemia, and heart failure (Table 1) (12, 69, 70, 155).

While genetic ablation of Kvβ1 demonstrated no cardiac developmental defects, a significant difference was noted in the current levels of $I_{to,f}$ within isolated cardiomyocytes of 10 week old males (2). In addition, the "knocking out" of Kvβ1 has demonstrated unique phenotypes resulting in neurological defects involved in learning and memory. Kvβ1.1 KO mice at three months (12 weeks) demonstrated a significant decrease in learning and memory assessed by the STFP task (social transmission of food preferences) (32). Interestingly aged Kvβ1.1 mutant (1 year old) actually demonstrated an enhanced neuronal excitability and performed better than WT controls on the Morris water maze test (85). Mice lacking both Kvβ1.1 and Kvβ2 demonstrated increased mortality in addition to increased cold-induced tremors (15). Recently it has been demonstrated that multiple gene analysis reports have identified Kvβ1.1 as a prime target for both mutated and missing in multiple pathologies including epilepsy, breast carcinoma, hypertension, cataract, and sudden cardiac death (4, 14, 45, 67, 80, 161).

Calcium may also play an intricate part of Kvβ's ability to regulate the cardiac action potential. Previous research demonstrated that intracellular calcium increases by ionomycin (ionphores) or IP_3 signaling blunts Kvβ1 induced inactivation of Kv1.1 resulting in increased steady-state Kv1.1 current (51). More recently it was demonstrated that calmodulin a intracellular calcium-binding messenger protein binds to the "chain" structure of the Kvβ1.1 subunit and inactivation

activity (131). While conducted in HEK cells it does stand to reason how cardiac intracellular calcium levels could affect Kvβ1.1 and the ion channels it binds to such as Kv4.2.

Tables and Figures

Table 1: Pyridine nucleotide alterations in pathological states

Cardiac Pathology	Pyridine Nucleotides	Model	Reference
GPD1-L Mutation	**NADH ↑**	**Lactate (10:1)**	**70,72**
Hypertrophy	**NAD ↓**	**Angiotensin II**	**110**
Hypertension	**NADH ↑**	**DOCA**	**69**
Ischemia	**NAD ↓**	**ischemia-reperfusion**	**12**

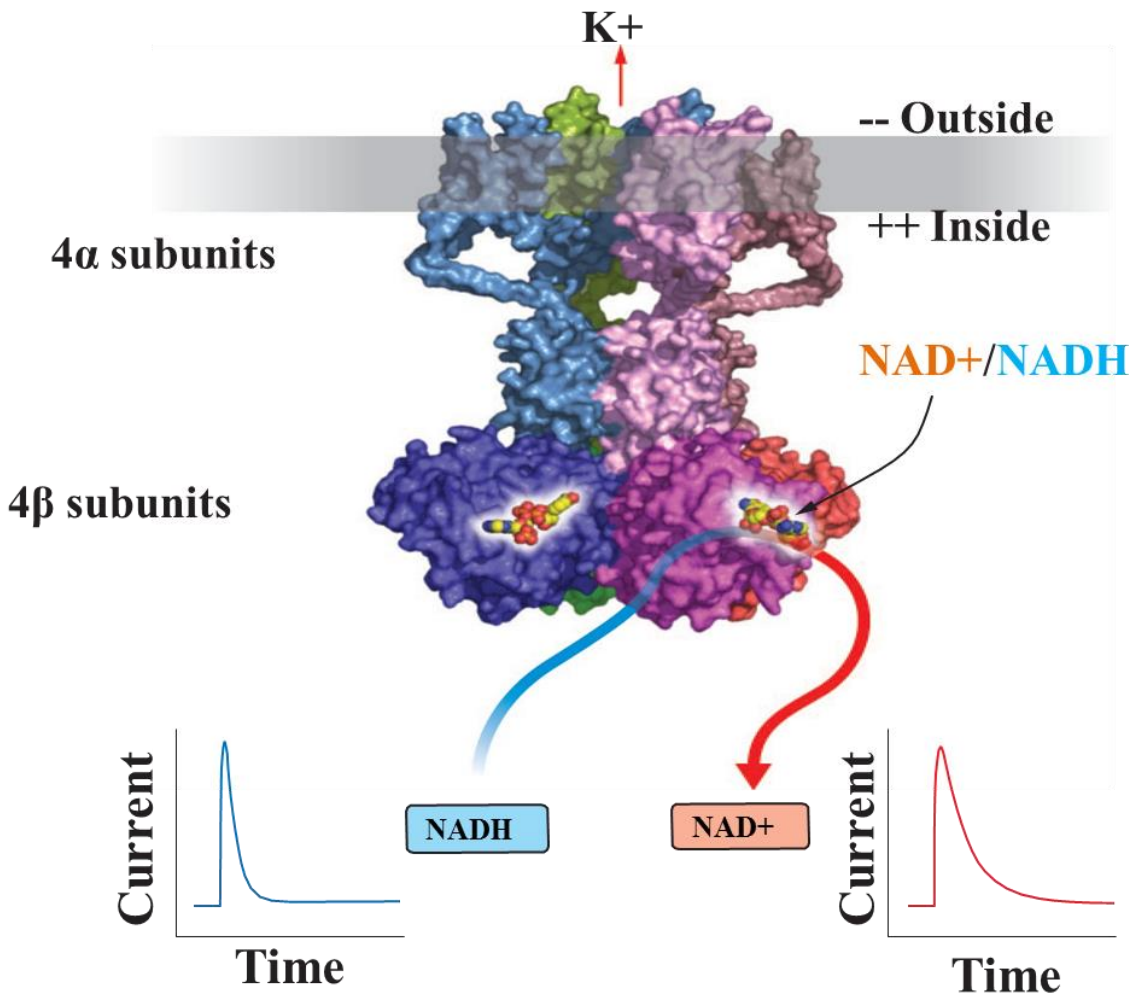

Figure 1: Kv-Kvβ interaction. A stylized structure of the Kv α-subunit bound with the Kvβ subunit (Kvβ1) at the membrane level. Pyridine nucleotides bound (in this example NAD and or NADH) causing alterations in Kv channel kinetics. Electrophysiologically recorded K^+ currents demonstrate when NADH is bound inactivation is favored thus inactivating at a much faster rate. However, when NAD is bound Kvβ mediated-inactivation is abolished and inactivation is slowed. From (Heinemann, S. H. & Hoshi, T. 2006. Multifunctional Potassium Channels: Electrical Switches and Redox Enzymes, All in One. Heinemann, S. H. & Hoshi, T. 2006. Multifunctional Potassium Channels: Electrical Switches and Redox Enzymes, All in One. *Science's STKE,* **2006,** pe33-pe33. Reprinted with the permission from AAAS.

CHAPTER TWO:

Characterization of Kvβ1.1 knockout mouse model and its cardiovascular implications: Electrical changes in both sexes but cardiac hypertrophy only in female.

Introduction

Cardiovascular disease (CVD) is a leading cause of death for women in the United States. In 2009, about 33,000 females died from high blood pressure and heart failure, in the U.S. (34). Sex differences have been reported in CVD, in which females are at lower risk for atrial fibrillation however, they present with higher incidences of Torsades de Pointes (TdP) and are therefore at greater risk for sudden death (7, 27, 79). In addition, females demonstrate more severe ischemic heart disease including stress induced cardiomyopathy, plaque erosion and microvascular dysfunction (17). Health disparities in females are highly prevalent and the treatment modalities are based on male driven parameters (18, 154).

One prominent sex disparity is in QTc interval and action potential duration (APD) indication dramatic sex specific differences in cardiac repolarization phase. This phenomenon is well documented in women taking anti-arrhythmic drugs demonstrating a greater risk of drug-induced long QT syndrome LQTS/TdP (63, 66, 79, 134). The prolonged QTc and AP durations suggests that there is a limited repolarization reserve in females, which blocks further prolongation of AP durations and generation of early after depolarization (EAD) (36, 157). Cardiac sex differences noted in humans has also been demonstrated in animal studies, which show an increase in QT duration as well as, an increase in incidences of early after depolarization in female rabbits after anti-arrhythmic drug exposure (24, 94, 109). Repolarization reserve in heart is constituted by

three main potassium currents (I_{Kr}, I_{Ks}, and I_{K1}) which work in synchrony and allow the return of membrane potentials to the resting state, and therefore play a vital role in cardiovascular function and disease (125). Mice demonstrate similar repolarization reserves to humans and are constituted by distinct potassium currents (I_{Kslow1}, I_{Kslow2}, and I_{ss}), and although slightly different in kinetics, the currents show similar contributions to action potentials (90). Disruption of the repolarization reserve can lead to CVD including arrhythmic events (13, 97). While overall murine action potential's are different when compared with humans key potassium channels such as those studied in this report are very similar between species. In addition, guniea pigs demonstrate extremely similar QT and ST wave elements in ECG signals and therefore may be an additional model to utilize.

Because potassium channels (Kv) are pivotal to the repolarization reserve, understanding how Kv channel accessory subunits can alter this reserve may provide novel mechanistic insights. The voltage-gated potassium channel subunit (Kvβ1) belongs to the aldo-keto reductases (AKR) superfamily which is found abundantly in the heart. The Kvβ subunit demonstrates a unique ability to bind and regulate many Kv channels including Kv4 and Kv1 channels (2, 19, 30, 112).

Previous research on Kvβ1 knockout mice demonstrated reduced K^+ channel inactivation(2) and after-hyperpolarization as well as increased neuronal excitability in the brain (32, 85). Genomic research has begun to shed light on the importance of Kvβ1 (Gene name KCNAB1) in cardiovascular health. In 2008, a patient passing from sudden cardiac death demonstrated a deletion in KCNAB1 (4). In addition, recent genomic studies identified KCNAB1 as a gene of interest for genetic association with blood pressure and causal variant in humans with hypertension (14, 80).

In this present work we demonstrate that 12-14 week old Kvβ1.1KO mice are physiologically altered compared with wild type (WT) controls. This is the first report that clearly delineates the physiological role of Kvβ1.1 in female murine hearts. In addition, we utilized physiological comparison between male and female to identify electrophysiological and vascular differences to understand the roles of Kvβ1.1.

Materials and Methods

Ethical Approval of Animals: Kvβ1.1 KO (global) (32) and C57BL6/NJ (wild type; WT) female and male mice were obtained from Jackson Laboratories, stock number 007747 (Bar Harbor, ME, US). Mice of 12-14 weeks of age were used (20 female mice with average weights of 19-21g and 15 male mice with average weights of 26-28g, of each strain). All animal protocol and use was approved by the Institutional Animal Care and Use Committee (IACUC) at the University of South Florida (Tampa, FL, USA), which is consistent with the practices approved by US National Institutes of Health guidelines. Investigators understand the ethical principles under which the journal operates and that this work complies with the journals animal ethics checklist. All the mice had continuous access to food and water, *ad libitum*. Mice were injected with heparin (360 USP, sigma) and euthanized with Somnasol (50 mg/kg body weight) by i.p. injection and heart tissue was excised after thoracotomy, snap frozen in liquid N_2 and stored at -80°C until further use.

Cell culture (H9C2) and siRNA: The H9C2 cells were purchased from ATCC (Manassas, VA, USA), and were cultured in 5% CO_2 incubator (Thermo Fischer Scientific, IL, USA) using standard DMEM medium (Invitrogen) supplemented with 10% Fetal Bovine Serum

(Invitrogen), penicillin and streptomycin (10mg/ml) antibiotics. For siRNA transfection experiments, the cells were transfected with 50 nM of either scrambled inhibitor or Kvβ1.1 siRNA (Cat# EMU086161, Sigma Aldrich, MO, USA) at 70% confluence using siLentFect™ lipid reagent (BioRad). Cells were observed for signs of toxicity for every 24 h under microscope. No detectable cell loss or change in cell morphology was observed in either groups. Total RNA was extracted 72 hrs post-siRNA treatment using Exiqon RNA isolation kit as described below.

Histochemistry: Female Kvβ1.1 KO and WT hearts were frozen after isolation by thoracotomy and then sectioned (25 μm) using a cryostat (Microm HM505 E, Walldorf, Germany). Sections were stained with hematoxylin/eosin for histological examination(104).

Echocardiography: Serial transaortic echocardiography (Visualsonic Vevo 770^{TM}, 30MHz linear signal transducer) (Toronto, Ontario, Canada) was taken under 2-3% isoflurane/oxygen anesthesia. The mice were depilated as required for imaging and placed on a 37^{o}C heated platform throughout the imaging procedure. Echo measurements were taken from at least three different cardiac cycles for each mouse. M-mode imaging from short-axis of the left ventricle (LV), using the papillary muscles for reference, was used to obtain measurements of LV posterior and anterior wall (LVPW/LVAW) thickness as well as LV internal dimensions (LVID'd and LVID's) in diastole and systole. Fractional shortening (FS%) and ejection fraction (EF%) were calculated as previously described(104). For measuring systolic flow Pulse wave (PW) – Doppler was used to image the ascending aortic arch as well as the pulmonary artery in long-axis to obtain mean flow velocity and velocity-time integral of both aortic arch and pulmonary artery.

Electrocardiography (ECG): ECG recordings were obtained from mice under 4-5% isoflurane/oxygen anesthesia using surface probes in lead II configuration. ECGs were acquired for a total duration of 15 min, with 1 min recordings obtained at 5 minute intervals. Heart rate was measured while ECG signals were obtained. Signal was acquired at 1000 μs rate by using PowerLab system operated with LabChart 7.2 software (AD Instruments, UK), and data was analyzed offline using the ECG module of LabChart 7.2 software, as reported elsewhere (8, 13). The intervals (ms) of RR, PR, QRS and JT were measured. QT interval was measured from the start of the Q peak to the point where the T wave returns to the isoelectric baseline (TP baseline), and heart rate corrected QT (QTc) interval was obtained using ($QTc = QT / ((RR/100)^{1/2})$(25, 82).

Blood Pressure Measurements: Non-Invasive tail-cuff method was utilized to measure blood pressure and heart rate in conscious mice. Mice were placed in plastic restrainers and placed on a water heater at 37°C for 10 min. A pressure transducer was placed on the tail of the mice. Mice were allowed to habituate to this procedure for 5 days before experiments were performed. Blood pressure (BP) and heart rate (HR) values were recorded using a Model CODA Standard, 1 animal Noninvasive blood pressure system (Kent Scientific, CT) with heating. Final measurements were averaged from 10 consecutive readings obtained from each mouse.

Monophasic Action Potentials: Monophasic action potentials (MAP) were recorded from *ex vivo* KO and WT female mouse hearts. Mice were injected with 1 mg heparin (180 USP, sigma) and euthanized with Somnasol (50mg/kg body weight) by i.p. injection. Hearts were

isolated through a bilateral thoracotomy and retrograde perfusion with Krebs-Hanseleit buffer (mM- 119 NaCl, 25 $NaHCO_3$, 4 KCl, 1.2 KH_2PO4, 1 $MgCl_2$, 1.8 $CaCl_2$, 10 D-glucose and 2 Sodium pyruvate, pH 7.4) at a constant flow rate of ~2.2 ml/min, 37°C (13). Monophasic action potentials were recorded from left ventricular (LV) epicardial surface using contact electrode (Harvard apparatus, MA). Hearts were stabilized for 15 minutes and AP data were acquired using 8 channel PowerLab system (AD Instruments, UK).

Quantitative Real-Time-PCR (qRT-PCR): Total RNA was isolated from the ventricular apex of Kvβ1.1 KO and WT female hearts using Exiqon miRCURY RNA Isolation kit (Exiqon, Woburn, MA) according to the manufactures protocol. Complimentary DNA (cDNA) from total RNA was synthesized and quantitative real-time PCR (qRT-PCR) analysis was performed for measuring mRNA expression of hypertrophic markers including MHCα, MHCβ, GATA6, BMP10, and PI3K. All the cDNA synthesis and qRT-PCR procedures were performed as described previously(104). The expression of mouse HPRT transcript was used as an endogenous reference. Data were expressed as mean fold change (±SEM; n=3).

Western Blotting: Protein lysates for Western blotting were prepared from both KO and WT female mouse hearts. Left ventricles were homogenized and procedures were performed as described previously (102-104). The supernatant was collected and stored at −80°C. Equivalent amounts of protein were loaded and separated by 4–20% gradient SDS polyacrylamide gels (Bio-Rad Laboratories). Proteins were detected with a dilution of primary antibody; MHCβ (MAB1548) and MHCα (AB50967) at 1:200 and1:1000, respectively. Target protein band

densities were quantified using Image-J software, and normalized with Ponceau S stained total protein band densities.

Pull-down Assay: To identify the interaction between Kvβ1.1 and MHCα in the heart, we conducted a pull-down assay using whole ventricular tissue lysate. Briefly, 5 µg of DDK-tagged Kvβ1.1 plasmid (Origene) was transiently expressed (72 hrs) in Cos-7 cells grown to 90% confluence in a 10 cm plate. Total cellular protein was extracted from Kvβ1.1-DDK expressing Cos-7 and mice ventricles by homogenization using extraction buffer containing (in mM) 50 mM Tris, pH 7.4, 150 mM NaCl, 5 mM EDTA, 1% Nonidet P40 (NP40) (ThermoScientific, USA) supplemented with 10 mM DDT, 1:100 protease inhibitor (Sigma-Aldrich, St. Louis, MO) and 1:100 protease inhibitor (sigma). Tissue lysate was then centrifuged at 10,000x g for 10 minutes at 4°C, and the supernatant was collected. Protein quantification was performed using Pierce 660 assay (Thermo Fisher Scientific, Waltham, MA). 200 µg of Kvβ1.1-DDK Cos-7 lysate was incubated with Anti-DDK Agarose beads (Origene, Rockville, MD) for 3 hrs at 4°C, and 500 µg of pre-cleared ventricular tissue lysate was then added and incubated overnight at 4°C. Bound proteins were then eluted and immunoblot analysis was conducted using MHCα antibody.

Pathway Analysis: Differentially expressed genes from qRT-PCR data were selected for network analysis using Ingenuity Pathway Analysis (IPA) software (Ingenuity Systems, Inc., CA, USA). Based on the existing literature, IPA identified the networks from its library of canonical pathways that were most significant to the data set. The significance of the association between the data set and the pathway network was measured by a ratio of the number of genes from the data set that map to the pathway divided by the total number of genes that map to the canonical pathway.

Statistical Analysis: A Student's *t*-test was used to identify significant pair-wise comparisons for all parameters between WT and KO mice. Statistical analyses were performed with Sigma Plot (version 11.0) and MS Excel. Data are expressed as mean ± SEM; and p-values ≤0.05 were considered statistically significant

Results

Kvβ1.1 KO females demonstrate altered cardiac structure and systolic function

The Kvβ1.1 KO female mouse hearts demonstrate a significant increase in heart weight compared with WT controls (**Figure 2A**). The Kvβ1.1 KO male mouse hearts however, demonstrated no significant heart weight difference when compared with WT male controls **(Figure 2B)**. Histological sections of female hearts showed an overall increased size of the KO hearts compared with WT controls (**Figure 2C and 2D**). Echocardiographic measurements confirm the overall size increase in heart as LV mass measurements showed a significant increase in KO females compared with WT controls (122±7 vs. 103±4 mg) (**Figure 3C**). M-mode short axis measurements demonstrate a significant increase in the LVID at both systole and diastole, in addition to the volume pumped at both systole and diastole (**Figure 3A and B**). Furthermore, the stroke volume was significantly higher in KO females compared with WT controls (41±1.8µl vs. 35±1.7µl) (**Figure 3D**). However, no differences were noted in LV wall thickness (including anterior and posterior) or functional indices including ejection fraction and fractional shortening between the female KO mice compared with WT controls (Table 2 and 3).

Arterial and blood pressure differences in Kvβ1.1 KO female mice

Blood pressure measurements in female KO mice demonstrated significant elevation at both systole and diastole compared with female WT control mice (**Figure 4A and B**). Male KO mice showed only a small and statistically non-significant elevation in blood pressure when compared with WT controls (**Figure 4D and E**). Heart rates between KO and WT in both sexes indicated no significant difference (**Figure 4C and F**). PW-Doppler imaging was used for assessing the ascending aorta and pulmonary artery to measure systolic flow parameters of the left and right side of the heart. KO mice demonstrate an increase in mean gradient pressure as well as velocity time integral (**Figure 5A-C**) in the ascending aorta when compared with WT mice, which is indicative of increased LV pressure in KO female mice. A small increase in VTI was also observed in the pulmonary artery, but this was not significantly different from WT controls (**Figure 5D**).

Kvβ1.1 KO prolongs QTc interval in both male and female mice

As show in **Figure 6A,** the averaged traces show significantly longer QTc interval in KO (51±1.8ms) female mice when compared with WT females (45±2.1ms) **(Figure 6B)**. In addition, the QRS interval was significantly prolonged in KO females compared with WT females (**Figure 6C**). Male Kvβ1.1 KO mice showed significantly longer QTc intervals **(Figure 6D),** however QRS interval did not change significantly **(Figure 6E)**. These data suggests that the repolarization phase in Kvβ1.1 KO mice is altered compared with WT controls. Additional ECG measurements including P duration demonstrated slight significance in KO females (Table 4 and 5).

Prolonged monophasic action potentials in Kvβ1.1 KO hearts

Monophasic action potential traces were recorded from left ventricular epicardial surface of hearts using *ex vivo* perfusion in females (**Figure 7A**) and males (**Figure 7C**). Analysis of the trace from female KO hearts revealed a significantly prolonged APD from 20-90% repolarization levels; APD_{90} (57±1.8 vs. 49±2.5), when compared with WT (**Figure 7B**). However, male KO hearts demonstrated significant prolonged APD's from 50-90% repolarization levels only **(Figure 7D)**. Nevertheless, these data suggest that Kvβ1.1 KO hearts demonstrate prolonged action potential durations.

Differential mRNA expression of key hypertrophic markers and Kv channels

As we observed significant differences in the structural, hemodynamic and electrical indices in KO female mouse hearts compared with WT, we examined the expression levels of various genes that have been previously linked to these phenotypes cardiac myosin; MHCα(6), MHCβ(7), PI3K, GATA4, GATA6 and BMP10. Data from the present study reveal that mRNA levels of MHCα were significantly increased in KO female mouse hearts compared to WT controls, whereas no change in MHCβ transcripts was noted (**Figure 8A**). The mRNA levels of GATA4, GATA6, and BMP10 significantly increased while PI3K decreased in KO female hearts compared with WT hearts (**Figure 8A**).

Differential expression of myosin isoform proteins

Gene expression changes noted in MHCα (**Figure 8A**) were confirmed by using Western blot, which showed a significant increase in MHCα expression within the LV in KO female mice

compared with WT male controls (**Figure 8B and 8C**). Western blot analysis also revealed small increase (not significant) in MHCβ expression in the LV KO heart compared with WT mice.

MHCα interacts with Kvβ1.1 subunit

To evaluate the protein-protein interaction, we performed a pull down assay to identify the association between Kvβ1 and MHCα. As shown in **Figure 8D**, lane 1 identifies MHCα as the protein that was pulled using the DDK-Kvβ1 affinity assay. However, no relevant protein was identified in lane 2 at the similar molecular weight range. Overall, these data demonstrates that Kvβ1 protein interacts with MHCα in the mouse heart.

Kvβ1.1 knockdown causes MHCα upregulation

We evaluated the co-regulation of Kvβ1 and MHCα by using siRNA knockdown in H9C2 cells (rat cardiomyoblasts). Inhibiting the expression of Kvβ1.1 in H9C2 cells clearly led to higher expression of MHCα in the cardiac cells. As shown in **Figure 8E**, we identified the regulation of key genes including GATA4, GATA6 and MHCα altered in the Kvβ1.1 knockdown group compared with the scrambled siRNA. These data confirm that Kvβ1 knockdown modulates the expression of the genes that were altered in the Kvβ1.1 KO mouse model.

Expression of key Kv channels and Kvβ subunits

The mRNA expression of key Kv channels and Kvβ subunits were not significantly altered (**Figure 9A and 9B**). Comparison of Kvβ1.1 levels between male vs female wild type mouse hearts shows significantly increased expression in females (**Figure 9C**).

Discussion

In the present study, we report the physiological role of Kvβ1.1 in the murine heart. Our morphometric and echocardiographic assessment clearly demonstrate that KO female mice have significantly enlarged hearts with altered cardiac function compared with their WT controls. Male KO mice however, demonstrated no alteration in heart size in comparison, emphasizing a sex specific difference in Kvβ1.1 KO female mice. The ECG and monophasic action potential analysis identified prolongation in QTc and APD's demonstrating that the repolarization reserve is depleted in both male and female Kvβ1.1 KO mice. At the molecular level, we identified novel protein-protein interactions between Kvβ1 and MHCα and confirmed that MHCα expression can be specifically modulated by Kvβ1 knockdown.

Electrical remodeling in Kvβ1.1 KO mice

Prolonged repolarization indices such as; QTc and APD, in KO mice suggest that Kvβ1.1 is necessary for Kv channel activity and therefore vital to the repolarization reserve. It is well known that Kv channels such as Kv1.x and Kv4.x are major contributors to the repolarization reserve in the heart. Alterations in Kv channels in heart can lead to arrhythmic events and altered cardiac metabolism (13, 96). Several studies in the past demonstrated that Kvβ subunits bind to and modulate the activities of Kv1.x and Kv4.x channels (112). Heterologous expression studies have shown that different splice isoforms of Kvβ1 can bind to and confer inactivation of both slowly or rapidly inactivating Kv1.x channels (117, 137, 138). It has been shown that Kvβ1.1 binds to Kv4.2 and Kv4.3 in mouse ventricles, and deletion of Kvβ1 leads to decreased $I_{to,f}$

current densities in male mice (2). Consistent with these evidence, our present data show prolonged APD and QTc in KO group, suggesting that Kvβ1.1 is an essential contributor to cardiac repolarization. Repolarization defects noted in KO female hearts showed significant hypertrophy, suggesting differential structural remodeling in females.

Vascular alterations in Kvβ1.1 KO mice

Power Doppler analysis indicates that increased vascular resistance may be the more likely cause of the observed hypertrophy in KO female mice since both the mean aortic gradient pressure and aortic velocity time integral (VTI) are significantly higher in KO females compared with WT controls. Blood pressure recordings demonstrated a significant increase in KO females when compared with WT female controls. KO males however, demonstrated a small and statistically insignificant elevation in blood pressure. An increase in blood pressure can result in pressure-overload on the heart leading to the development of left ventricular hypertrophy (LVH) that can progress further to hypertensive heart disease (22). Echocardiographic analysis also supports this idea as female KO mice have an increased LV internal diameter at diastole and systole indicating LV dilatation (23), and increased left ventricular mass which is corroborated by the higher cross sectional area observed using stained tissue sections, which collectively suggests that female KO mouse hearts are hypertrophic (13, 104). Lack of any significant change in ejection fraction, which reflects a fractional change in the LV end diastolic volume, indicates no differences in the fractional LV output at each cycle. Despite this, we observed increased aortic blood flow rate as well as KO females presenting with higher blood pressure than WT controls, which could, at least in part, contribute to the development of cardiac hypertrophy.

Kvβ1.1 alterations to cardiac MHCα expression

Cardiac remodeling involves changes in expression of key genes involved in regulating the electrical and the function of the heart. Therefore, we assessed mRNA and/or protein expression of key genes in the heart. We found that myosin isoform expression was significantly altered in the heart of KO females. Significantly larger elevation of MHCα (fast isoform) expression; both mRNA and protein, clearly indicates features of a hypertrophic response in KO female heart. Further, mRNA expression of Kvβ1.1 in heart demonstrated a significant increase within females compared to males in wild type mice indicating that Kvβ1.1 may play a significant cardiac specific role in females. To develop an overall understanding of the Kvβ1.1 gene at the molecular level, we utilized the Ingenuity Pathway Analysis (IPA) and provided experimental data as input for predicting possible pathways that are involved in the cardiac remodeling. Based on this analysis, the final targets for cardiac hypertrophy in murine heart are GATA-4, GATA-6, and MHCα (MYH6), which are majorly altered in KO female hearts (**Figure 10**). The transcription factors GATA-4 and GATA-6 have previously been demonstrated to have a profound effect on MHCα and β expression (47, 77, 83, 162). Furthermore, PKA and PKC, which are known targets affected by cardiac hypertrophy, demonstrate significant interactions with GATA4, which is one of the key transcription factor that activates MHCα (MYH6) (128, 145). Although how Kvβ1.1 or absence of Kvβ1.1 alters the expression of GATA-4, GATA-6 and MHCα (MYH6) remains unclear, protein-protein interaction between Kvβ1.1 and MHCα in conjunction with elevated MHCα expression in Kvβ1.1 KO mouse hearts and Kvβ1.1 siRNA treated H9C2 cells strongly suggests a potent inhibitory role of Kvβ1.1 in MHCα regulation. Collectively, the expression data and network analysis suggests that in female KO mice, there is

an upregulation of the hypertrophic pathway that involves altered expression of myosin heavy chain genes as well as key transcription factors including GATA-4.

Study limitations

In this study, mice with global knockout of Kvβ1.1 gene were utilized for experimentation. Our study demonstrated significant cardiac structural and hemodynamic differences in the female KO mice. However, since Kvβ1.1 female KO mice show high blood pressure, it is likely that vascular changes may be involved in causing cardiac hypertrophy. Future studies are necessary to identify the vascular component and how deletion of Kvβ1.1 affects the female mice.

Conclusion

In conclusion, we identified structural, electrical and hemodynamic differences in Kvβ1.1 KO in murine hearts. This is the first study demonstrating that deletion of Kvβ1.1 leads to increased blood pressure, electrical changes and cardiac hypertrophy in the female murine hearts. We identified that the male mice failed to develop cardiac hypertrophy and high blood pressure despite altered electrical activity. Overall, the female mouse hearts depict distinct physiological changes up on deletion of Kvβ1.1 gene compared with male mice. At molecular level, the female hearts confirm the major hallmarks for cardiac hypertrophy such as MHCα and it's binding to Kvβ1.1. Therefore, this study brings fundamental new information for understanding the roles of Kvβ1.1 in female murine hearts and its relation to cardiovascular physiology. In future experiments ovariotomy of female mice may demonstrate a unique interaction between estrogen levels and Kvβ1.1 that highlights a male-female difference in function.

Tables and Figures

Table 2: Echocardiography M-mode Measurements

Mice	LVAW(s) mm	LVAW(d) mm	LVPW(s) mm	LVPW(d) mm
Kvβ1.1$^{-/-}$	**1.3±0.05**	**0.88±0.04**	**1.1±0.03**	**0.8±0.01**
Wild type	**1.3±0.05**	**0.87±0.04**	**1.1±0.06**	**0.8±0.03**
P-value	**NS**	**NS**	**NS**	**NS**

Table 3: Echocardiography M-mode Measurements

Mice	V(s) µl	V(d) µl	EF%	FS%	CO (ml/min)
Kvβ1.1$^{-/-}$	**27.7±1.6**	**69±3.1**	**60±1.2**	**31.6±0.8**	**18±0.9**
Wild type	**21.4±2.2**	**57±2.8**	**63±2**	**34±2**	**15.8±0.8**
P-value	**0.03**	**0.008**	**NS**	**NS**	**0.07**

Table 4: ECG Measurements (Females)

Female Mice	RR Interval (ms)	PR Interval (ms)	P Duration (ms)	QT Interval (ms)	JT Interval (ms)
Kvβ1.1$^{-/-}$	**148±3**	**43±1.6**	**12±0.7**	**20±0.7**	**10±0.7**
Wild type	**144±3**	**40±0.7**	**10±0.5**	**17±0.7**	**9.5±0.8**
P-value	**NS**	**NS**	**0.04**	**0.02**	**NS**

Table 5: ECG Measurements (Males)

Male Mice	RR Interval (ms)	PR Interval (ms)	P Duration (ms)	QT Interval (ms)	JT Interval (ms)
Kvβ1.1$^{-/-}$	**144±4**	**42±0.5**	**9.8±0.6**	**22±0.6**	**14±0.7**
Wild type	**140±2.3**	**53±4.5**	**12±0.8**	**20±0.5**	**11±0.5**
P-value	**NS**	**0.04**	**NS**	**0.007**	**0.002**

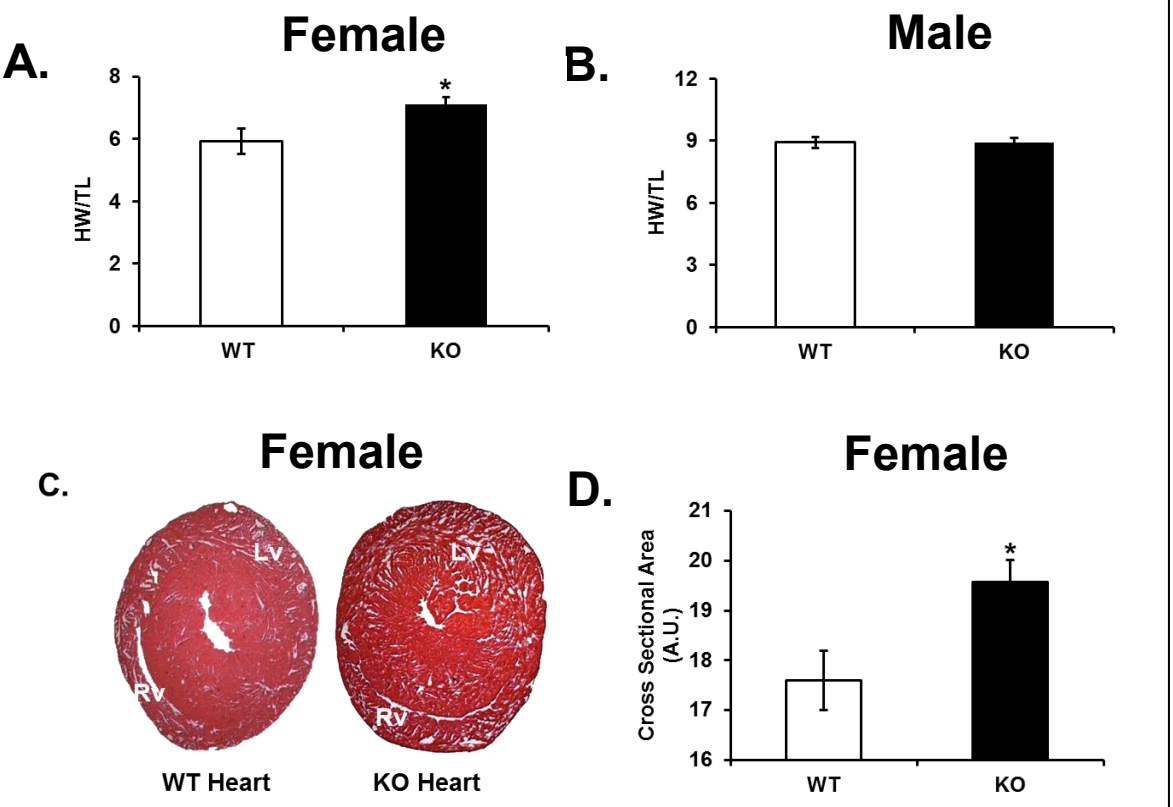

Figure 2. Cardiac structural analysis by morphometry: A. Female heart weight normalized with tibia length from WT and KO hearts, bar graph is mean±SEM (n=10) and *p<0.05. **B.** Male heart weight normalized with tibia length from WT and KO hearts, bar graph is mean±SEM (n=15). **C.** Cross sectional image of the heart from wild type (WT) and knockout (KO) female mice. Heart sections were taken at 25-µm thick and stained with hematoxylin/eosin; left ventricle (Lv) and right ventricle (Rv) are labeled. **D.** Cross sectional area of hearts measured with Image-J software, and mean±SEM plotted using a bar graph (n=4) and *p<0.05.

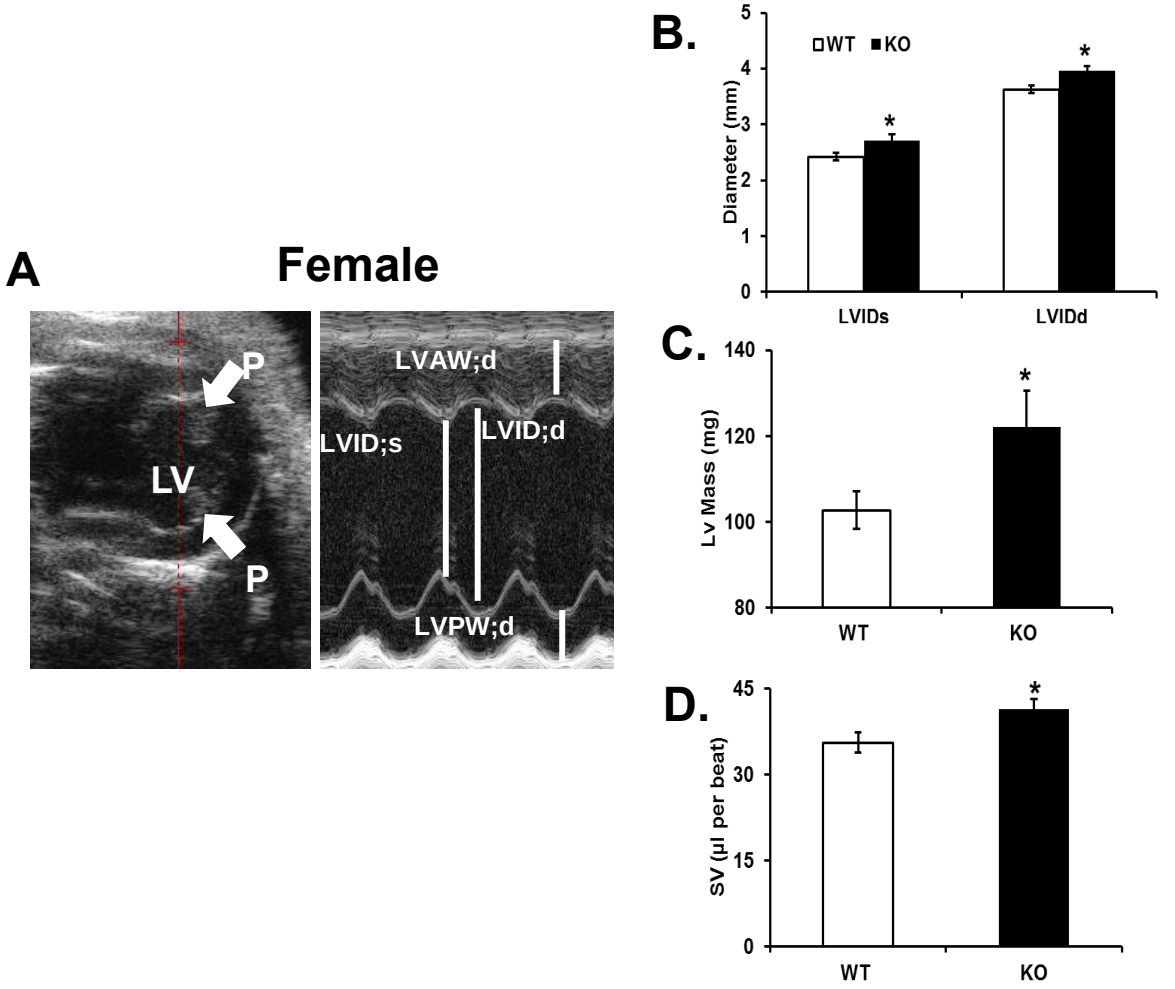

Figure 3. Female cardiac measurements by echocardiography: A. B-mode short axis image of the left ventricle (LV) with papillary muscles visible (P). M-mode image of the interior of the LV with LVID;s and LVID;d (left ventricular internal dimension at systole and diastole) along with LVAW;d and LVPW;d (left ventricular anterior/posterior wall at diastole). **B.** LVID;s and LVID;d dimensions measured between wild type (WT) and knockout (KO). Bar graph is mean±SEM (n=13) and *p<0.05. **C.** Lv Mass estimated using M-mode images, bar graph represents mean±SEM (n=13) and *p<0.05. **D.** Stroke volume (SV) per beat obtained from M-mode images, bar graph is mean±SEM (n=13) and *p<0.05.

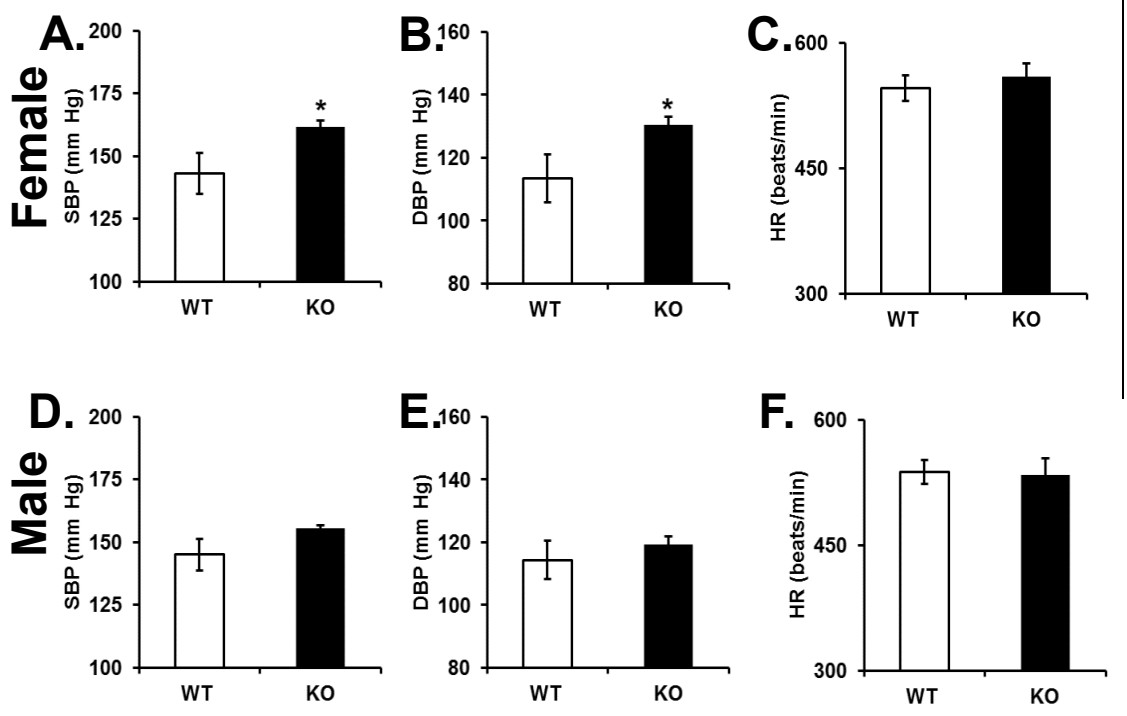

Figure 4. Blood pressure measurements: A. Female systolic blood pressure (SBP) measurements from WT and KO mice, bar graph is mean±SEM (n=8 mice) and *p<0.05. **B.** Female diastolic blood pressure (DBP) measurements from WT and KO mice, bar graph is mean±SEM (n=8 mice) and *p<0.05. **C.** Female heart rate (HR) measurements from WT and KO hearts, bar graph is mean±SEM (n=8 mice). **D.** Male systolic blood pressure (SBP) measurements from WT and KO hearts, bar graph is mean±SEM (n=8 mice). **E.** Male diastolic blood pressure (DSP) measurements from WT and KO hearts, bar graph is mean±SEM (n=8 mice). **F.** Male heart rate (HR) measurements from WT and KO hearts, bar graph is mean±SEM (n=8 mice).

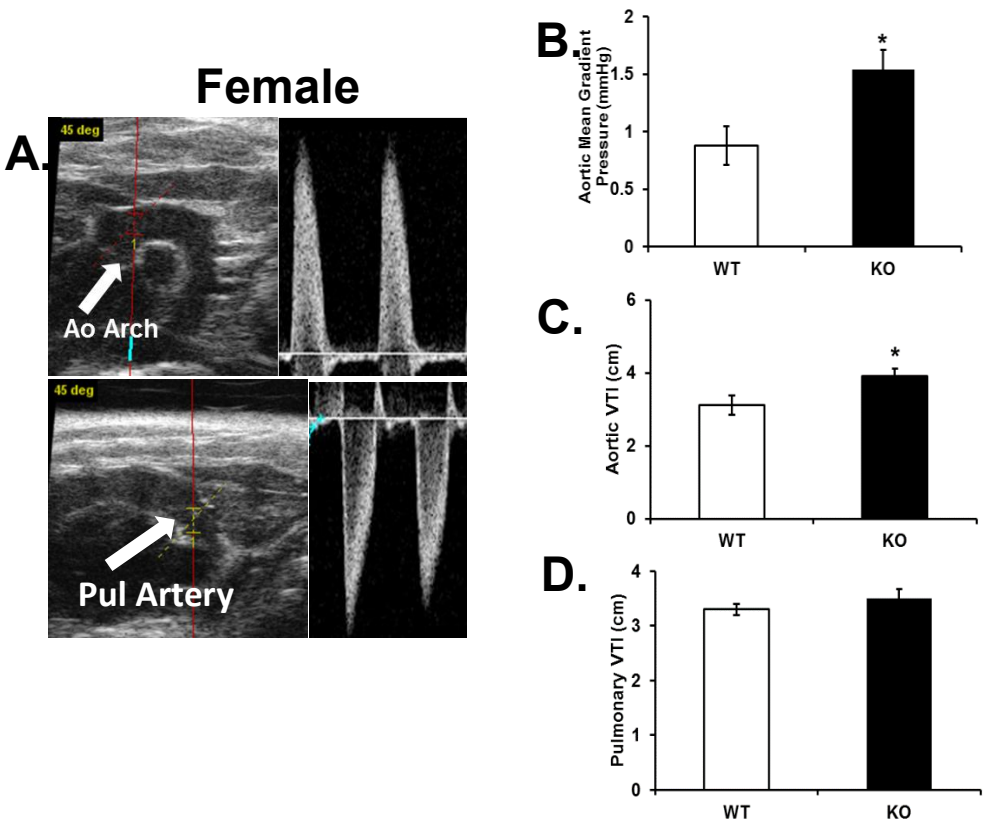

Figure 5. A. Female Hemodynamic changes: B-mode image of the ascending aorta (Ao Arch) and PW Doppler image of the ascending aorta blood flow. B-mode image of the pulmonary artery (Pul Artery) and PW Doppler image of the pulmonary artery blood flow **B.** Aortic mean gradient pressure in millimeters per mercury measured between wild type (WT) and knockout (KO). Bar graph is mean±SEM (n=8) and *p<0.05. **C.** Aortic velocity time integral (VTI) taken from PW Doppler imaging, bar graph is mean±SEM (n=8) and *p<0.05. **D.** Pulmonary VTI taken from PW Doppler imaging, bar graph is mean±SEM (n=8).

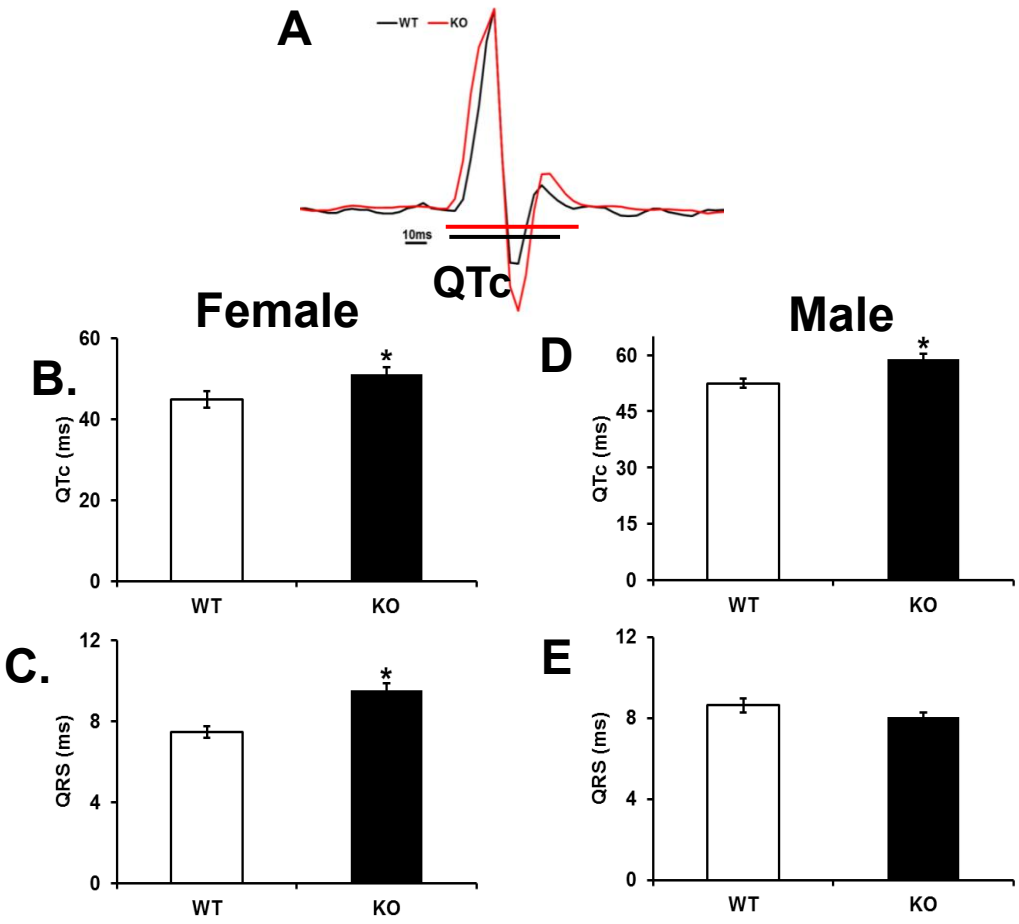

Figure 6. ECG recordings: A. Averaged trace of lead-II ECG recording from WT (black) and KO (red) showing QTc duration from female mice. **B.** Female QTc interval in WT and KO mice, and bar graph represents mean±SEM (n=10) and *p<0.05. **C.** Female QRS duration in WT and KO mice and bar graph represents mean±SEM (n=10) and *p<0.05. **D.** Male QTc interval in WT and KO mice, and bar graph represents mean±SEM (n=10) and *p<0.05. **E.** Male QRS duration in WT and KO mice and bar graph represents mean±SEM (n=10).

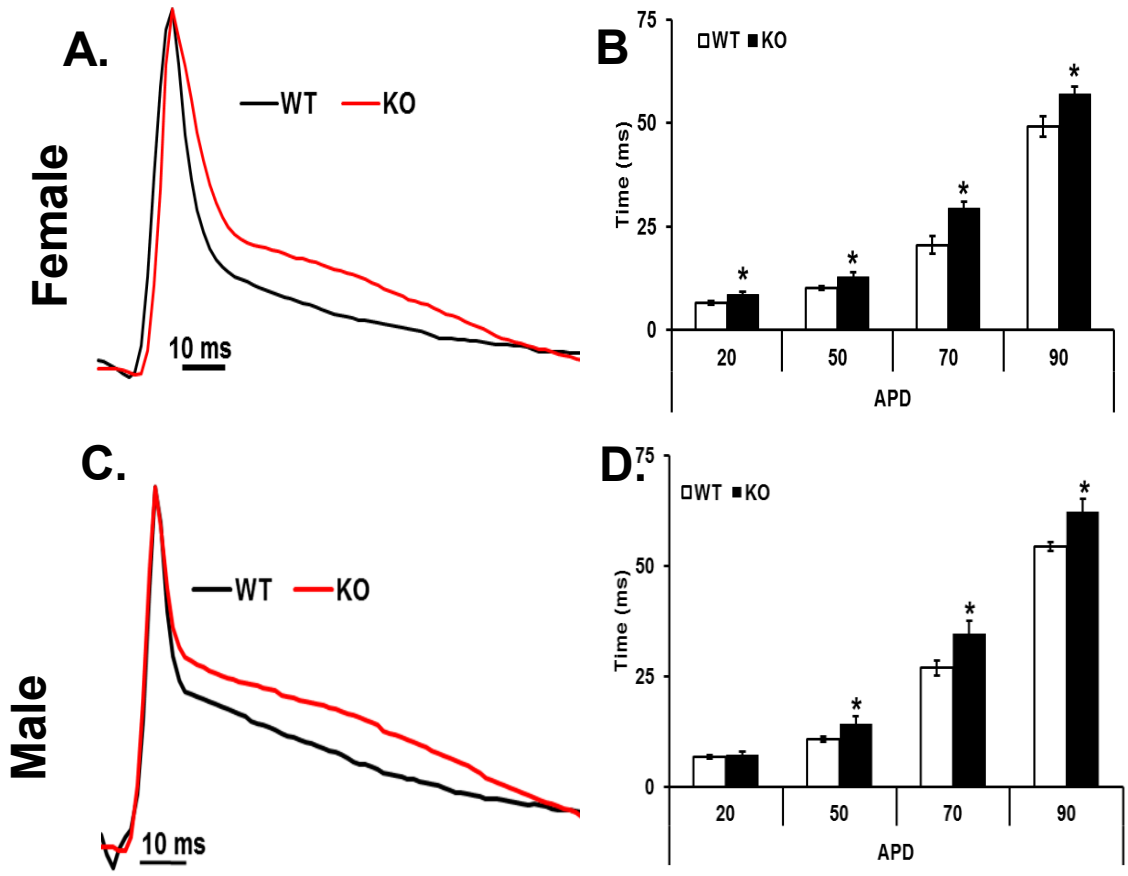

Figure 7. Ventricular repolarization changes: A. Averaged recordings of monophasic action potential in WT (black) and KO (red) from females. **B.** Female action potential durations (milliseconds) at 20, 50, 70, and 90% repolarization in WT and KO mice, bar graph shows mean±SEM (n=6) and *p<0.05. **C.** Averaged recordings of monophasic action potential in WT (black) and KO (red) (n=3) from males. **B.** Male action potential durations (milliseconds) at 20, 50, 70, and 90% repolarization in WT and KO mice, bar graph shows mean±SEM (n=9) and *p<0.05. Monophasic action potential recordings were obtained at 37^{o}C perfusion.

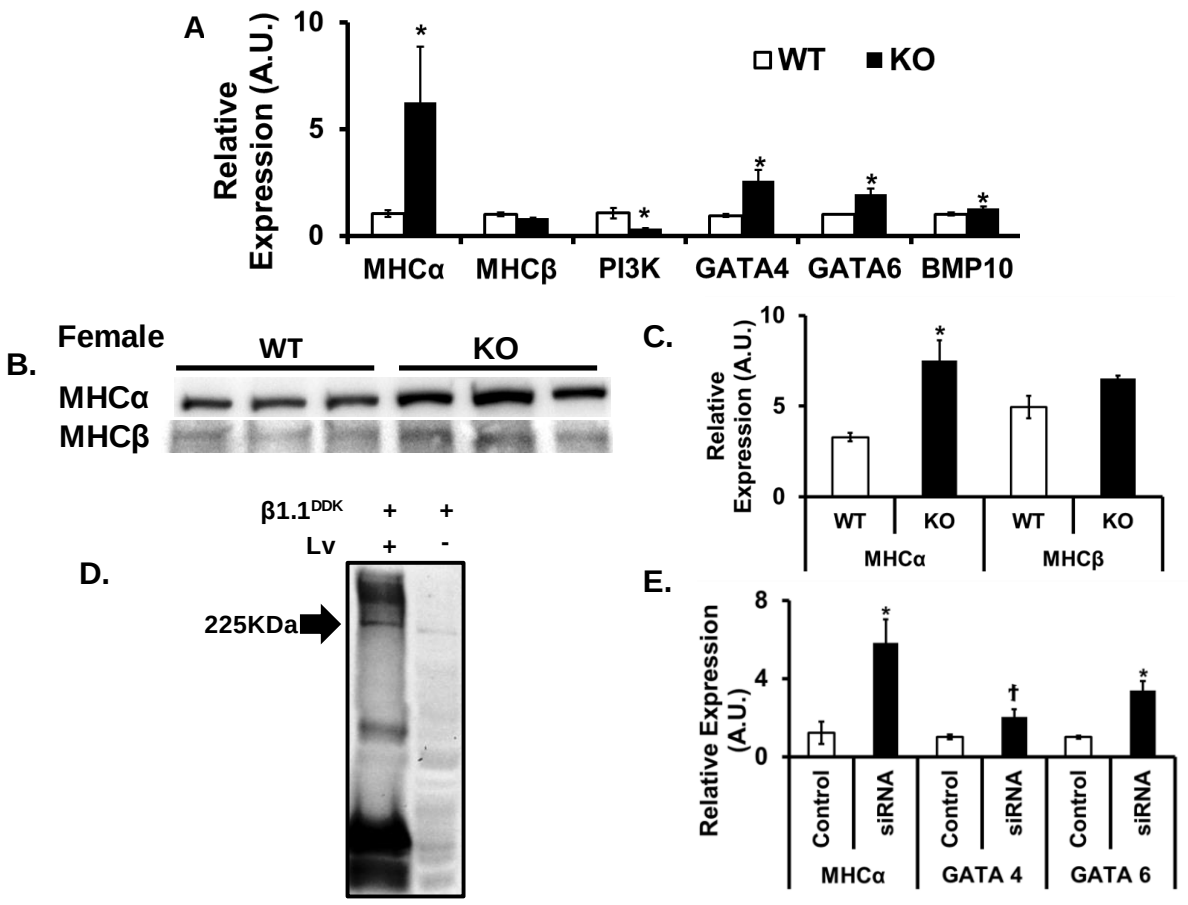

Figure 8. Female cardiac real-time PCR expression, protein, and protein-protein interaction analysis: A. Expression of myosin heavy chain isoforms (MHC) α and -β; PI3K, GATA4, GATA6 and, BMP10 known cardiac specific hypertrophy markers, bar graph is mean±SEM (n=3) and *p<0.05. Genes were normalized with a housekeeping gene (HPRT). **B.** Western blot images of MHCα and MHCβ from WT and KO left ventricular homogenate. **C.** Bar graph is mean±SEM (n=3) and *p<0.05, bands were normalized with Ponceau S stained full lanes. **D.** Western blot image of lane 1; KO left ventricle (Lv) and Cos-7 cells transfected with Kvβ1.1-DDK plasmid ($\beta1.1^{DDK}$) and lane 2; Cos-7 cells transfected with Kvβ1.1-DDK plasmid ($\beta1.1^{DDK}$) alone. Lane 1 was incubated overnight with DDK-coated agarose beads. MHCα (1:200) primary antibody was incubated overnight with blot, a 225KDa band was noted in lane 1 with a limited band seen in lane 2. **E.** PCR expression of myosin heavy chain α as well as GATA4 and GATA6 72-hrs post Kvβ1.1 siRNA treatment in H9C2 (rat cardiomyoblasts) bar graph as mean±SEM (n=3) and *p<0.05.

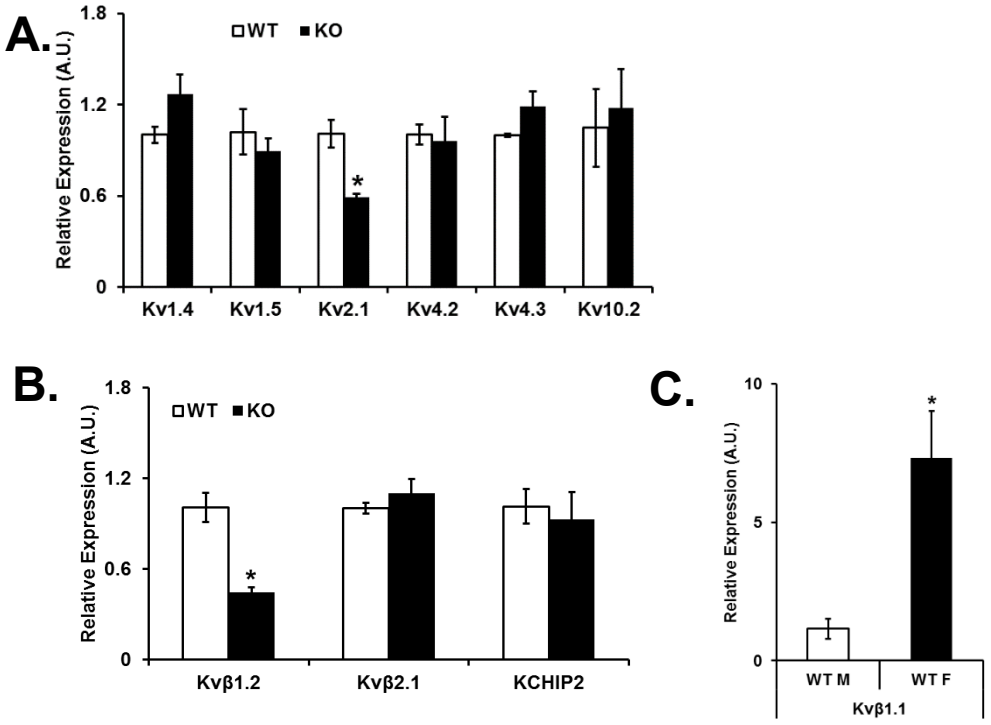

Figure 9. Real-time PCR expression analysis: A. Female expression of voltage-gated potassium channels involved in cardiac repolarization including Kv1.4, Kv1.5, Kv2.1, Kv4.2, Kv4.3 and, Kv10.2 bar graph is mean±SEM (n=3) and *p<0.05. Genes were normalized with a housekeeping gene (18s). **B.** Expression of voltage-gated potassium channel subunits Kvβ1.2, Kvβ2 and, KCHIP2 bar graph is mean±SEM (n=3) and *p<0.05. **C.** Expression of voltage-gated potassium channel subunit Kvβ1.1 in wild type male (WT M) vs. wild type female (WT F) mouse heart, bar graph represents mean±SEM (n=3). Genes were normalized with a housekeeping gene (HPRT).

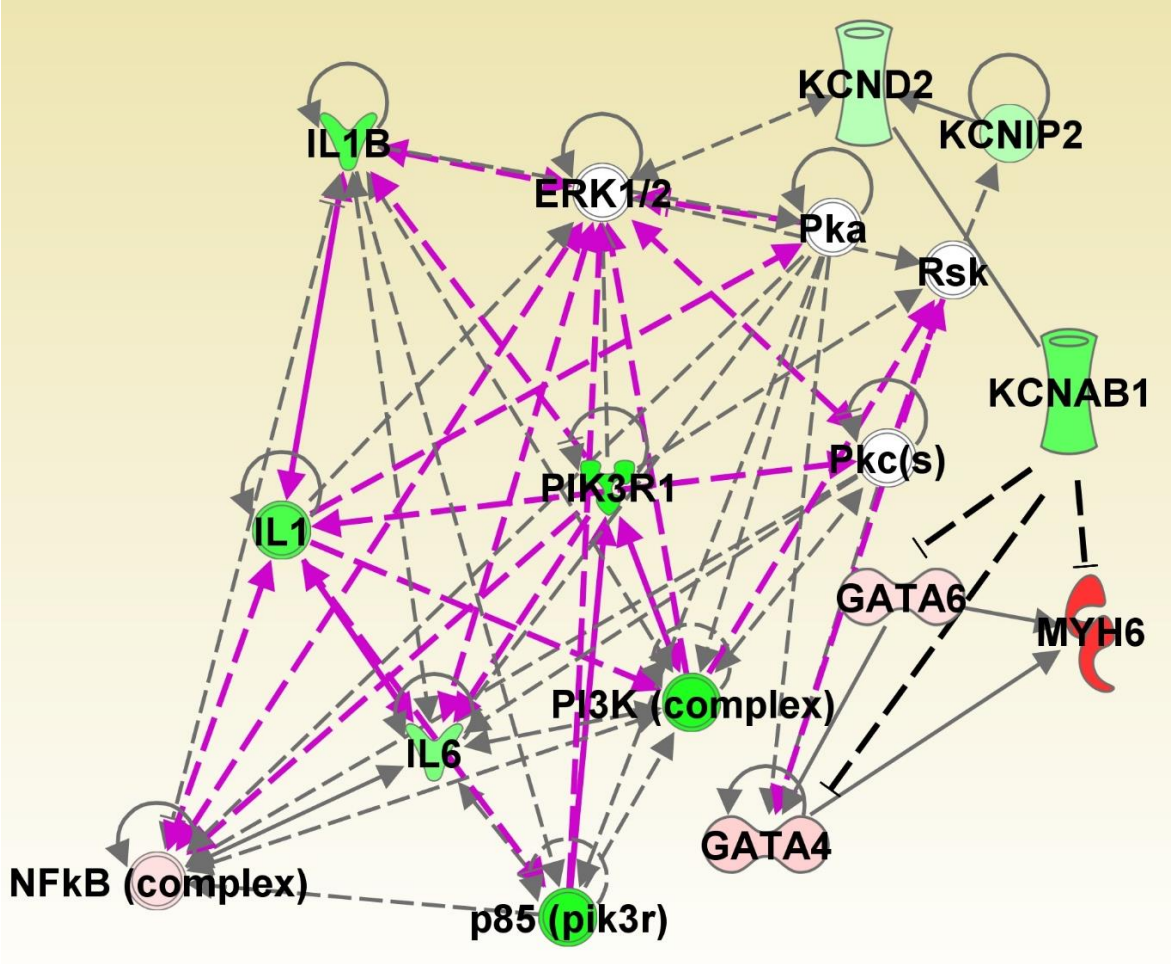

Figure 10. Gene network analysis: Top two networks identified by ingenuity pathway analysis (IPA) based on qPCR-expression data were merged. Potential interactions between KCNAB1 and MYH6 (MHCα) or GATA factors were incorporated into the analysis and indicated by dotted black line. Relative gene expression changes between WT and KO group were depicted by a color gradient from green to red, green represents higher expression for WT, whereas red represents KO.

CHAPTER THREE:

Kvβ1.1 senses pyridine nucleotide changes in the heart and modulates cardiac electrical activity

Introduction

Cardiac injury including cardiac hypertrophy and myocardial ischemia demonstrate a decrease in NAD^+ and sharp increase in NADH (12, 57, 110). Therefore modulation of NAD^+ by supplementing the substrate or activation of the NAD^+ synthetic pathway increases intracellular NAD^+ which has been demonstrated as a plausible avenue of cardiac intervention in recent years. Exogenous NAD^+ injections resulted in significant rescue in agonist-induced cardiac hypertrophy in mice (111). Administration of nicotinamide mononucleotide (NMN) and nicotinamide phosphoribosyltransferase resulted in a significant increase in NAD^+ levels in the heart as well as reduced infarct size and improved cardiac myocyte survival after ischemia reperfusion injury (46, 155). The increase in NAD^+ levels leading to cardiac protection may be due to its ability to alter ion channel activity (53). Intracellular NADH was demonstrated to significantly alter the cardiac sodium channel (Nav1.5) and reduce peak currents as well as inhibit the Na^+/Ca^{2+} (NCX) exchanger in ventricular myocytes (71, 73).

The shaker potassium channel subunits (Kvβ), which are the members of the aldoketo reductase superfamily, are highly expressed in the heart and bind to voltage-gated potassium channels; Kv1 and Kv4 (21, 53, 117). Kv channels play a key role in cardiac repolarization, specifically in to the determination of the duration of the action potential plateau observed in phase 1 (91). In

mouse ventricle it is well known that much of the $I_{to,f}$ current is encoded by the molecular correlate Kv4.2/Kv4.3 responsible for the rapidly activating and inactivating potassium current (58, 106, 125). Further the Kv4.2 channel plays a critical role in the early cardiac repolarization as well as excitation contraction-coupling (124) and arrhythmias (10). Previous research also highlights the importance of potassium channel subunits including KCHIP2 (39) and Kvβ1(21) and their role in alternating Kv4.2/Kv4.3 affecting overall Ito current in cardiomyocytes and heterologous systems.

Previously, it was demonstrated that Kvβ1-3 bind pyridine nucleotides with high affinity and alter Kv channel gating and regulation (53, 137, 139). Addition of NAD^+ abolished Kvβ1 induced inactivation of Kv1.5 currents, whereas inclusion of NADH in the patch-pipette solutions supported inactivation (139). These reports overall, support the idea that reduced pyridine nucleotides (NADPH or NADH) inactivate and oxidized pyridine nucleotides $NADP^+$ or NAD^+) abolish Kvβ1 mediated inactivation and gating of Kv currents. Previous reports identified an increased learning and memory, neuronal excitability and synaptic plasticity in aged Kvβ1.1 knockout (KO) mice (85, 89). Kvβ1 KO also demonstrated a significant difference in Kv currents within left ventricular apex myocytes in 6-10 week old male mice (2). Moreover, Kvβ1.1 co-immunoprecipitates with Kv4.2 suggesting that Kvβ1.1 regulation of Kv4.2 activity may be of primary interest under pathophysiological stress.

Earlier studies using heterologous expression systems have identified that Kvβ subunits bind pyridine nucleotides [NAD(P)H/NAD(P)] with high affinity and modulate the gating and kinetics of Kv channel (53). Moreover, cardiac injury frequently involves elevated $NADH/NAD^+$ redox potential. Hence, it is plausible that Kvβ1.1 is an essential player in relaying the inhibitory effects of increased NADH stress on cardiac repolarization. We therefore hypothesized that

Kvβ1.1 is an essential mediator for pyridine nucleotide changes in the heart. We tested this hypothesis by utilizing Kvβ1.1 knockout mice (KO) and assessed the physiological and biochemical consequences of pyridine nucleotide modulation.

Material and Methods

Animals: Kvβ1.1 KO (global knockout) and WT mice (C57BL/6NJ) were obtained from Jackson Laboratories (Bar Harbor, ME, US) (141). Mice of 16-20 weeks of age were used and fed with food and water *ad libitum*. All animal work was approved in advance by the Institutional Animal Care and Use Committee at the University of South Florida (Tampa, FL, USA). Mice were genotyped to confirm the genetic deletion of Kvβ1.1 (**Figure 11A**).

Cardiomyocyte Isolation: Ventricular cardiomyocytes were isolated using an enzymatic dispersion technique. Briefly, hearts were cannulated and retrograde perfused with Ca2+-free isolation buffer containing (in mM; 117.3, NaCl, 5.3 KCl, 26.2 NaHCO3, 1 Na2HPO4, 20 HEPES, 10 Taurine, 20 2,3-butanedione monoxime (BDM), 6 D-glucose, pH 7.4, for 5 min at 37°C. The perfusate was then switched to isolation buffer containing 0.4 mg/mL Liberase Blendzyme 4 (Roche, Indianapolis, IN) and 20 μM CaCl2, and perfused for 10 min. Following digestion, the apex was excised and triturated in the Ca^{2+}-free isolation buffer containing 1% bovine serum albumin (BSA). The resulting cell preparation was passed through ~297μm polypropylene mesh to remove tissue debris. Isolated myocytes were then washed in isolation buffer without BDM, while adding CaCl2 in increments of 0.2 mM at 5 min intervals to reach a final concentration of 1.2 mM. Cells were then utilized for electrophysiological recordings within 4-5 hrs. Cells were placed on glass coverslips and perfused with an external solution

containing (in mM) NaCl 135, KCl 5.4, CaCl2 1.8, MgCl2 1.1, HEPES 10, D-glucose 5.5, pH 7.4 at room temperature.

Patch-clamp recording for isolated cardiomyocytes: Current clamp recordings were carried out on isolated cardiomyocytes using a perforated patch configuration. Isolated adult cardiomyocytes were plated on glass coverslips and allowed to rest in external solution for 10-30 minutes. The external solution for recordings consisted of (in mM): NaCl 135, KCl 5.4, CaCl2 1.8, MgCl2 1.1, HEPES 10 and D-Glucose 5.5, pH 7.4. Patch pipettes were fabricated from borosilicate glass, pulled to a resistance of 1-1.5 MΩ. The internal (patch pipette) solution consisted of (in mM): Aspartic acid 100, KCl 35, MgCl2 1.0, CaCl2 1.8, NaCl 4.5, EGTA 10, ATP 5, pH 7.2. Membrane potential traces were acquired at room temperature using an Axopatch-200B patch-clamp amplifier (Molecular Devices, Sunnyvale, CA) and pClamp 10 software (Molecular Devices, Sunnyvale, CA). Electrical access to the cell was achieved through perforated-patch configuration using 240 μg/ml amphotericin B (0.1% DMSO), dissolved in the internal solution. Action potentials were evoked from the cells under current-clamp mode by applying 2 msec current pulses delivered at 1 Hz. Pulse amplitudes were 2x threshold levels (1-2 nA). Membrane potentials were sampled at 10 kHz. Control action potentials were recorded for 1 minute. Cells were then perfused with external solution containing 10 mM lactate for 5 min and action potentials evoked again and recorded for 1 minute using the same pulse parameters as described before. Data were exported and analyzed using the Peak Analysis Module of LabChart 7.2 (AD Instruments, Colorado Springs, CO).

Cell culture (COS-7) and transfection procedures: COS-7 cells were purchased from ATCC (Manassas, VA, USA). COS-7 cells are green-monkey kidney fibroblast cells and were cultured in 5% CO2 incubator (Thermo Fischer Scientific, IL, USA) using standard DMEM medium (Invitrogen) supplemented with 10% Fetal Bovine Serum (Invitrogen), and 1% penicillin and streptomycin antibiotics. For cDNA transfection experiments, the cells were transfected with 2-6µg of either mouse Kv4.2 alone or in combination with Kvβ1.1-GFP (Cat# MC206092, MG206299 Origene, MD, USA), at 70-80% confluence using Lipofectamine™ LTX transfection system (Invitrogen, NY, USA) (137). Cells were monitored for signs of toxicity every 24hr under an EVOS XL Core Light Microscope (AMG Bothell, WA). No detectable cell loss or change in cell morphology was observed in transfected group. After 48 hours of transfection, cells were used for electrophysiological recordings.

Patch-clamp recording for transfected COS-7 cells: Whole-cell patch-clamp recordings were performed on COS-7 cells. Briefly, COS-7 cells transfected with Kv4.2 with or without Kvβ1.1-GFP plasmids were trypsinized (0.25%) and washed with serum free media just prior to plating on glass coverslips and allowed to rest in external solution consisting of (in mM): NaCl 135, KCl 5.4, MgCl2 1.1, CaCl2 1.8, HEPES 10 and Glucose 5.5 at pH 7.4 for 10-30 minutes. Patch pipettes were fabricated from borosilicate glass, pulled to a resistance of 1-3 MΩ. The internal (patch pipette) solution consisted of (in mM): Aspartic acid 100, KCl 35, MgCl2 1.0, CaCl2 1.8, NaCl 4.5, EGTA 10, ATP 5 at pH 7.2 with KOH. Axopatch-200B patch-clamp amplifier (Molecular Devices, Sunnyvale, CA) operated by pClamp 10 software (Molecular Devices, Sunnyvale, CA) were used to record membrane currents, which were analyzed and digitized with 12-bit resolution. Patch pipettes with 1–3 MΩ resistance were used to obtain GΩ

tight seals and membrane under the patch pipette was ruptured using negative pressure to achieve the whole-cell configuration. Whole cell currents were elicited by applying depolarizing voltage steps from −60 to +60 mV in 10 mV steps to the cells from a holding of −80 mV for 300 ms. The decay rates were determined by a single exponential fit to the inactivating phase of the current over (300ms) a range of voltages from 0 to +60mV. To analyze the current voltage relations the Ipeak was measured at different voltages (-60 to +60 mV) and plotted vs membrane potential. Voltage dependence of inactivation was measured by using the two-pulse protocol, from a holding potential of −80 mV, different test potentials from −120 to +60 mV in 10 mV steps, were applied for 300 msec. The steady-state inactivation curves were fit with a Boltzmann function.

Pull-down and Immunoblotting: To identify the interaction between Kvβ1.1 and Kv4.2 in the heart, we conducted a pull-down assay using whole ventricular tissue lysate. Briefly, 5 µg of DDK-tagged Kvβ1.1 plasmid (Origene) was transiently expressed (48 to 72 hrs) in COS-7 cells that were grown to 90% confluence in a 10 cm plate. Total cellular protein was extracted from Kvβ1.1-DDK expressing Cos-7 and mice ventricles by homogenization using extraction buffer containing (in mM) 50 mM Tris, pH 7.4, 150 mM NaCl, 5 mM EDTA, 1% Nonidet P40 (NP40) (ThermoScientific, USA) supplemented with 10 mM DDT, 1:100 protease inhibitor (Sigma-Aldrich, St. Louis, MO) and 1:100 protease inhibitor (sigma). Tissue lysate was then centrifuged at 10,000x g for 10 minutes at 4°C, and the supernatant was collected. Protein quantification was performed using Pierce 660 assay (Thermo Fisher Scientific, Waltham, MA). Approximately 200 µg of DDK-tagged Kvβ1.1 Cos-7 lysate was incubated with Anti-DDK Agarose beads (Origene) for 3 hrs at 4°C, and 500 µg of pre-cleared ventricular tissue lysate was

then added, and incubated overnight at 4°C. Bound proteins were then eluted and immunoblot analysis was conducted using Kv4.2 antibody as explained before.

Electrocardiography: Mice were anesthetized with 2-3% isoflurane/oxygen anesthesia and lead–II electrocardiography (ECG) was recorded with Power lab (AD Instruments, UK) amplifier and data acquisition system, analysis was performed by using Labchart 7.2. The end of T wave is fixed at the point where the waveform returns to isoelectric line and ECG parameters including QTc were assessed as reported before (13, 129).

Monophasic action potentials: Monophasic action potentials (MAPs) were recorded from *ex vivo* heart preparations as reported before (13, 141). Mice were injected with 1 mg heparin (180 USP, sigma) and euthanized with Somnasol (50 mg/kg) by i.p. injection. Hearts were isolated through a bilateral thoracotomy and retrograde perfusion with Krebs-Hanseleit buffer (mM- NaCl 119, $NaHCO_3$ 25, KCl 4, KH_2PO4 1.2, $MgCl_2$ 1, $CaCl_2$ 1.8, D-glucose 10 and Sodium pyruvate 2, pH 7.4) was carried out at a constant flow rate of 2.0 ml/min, 37°C. Monophasic action potentials were recorded from left ventricular (LV) epicardial surface using contact electrode (Harvard Apparatus, MA). Hearts were stabilized for 10 minutes and MAP data were acquired using 8 channel PowerLab system (AD Instruments, UK).

Modulation of NADH alters monophasic action potential durations: MAPs were recorded from WT or KO mouse hearts to assess the activity in response to biochemical modulation of NADH (71). An increased NADH level in *ex vivo* heart tissue was accomplished by including 20 mM Sodium lactate in the Krebs-Hanseleit buffer. Baseline MAPs from LV

were acquired with normal buffer without lactate. Subsequently hearts were perfused for 20 min with a 20 mM lactate containing buffer and MAP's were acquired using 8 channel PowerLab system (AD Instruments, UK). Increase in NADH levels by perfusion for 20 min with high lactate vs. no lactate added buffer was confirmed in WT hearts. Further, NADH levels were also assessed and compared between the WT and KO mice after lactate buffer perfusion for 20 min.

Pyridine nucleotide assay: Whole hearts from saline or ISO exposed WT and KO mice in addition to WT and KO hearts exposed with lactate were freeze clamped and stored at -80°C until analysis. Heart tissue was pulverized under liquid N2 in a mortar and pestle, and pyridine nucleotide; NADH/NAD^+, ratio was assessed from 20 mg tissue of each sample by utilizing EnzyChrome NAD^+/NADH kit (Bioassays, Hayward, CA) according to the manufacturer's recommendations. Sample absorbance was measured at 560 nm using a 96-well plate reader (Biotek, VT, USA), and normalized to total protein level. Ratio of NADH/NAD^+ were computed for all groups.

Quantitative Real-Time-PCR (qRT-PCR): Total RNA was isolated from left ventricles of hearts using the Exiqon miRCURY RNA Isolation kit (Exiqon, Woburn, MA) according to the manufactures protocol. Complimentary DNA from total RNA was synthesized and quantitative real-time PCR (qRT-PCR) analysis was performed for potassium channel subunit genes Kvβ1.2, Kvβ1.3, Kvβ2, and KCHIP2; potassium channel genes Kv4.2, 1.4, 1.5, sodium channel Nav1.5; and calcium regulators SERCA2, Calcineurin, PI3K, and PLB (Phospholamban) . The cDNA synthesis and qRT-PCR procedures were performed as described previously (103, 141). The expression of mouse 18s was used as an internal control.

Western Blots: Protein extracts from left ventricle (LV) of knock out (KO) and wild type (WT) mice hearts were isolated and quantified as described previously (13, 103) for Western blot analysis. Proteins were detected with a dilution of primary antibody as follows: 1:200 (Kv1.5), 1:500 (Kvβ1.1) 1:1000 (Kv4.2), 1:10,000 (GAPDH). Primary antibodies Kv4.2 and GAPDH were obtained from Millipore (Darmstadt, Germany), Kv1.5 from Alomone (Jerusalem, Israel), Kvβ1.1 from Genetex (Irvine, CA, USA) and, Kvβ1.1 from Neuromab (Davis, CA, USA). Immunoblots were quantified using *Image J* software and mean (±SEM) values were plotted as bar diagrams.

Mouse model of cardiac hypertrophy: Age matched Kvβ1.1 KO and WT mice were infused with either saline or isoproterenol hydrochloride (ISO) (Sigma-Aldrich, MO, US) for 14 days at a dose of (30mg/kg/day) using osmotic mini-pumps (Alzet, Durect; model 2002) according to the previously published report (147). Mice were anesthetized with 2.5% isoflurane (Butler Schein, OH, US); pumps were placed subcutaneously and monitored for 14 days.

Statistical Analysis: Statistical analyses were performed with Sigma Plot (v.11.0). When comparing two groups, an independent Student's t-test was used. Data are expressed as mean ± SEM; and $p \leq 0.05$ were considered significant.

Results

Kv4.2 interaction with Kvβ1.1:

We utilized KO mice that lack the Kvβ1.1 subunit by the insertion of a PGKneobpA/neo cassette in the first exon, which is responsible for coding Kvβ1.1 splice isoform (32) (**Figure 11A**). As shown in **Figure 11B**, Western blot confirmed the expression of Kvβ1.1 protein in the wild type mouse heart, however the Kvβ1.1 KO mouse showed the absence of Kvβ1.1 expression. COS-7 cells transfected with Kvβ1.1 tagged with DDK were utilized for pull-down assays. The Kvβ1.1-DDK was incubated with cardiac homogenate and DDK-coated agarose beads overnight, precipitates were resolved using gel electrophoresis and immunoblotted with Kv4.2 antibody. As shown in **Figure 11C**, Kvβ1.1 pulls-down Kv4.2 from mouse heart lysates demonstrating protein-protein interaction and binding. To confirm that DDK beads successfully bind to Kvβ1.1 with specificity, COS-7 lysates overexpressing Kvβ1.1-DDK plasmid were pulled down with DDK-coated agarose beads alone, and immunoblotted with anti-DDK antibody, which demonstrates Kvβ1.1-DDK expression as well as no significant band in COS-7 alone (**Figure 11D**).

Kvβ1.1 KO hearts demonstrate similar physical dimensions:

Whole heart sections of both WT and KO mice demonstrate comparable morphometric measurements including the right ventricle (RV), left ventricle (LV) and septum (SEP) (**Figure 12A**). Overall, area measurements from the cross-sections demonstrate no significant difference (**Figure 12B**). Heart weights normalized to tibia length also demonstrated similar weights in both WT and KO mice (**Figure 12C**).

Kv4.2 inactivation decay (tau) in the presence of Kvβ1.1 and lactate:

We utilized COS-7 cells transfected with mKv4.2 with and without mKvβ1.1-GFP and perfused with 10 mM lactate solution to increase the intracellular NADH levels. Kv4.2 alone with and without lactate demonstrated no significant differences in overall current kinetics (**Figure 13A and 13C**) as well as in time constants (**Figure 13E**) at voltages -20 to +60 mV. At baseline with no lactate exposure, Kv4.2+Kvβ1.1 demonstrated no significant current kinetics compared with Kv4.2 currents (**Figure 13A and 13B**). However, only in the presence of Kvβ1.1, the addition of lactate resulted in a significant decrease in inactivation time constants at voltages of -20 to +60mV (**Figure 13D and 13F**). However, inactivation time constants were not significantly different between Kv4.2 alone and Kv4.2+Kvβ1.1 groups, with or with lactate addition.

Current voltage relationship of Kv4.2 in the presence of Kvβ1.1 and modulation by lactate:

Analysis of current voltage (I-V) relationship of Kv4.2 exhibits an increase in current with channel activation at -20 mV, both before and after lactate exposure. The I-V curves were similar in Kv4.2+Kvβ1.1 group, and addition of lactate caused no additional differences (**Figure 14A and 14B**). For the steady state inactivation measurements recorded by using the two-pulse protocol (**Figure 14**) the I-V curves showed a steep decrease in the inactivation profile in both Kv4.2 alone and +lactate with a small non-significant hyperpolarization shift ($p>0.05$ at -40mV). The $V_{1/2}$ of inactivation demonstrated that there was no significant difference between Kv4.2 alone and with the addition of lactate (-50.2 ± 3.1 mV and -52.3 ± 1.8 mV, $p = 0.442$). While

Kv4.2 + Kvβ1.1 demonstrated a significant hyperpolarizing shift with addition of lactate, a $V_{1/2}$ of inactivation (-48.3 ± 1.1 mV and -58.6 ± 0. 9 mV, p = 0.01) (**Figure 14D**). Kv4.2 alone and Kv4.2 + Kvβ1.1 demonstrated no significant hyper polarizing shift. These data suggest that the addition of lactate causes an increase in the Kvβ1.1 mediated hyperpolarization shift in Kv4.2 currents.

Isolated cardiomyocyte action potentials:

Left ventricular apex adult cardiomyocytes were isolated from the hearts of 16-20 weeks WT and KO mice and subjected to current-clamp recordings. Baseline action potential's were recorded after which external buffer was switched to a buffer containing lactate (10mM) and allowed to perfuse for 10 minutes. WT cardiomyocytes demonstrated significant increases in the action potential durations at APD 20 and 50% ($p<0.05$) repolarization along with an increase at APD 70 ($p<0.1$) after exposure with 10 mM lactate (**Figure 15C-E**). However, KO myocytes demonstrated no significant difference in APD durations (APD20-70) after lactate exposure compared with no lactate (**Figure 15C-E**). Action potential durations between WT and KO myocytes at baseline or (-) lactate demonstrated a significant increase in KO at APD 20, however while increased at APD 50 an 70 they were not significantly different from WT. These data suggest that by increasing the intracellular NADH levels by lactate perfusion, the action potential duration is significantly prolonged. However in the Kvβ1.1 KO cardiomyocyte the increase in NADH by lactate fails to prolong the APD suggesting a significant role for Kvβ1.1 in cardiac action potential regulation under high intracellular NADH levels.

Changes in monophasic action potential (MAP) in lactate perfused hearts:

Ex vivo MAP traces were recorded from WT and KO hearts before and after lactate perfusion with a modified Kreb's-Hanseleit buffer consisting of 1mM pyruvate and 20 mM lactate (**Figure 16A and Figure 16B**). MAP waveforms show typical triangular peaks with a rapid depolarization upstroke followed by a downward spike representing repolarization activity. Analysis of MAP durations (ms) at APD 20, 50, and 70% repolarization demonstrated significant prolongation in the WT hearts after 10 minutes of lactate perfusion (**Figure 16C-E**). No significant prolongation was noted in KO hearts after 10 minutes of lactate exposure (**Figure 16C-E**). KO mouse hearts showed APD prolongation at baseline as compared to WT hearts (**Figure 16C-E**). The addition of lactate to the ex vivo WT and KO hearts demonstrated significant increases in NADH (µM/µg) after lactate exposure (**Figure 16F**). To determine that lactate alterations are caused by the increase in NADH and not as a result of non-specific effects, we utilized pyruvate in the buffer and perfused WT hearts as a rescue strategy. After 10 minutes of pyruvate perfusion, the APDs returned to levels similar to baseline (**Figure 16G**). Heart rate of WT and KO hearts at baseline or (-) lactate recordings demonstrated no significant difference indicating that changes observed to AP's were not due to heart rate variation (**Figure 16H**). These results indicate that lactate perfusion leads to cardiac NADH increase and prolongation in action potential duration in wild type mouse hearts, but not KO hearts. Hence, it is plausible that the repolarization phase can be altered by modulation of NADH levels and that the Kvβ1.1 subunit is a key sensory component to relay the NADH alterations.

Changes in monophasic action potentials in ISO-infused hearts:

Chronic ISO-infusion causes cardiac hypertrophy. We recorded MAPs from saline or ISO infused WT and KO mice hearts (**Figure 17A and 17B**). Analysis of MAP traces demonstrates that chronic ISO exposure of WT mice prolongs cardiac APDs. As shown in **Figure 17C-E**, ISO treatment of WT mice led to a significant prolongation of APD20, 50, and 70, when compared with that of saline (**Figure 17C-E**). Contrarily, no significant differences were observed in the APDs of saline vs. ISO exposed KO mice at APD20, 50, and 70 (**Figure 17C-E**). Previous reports suggest that remodeling associated with cardiac hypertrophy also results in a significant shift in NADH/NAD^+ levels. Hence, we reasoned that elevated NADH may reduce NADH/NAD^+ ratio, and contribute to the APD prolongation seen in WT mouse hearts. Indeed Infusion of ISO resulted to a significant increase in cardiac NADH/NAD^+ ratios in both WT and KO mice (**Figure 17F**). These results suggest that NADH elevation can lead to APD prolongation, and that Kvβ1.1 subunit is essential to electrical signaling.

ECG activity in ISO-infused Kvβ1.1 KO hearts:

To evaluate the electrical activity in the mice, we utilized lead II ECG recordings. The WT and KO mice were exposed to either saline or ISO and ECG recordings were obtained on day 14 (**Figure 18A**). The PR interval along with the P duration demonstrates a significant decrease in KO saline (baseline) compared with WT controls. P-duration in both WT-ISO and KO-ISO were significantly increased from their respective controls (**Figure 18E**).

WT-ISO mice demonstrated significantly increased QTc and JT intervals compared with the saline group, suggesting a decreased repolarization reserve after ISO infusion (**Figure 18F and 18G**). The QTc and JT interval in the KO-Saline and KO-ISO mice remain unchanged indicating

that electrical activity was unaltered with isoproterenol infusion (**Figure 18F and 18G**). The mice showed a significant QTc and JT interval prolongation at baseline between WT and KO mice (**Figure 18F and 18G**). QRS intervals remained unaltered in all groups (**Figure 18H**) ECG data clearly validate the notion that isoproterenol induced QT prolongation is attenuated in the KO compared with WT.

Cardiac ion channel expression:

To gain insights into the transcriptional status of key Kv channels in Kvβ1.1 KO hearts, qRT-PCR assay was used to assess the expression of Kv channel subunit genes including Kvβ1.2, Kvβ1.3, Kvβ2 and, KChIP2, which showed no significant differences between WT and KO hearts (**Figure 19A**). Also, key ion channels known to interact with Kvβ1.1 including Kv4.2, Kv1.4, Kv1.5 as well as ion channels affected by pyridine nucleotides; Nav1.5, were also assayed, which revealed no significant differences between WT and KO hearts (**Figure 19B**) (71). Furthermore, expression of key mediators of calcium signaling including SERCA2, Calcineurin, PI3K, and, Phospholamban (PLB) was found to be comparable in the WT and KO hearts (Fig. 10C). These results suggest that the electrical changes observed are therefore likely caused by kinetic alterations as opposed to gene expression changes. Whole hearts were homogenized and membrane extracts separated for Western blot analysis of Kv4.2 and Kv1.5 expression revealing no significant difference between WT and KO membrane fractions (**Figure 19D and 19E**).

Discussion

In the present study, we identified that Kvβ1.1 is a major physiological regulator in the heart. Modulation of pyridine nucleotides is sensed by the Kvβ1.1 subunit and helps relay the

biochemical information for regulating the electrical activity. We identified that the cellular action potential is modified with the addition of lactate and regulated by the presence of Kvβ1.1. The basal tonic regulation of action potential is tightly coupled to the ion channel function via Kv4.2, through which the action potential is significantly regulated. Identification of increased intracellular NADH levels via perfusion of lactate was utilized as a model to probe its effects on action potential and Kv current changes (71). In presence of Kvβ1.1 subunit, using the WT cardiomyocytes, we identified that the action potential is prolonged upon NADH increase, and lack of Kvβ1.1 subunit significantly diminished the modulatory role of NADH on the action potential. These experiments for the first time clearly demonstrate that Kvβ1.1 is necessary for regulation of basal action potential duration as well as imparts the ability to sense the changes in the pyridine nucleotides in the cardiomyocytes in a precise fashion.

Previous studies identified that Kvβ subunit belongs to the aldoketo reductase superfamily. The Kvβ1 belongs to the AKR6 family and depict very tight binding to NADH/NAD^+. Crystal structure analysis revealed that $NADP^+$ is very tightly bound to the Kvβ subunit and co-crystallizes with the Kvβ protein (40). Affinity studies performed to identify the dissociation constant (Kd) showed that that the affinity is in the micro molar range (72, 138). Therefore, the fundamental information for the binding characteristics and ion channel modulation were previously published, however, the physiological roles of Kvβ subunits remain unknown. In the present study we connect the biochemical basis and the ion channel physiology to cardiac electrical activity. Based on the biochemical changes caused by modulation of NADH/NAD^+, the Kv current is regulated by Kvβ1.1 subunit in a subtle but significant manner and that these connections ultimately lead to action potential and ECG changes in the mice heart.

While cardiac action potential is an ensemble of many ionic currents (K, Na, Ca) and its activity during depolarization and repolarization depend on many ion channels (38). The role of Kvβ1.1 seems to be tightly coupled to Kv current modulation affecting the repolarization in the presence of NADH/NAD^+. Previously, we identified that Kv current is modulated by Kvβ subunits in the presence of oxidized (NAD^+/$NADP^+$) and reduced pyridine nucleotides (NADH/NADPH) (137-139). Under reducing (NADH) conditions, the Kv current inactivation was supported while the addition of oxidized pyridine nucleotides (NAD^+) provided Kv current activation. These studies form the experimental basis for testing the physiological roles of Kvβ1.1 in the heart. Using heterologous COS-7 expression system, we co-expressed Kv4.2 along with the Kvβ1.1 subunit to identify the influence of NADH via lactate perfusion. As noted previously with Kv1.5+Kvβ1 pairing, we found that Kvβ1.1 produces a faster inactivation tau with Kv4.2 in the presence of NADH. Further, we demonstrated that steady-state inactivation of Kv4.2 was significantly shifted to a more hyperpolarized state by Kvβ1.1in the presence of elevated NADH.

The *ex vivo* MAPs show that action potentials were significantly prolonged in wild type hearts upon addition of lactate, whereas the action potential prolongation was completely reversed with the addition of pyruvate, which is a known energy substrate that can restore the intracellular levels of NAD^+, clearly identifying the role of NADH/NAD in cardiac electrical activity. Moreover, the lack of Kvβ1.1 subunit failed to impart the ability of heart to respond to NADH/NAD changes, pointing to the importance of the Kvβ1.1 subunit in cardiac physiology both at the cellular and tissue level. We next asked the physiological significance of Kvβ1.1 in cardiac physiology in regard to ECG changes and if Kvβ1.1 has a physiological role in terms of modulating ECG. To test this, we utilized the Kvβ1.1 knockout mice and recorded ECG from wild type and KO mice and identified that lack of Kvβ1.1 subunit leads to prolonged QTc and JT

interval in 16 - 20 week old mice. The QTc is a standard measure of cardiac ventricular depolarization and repolarization activity, providing the ability to delineate the contribution of Kvβ1.1 to ECG changes (113). Further the KO mice demonstrated a significant decrease in P-duration and PR interval compared with WT mice. P-duration and PR interval changes have demonstrated pro-arrhythmic phenotypes (68). While the significant decrease in PR duration in KO has yet to be defined, quantitative trait loci mapping demonstrated that chromosome 3 influences the variance of the PR interval, interestingly Kvβ1.1 (KCNAB1) is found on chromosome 3 (126). A significant increase in P duration in WT and KO after ISO exposure has been previous demonstrated in hypertrophic models (120, 132). These data demonstrate a significant physiological role for Kvβ1.1 subunit in the heart in which coupling of Kvβ1.1 subunit to the Kv channel can significantly alter the cardiac action potential and ECG parameters. We further investigated the role of Kvβ1.1 subunit in the physiological changes in cardiac NADH/NAD levels. For this we utilized the well-established cardiac hypertrophy model by infusing isoproterenol for 14 days in wild type or KO mice. Hypertrophy and injury caused by ISO infusion has been shown to cause prolongation of QTc (135), and monophasic action potentials (MAP) (33) as well as a significant decrease in Kv4.2 and 4.3 current (100). While hypertrophy can result in significant cardiac alterations including the increase in PKA which regulates many regulatory proteins in cardiac contraction-relaxation cycle such as ryanodine receptor 2, and L-type Ca channels it is important to note that QRS interval was not altered after ISO exposure in either WT or KO mice (142). In addition, numerous hypertrophic research has demonstrated that L-type calcium currents remained unchanged (56). Furthermore, preliminary evidence demonstrates that reduced Ito density represents a very early event in response to

decreased pump performance (76, 150). Therefore, decreased Ito appears to be a significant contributor to action potential prolongation in cardiac hypertrophy (150).

Isoproterenol perfusion caused a significant increase in cardiac NADH/NAD ratio levels leading to prolonged QTc intervals in the wild type mice; however the KO mice lacking the Kvβ1.1 subunit failed to respond to the NADH/NAD ratio increase caused by cardiac hypertrophy. The cardiac lead II ECG signal allows monitoring the left ventricular activity in a precise manner. The QTc is a standard measure of cardiac ventricular depolarization and repolarization activity, providing the ability to delineate the contribution of Kvβ1.1 to ECG changes in the presence of NADH (113). Since the KO mice failed to demonstrate further prolongation in the QTc with ISO treatment, it is likely that the NADH generated due to hypertrophic response is not sensed and hence NADH induced QTc prolongation was abolished in the KO mice. Therefore, based on cellular model using Kv4.2+Kvβ1.1 expression system, cardiomyocyte action potential, and tissue *ex vivo* action potentials, we identified and established the physiological responses of heart in the presence and absence of Kvβ1.1 subunit for its ability to sense change in NADH/NAD levels. Overall, these changes point to the idea that because Kvβ1.1 is an obligatory mediator for sensing NADH/NAD changes in the heart, it is likely that ECG changes caused by cardiac hypertrophy are due to high NADH levels and presence of Kvβ1.1 allows the heart to sense the pyridine nucleotide changes.

Heterologous expression studies using xenopus oocytes or mammalian expression system established that Kvβ1 could bind to multiple Kv channel partners (60, 112, 127). Rat heart studies identified that Kvβ1.1 binds Kv1.5, while other studies showed that Kvβ1.1 binds to Kv4 channel (108, 156). Co-immunoprecipitation in mouse heart revealed that Kvβ1.1 binds with Kv4.2 and is likely a preferential binding partner in the mouse heart (2). By using the pull down

approach in the present study, we identify the binding of Kvβ1.1 with Kv4.2, which is in agreement with previous report (2). Triggered arrhythmia is a significant feature in determining the role of specific ion channels or its regulatory subunits. To identify the arrhythmogenic potential of Kvβ1.1 we utilized WT or KO hearts and subjected to S1S2 protocol and identified that 2 out of 5 hearts show sustained arrhythmia in KO mice pointing towards the contribution of Kvβ1.1 and its role in regulating action potential basis. Therefore based on the triggered arrhythmogenic basis the lack of Kvβ1.1 leads to increased arrhythmia susceptibility implicating a physiological role for Kvβ1.1 in the heart. Overall, these studies provide a strong basis that Kvβ1.1 can bind to Kv4.2 and other Kv channels, and therefore likely contributes to the cardiac electrical activity in a physiologically significantly manner.

Conclusions

Overall in the present study we demonstrate that Kvβ1.1 subunit offers sensing of changes in NADH/NAD in the heart. The modulation of Kv4.2 currents in the presence and absence of Kvβ1.1 under increased NADH levels points towards the ability of Kvβ1.1 subunit to mediate inactivation of Kv4.2 currents. The changes in action potential duration and contribution of Kvβ1.1 in cardiomyocyte and *ex vivo* hearts identify the specific roles of Kvβ1.1 mediation in sensing NADH changes under both cellular and ex vivo settings. In addition, the in vivo changes at ECG level using the cardiac hypertrophy model causing increased intracellular NADH levels clearly shows that the electrical activity and changes to NADH increase are mediated by Kvβ1.1 subunit since the KO mice failed to respond to hypertrophic stimulation. Taken together, the physiological changes and the biochemical basis provide novel mechanistic insights with distinct Kvβ subunit mediated responses in cardiovascular physiology.

Tables and Figures

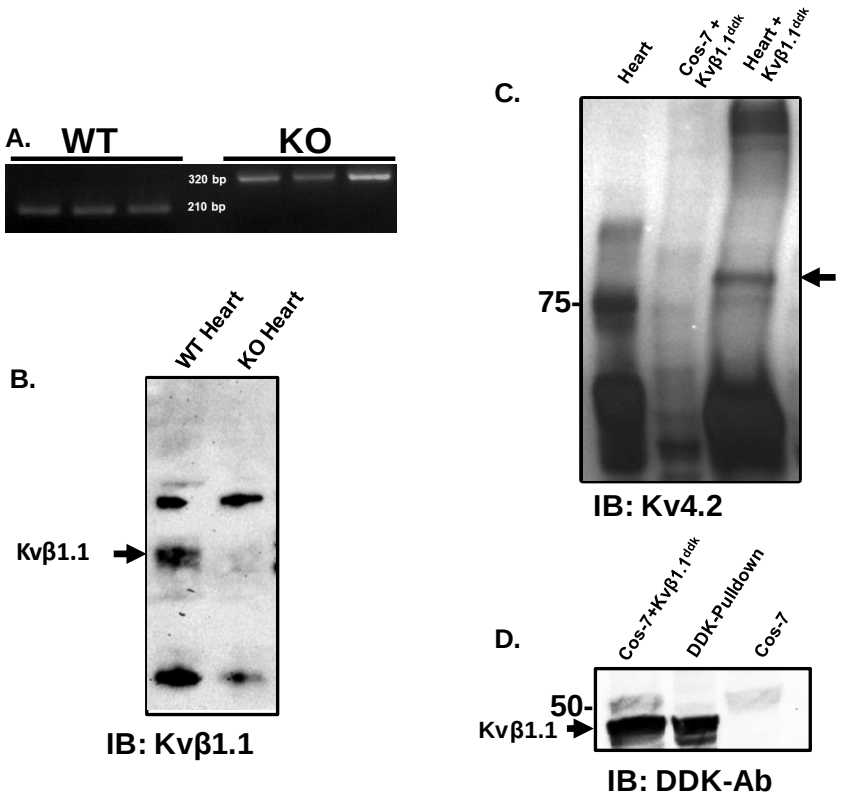

Figure 11: Kvβ1.1 and Kv4.2 interaction A. Genotype of WT and KO mice. PCR product separated by gel electrophoresis for identifying wild type (WT) at 210 bp and knockout (KO) at 320 bp. **B.** WT and KO heart homogenates. Primary antibody was Kvβ1.1 (1:200). **C.** WT heart homogenate (first lane), COS-7 cells transiently transfected with Kvβ1.1-DDK (second lane), were combined and incubated with DDK coated agarose beads overnight (third lane). Primary antibody was Kv4.2 (1:500). **D.** COS-7 cells transfected with Kvβ1.1-DDK (first lane) and incubated overnight with DDK coated agarose beads (second lane) while untransfected COS-7 cells showing no DDK band (third lane). Primary antibody was DDK (1:200).

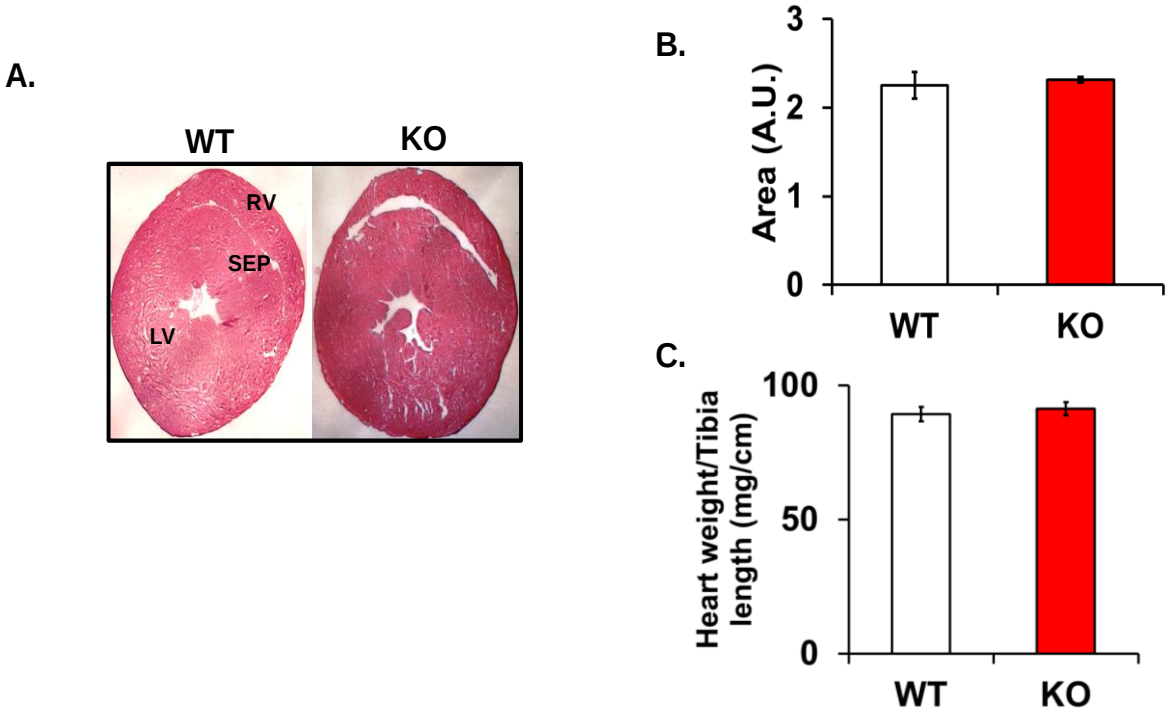

Figure 12: Physical parameters of the Kvβ1.1 knockout heart A. Twenty five micron (µm) cross-sections of heart stained with H&E for identifying the differences in shape and size, regions labeled as LV (left ventricle), RV (right ventricle), and, SEP (septum). **B**. Total H&E cross-sectional area (arbitrary units, A.U) of the heart quantified and compared between WT and KO mice. The data represented are mean ± SEM (n=3 hearts). **C.** Normalized heart weights by tibia length of both wild type (WT) and knockout (KO) mice. The data represented are mean ± SEM (n=10 mice).

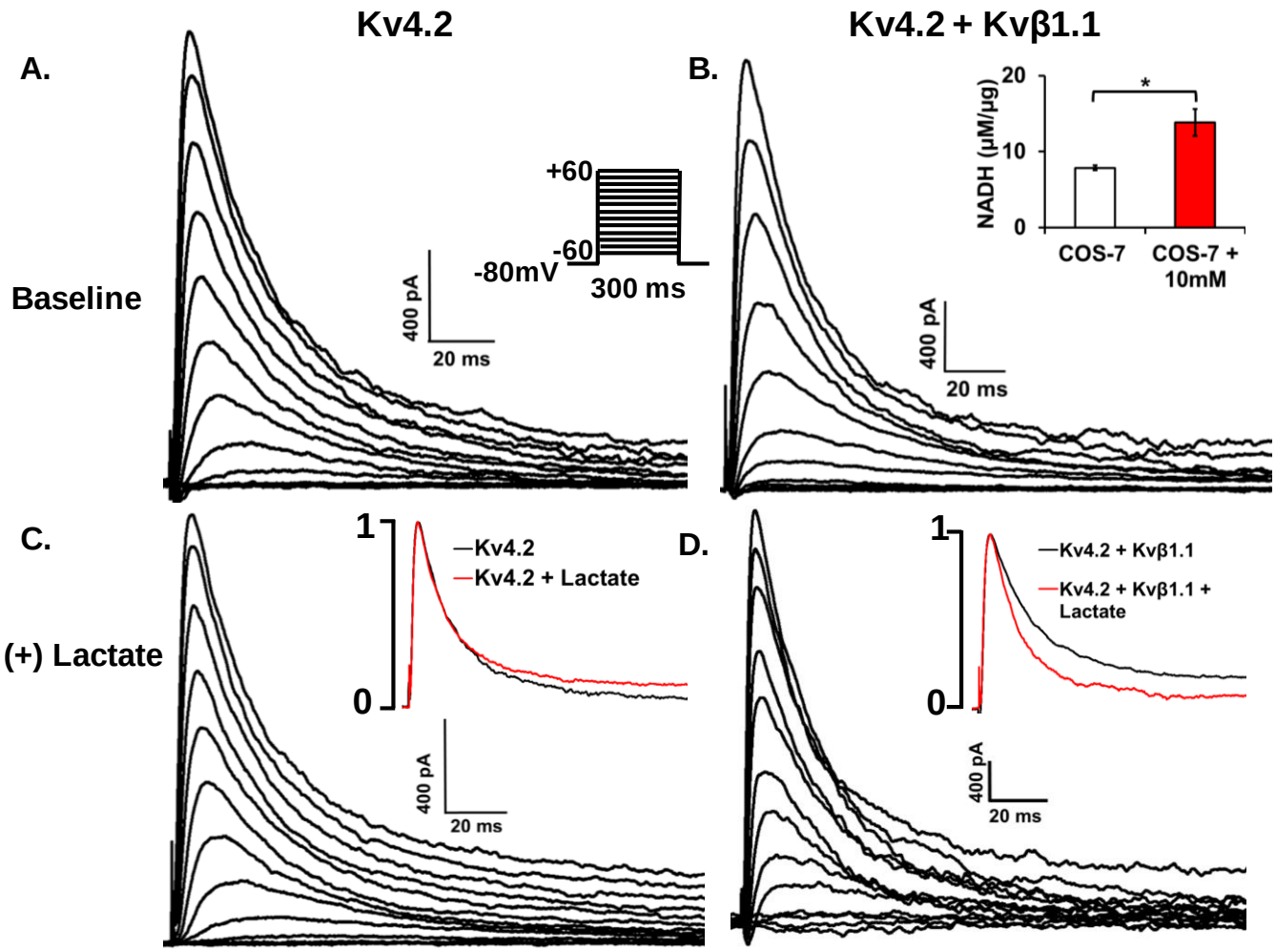

Figure 13: COS-7 cells transfected with Kv4.2 demonstrate redox (NADH/NAD) dependent alterations in the presence of Kvβ1.1 A. Current traces from representative COS-7 cells transfected with Kv4.2 alone. **B.** Kv4.2 with Kvβ1.1. Inset of NADH (µM/µg) levels with 10mM lactate exposure. The data represented are mean ± SEM (n=3 hearts) * represents $p<0.05$ **C.** Kv4.2 alone with lactate (10mM) exposure. **D.** Kv4.2 and Kvβ1.1 with lactate (10 mM) exposure; the voltage template is shown in Kv4.2 baseline. Overlay Inset currents of baseline (black) and lactate (red) are shown at +40mV.

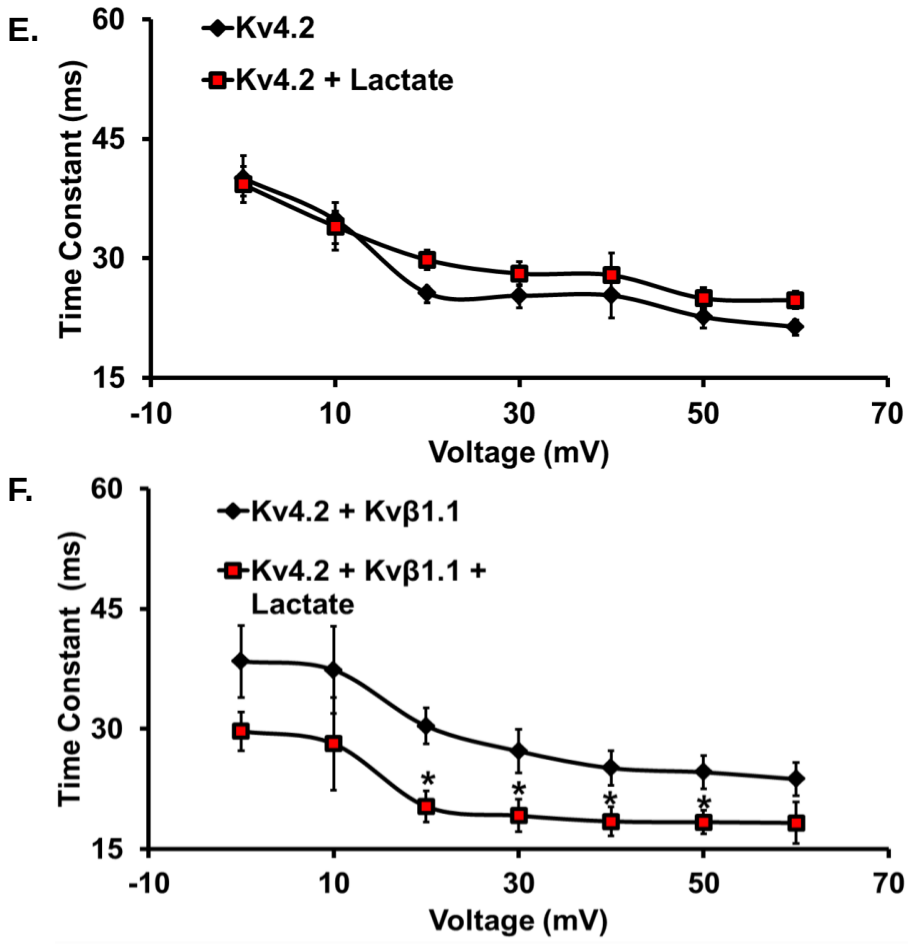

E. The time constant of decay demonstrates no significant difference between Kv4.2 with and without lactate exposure. The data represented are mean ± SEM (n=10 cells in each group). **F.** Time constant (tau) of decay demonstrates significant decrease in Kv4.2 with Kvβ1.1 in the presence of lactate exposure. The data represented are mean ± SEM (n=10 cells in each group) * represents $p \leq 0.05$

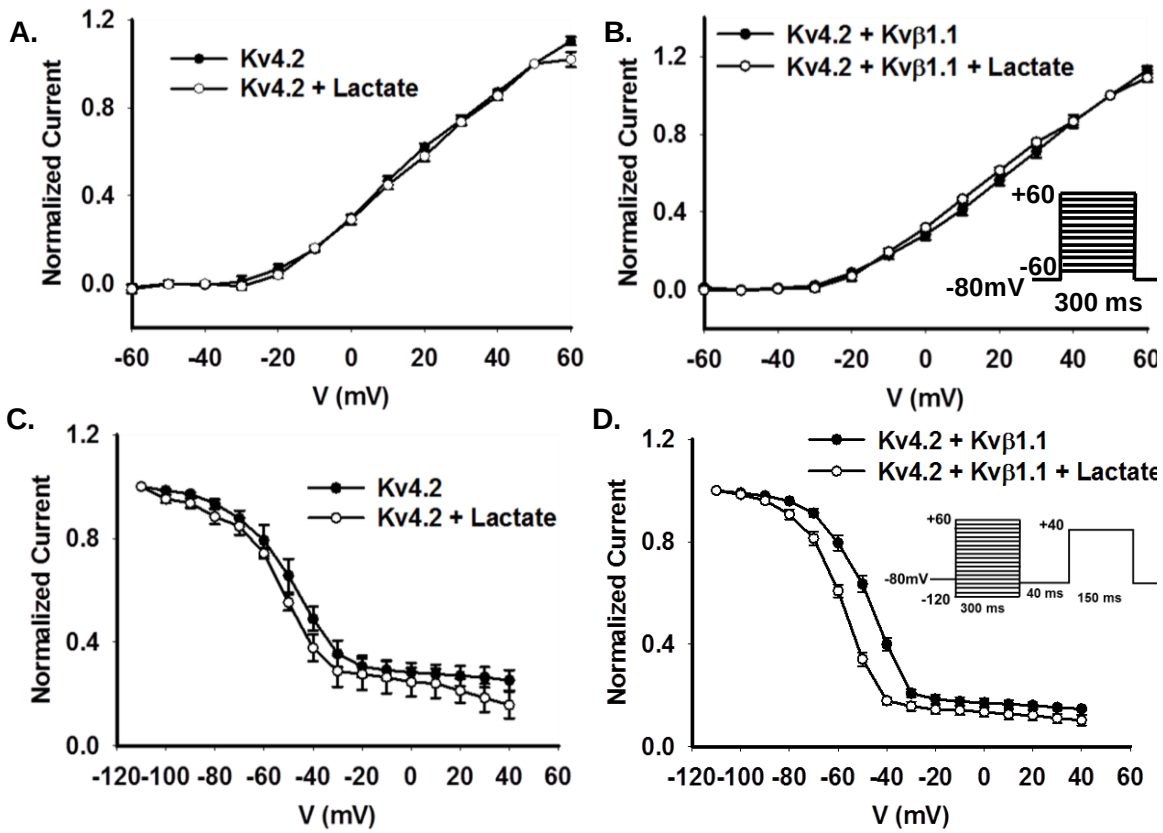

Figure 14: COS-7 cells transfected with Kv4.2 demonstrate alterations in inactivation in the presence of Kvβ1.1 and lactate A. Normalized current curve for Kv4.2 with and without lactate demonstrate no significant difference in activation. The data represented are mean ± SEM (n=10 cells in each group). **B.** Normalized current curve for Kv4.2+Kvβ1.1 with and without lactate demonstrate no significant difference in activation. The voltage dependence of activation was determined by normalizing outward currents at indicated voltages to +50 mV. The data represented are mean ± SEM (n=10 cells in each group). The voltage template is shown in Kv4.2 and Kvβ1.1 baseline. **C.** Normalized current curve for Kv4.2 with and without lactate demonstrate no significant difference in the steady-state inactivation curve. The data represented are mean ± SEM (n=10 cells in each group). **D.** Normalized current curve for Kv4.2+Kvβ1.1 with and without lactate demonstrate a significant hyperpolarizing shift in the presence of lactate. The voltage dependence of inactivation was determined by normalizing outward currents at indicated voltages to -110 mV. The data represented are mean ± SEM (n=10 cells in each group). The voltage template is shown in Kv4.2 and Kvβ1.1 lactate.

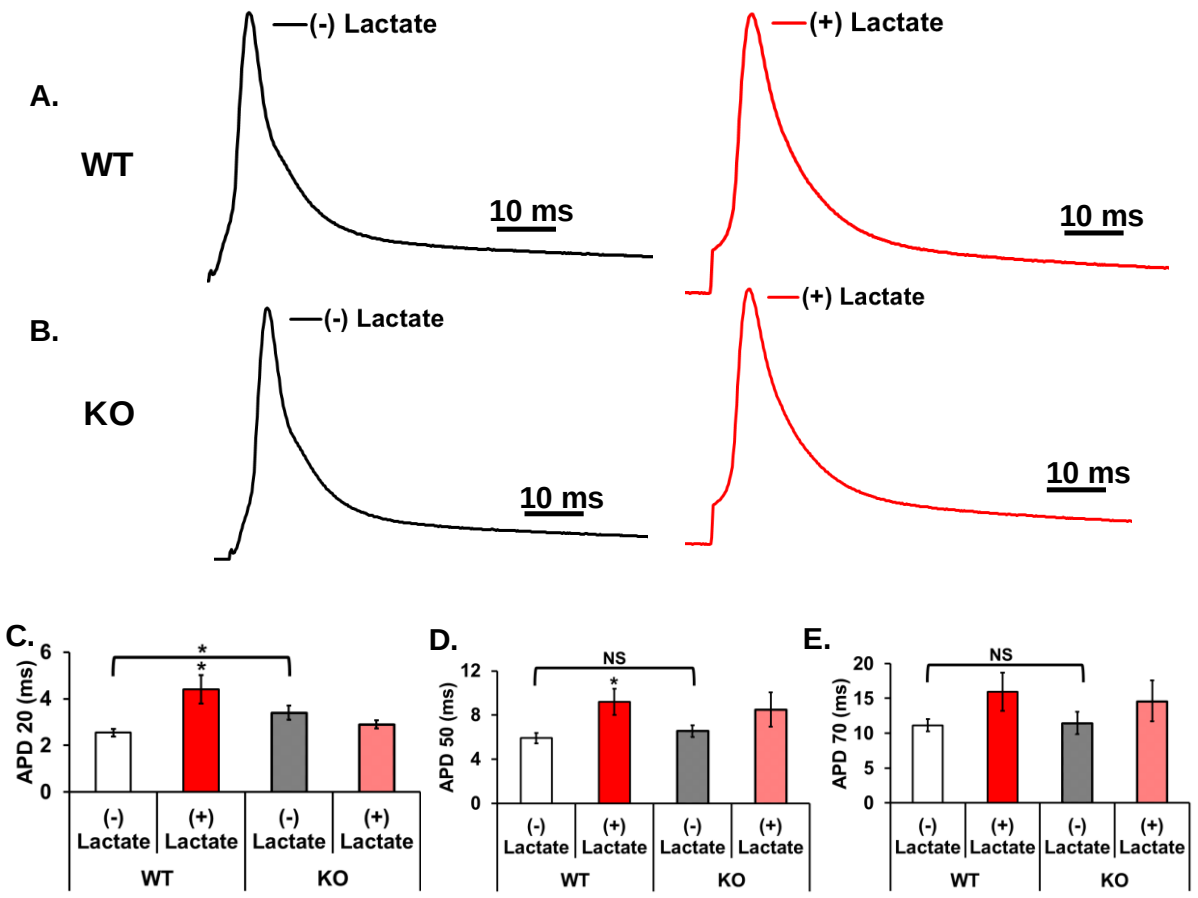

Figure 15: Isolated cardiomyocyte Action Potentials (AP). A. Representative AP traces from a single cell isolated from a WT mouse heart recorded in the absence (Baseline, black line) and presence of 10 mM lactate (Lactate, red line) in the external solution. **B.** Representative action potentials from a single cell isolated from a KO mouse heart recorded in the absence (Baseline, black line) and presence of 10 mM lactate (Lactate, red line) in the external solution. Action potentials were evoked from the cells under current-clamp mode by applying 2 msec current pulses delivered at 1 Hz. Representative AP traces have been edited to remove the stimulation artifact. **C.** Action potential durations (APDs) at 20% (APD 20) repolarization (-) lactate (white bar) and (+) lactate exposure (red bar) in WT mice and (-) lactate (grey bar) and (+) lactate (pink bar) in KO mice. **D.** Action potential durations (APDs) at 50% (APD 50) repolarization (-) lactate (white bar) and (+) lactate exposure (red bar) in WT mice and (-) lactate (grey bar) and (+) lactate (pink bar) in KO mice. **E.** Action potential durations (APDs) at 70% (APD 70) repolarization (-) lactate (white bar) and (+) lactate exposure (red bar) in WT mice and (-) lactate (grey bar) and (+) lactate (pink bar) in KO mice. The data represented are mean± SEM (n=7-9 cells in each group). Scale bars = 10 ms, *represents $p \leq 0.05$.

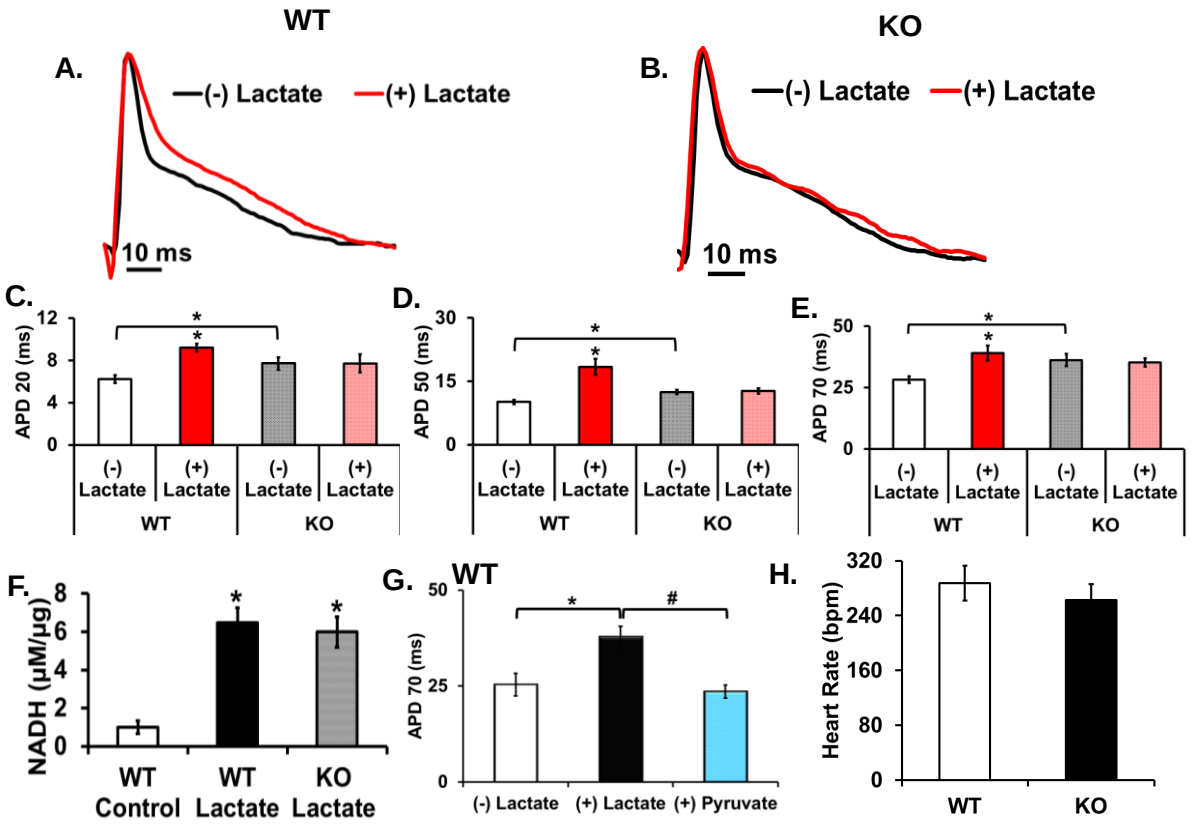

Figure 16: Pyridine nucleotide modulation alters Monophasic Action Potentials (MAPs) A. Representative monophasic action potential trace from a WT mouse heart recorded in the absence ((-) Lactate, black line) and presence of 20 mM lactate ((+) Lactate, red line) in the external solution. **B.** Representative MAP trace from a KO mouse heart recorded in the absence ((-) Lactate, black line) and presence of 20 mM lactate ((+) Lactate, red line) in the external solution. **C.** LV surface MAP durations at 20% (APD 20) in WT (+) lactate demonstrated a significant increase in duration, while KO group MAPs were indistinguishable. **D.** LV surface MAPs at 50% (APD 50) in WT (+) lactate demonstrated a significant increase in duration, while KO group action potentials were indistinguishable. **E.** LV surface MAPS at 70% (APD 70) in WT (+) lactate demonstrated a significant increase in duration, while KO group MAPs were indistinguishable. The data represented are mean ± SEM (n=7-10), * represents $p \leq 0.05$ (-) lactate vs. (+) lactate and WT (-) lactate vs. KO (-) lactate. **F.** Relative NADH levels were examined in hearts after lactate-perfusion from WT or KO when compared with WT hearts perfused with no lactate (Control), n=4, *$p \leq 0.05$, compared with control. Bar represents 10 ms scale. **G.** LV surface action potentials at APD 70 in WT (-) lactate, (+) lactate, (+) pyruvate demonstrated a significant increase in duration (lactate) and then a significant reduction in duration (pyruvate). The data represented are mean ± SEM (n=6), * represents $p \leq 0.05$ lactate vs. baseline, # represents $p \leq 0.05$ lactate vs. pyruvate. **H.** Heart rate from LV surface action potentials, data represented are mean ± SEM (n=7-10).

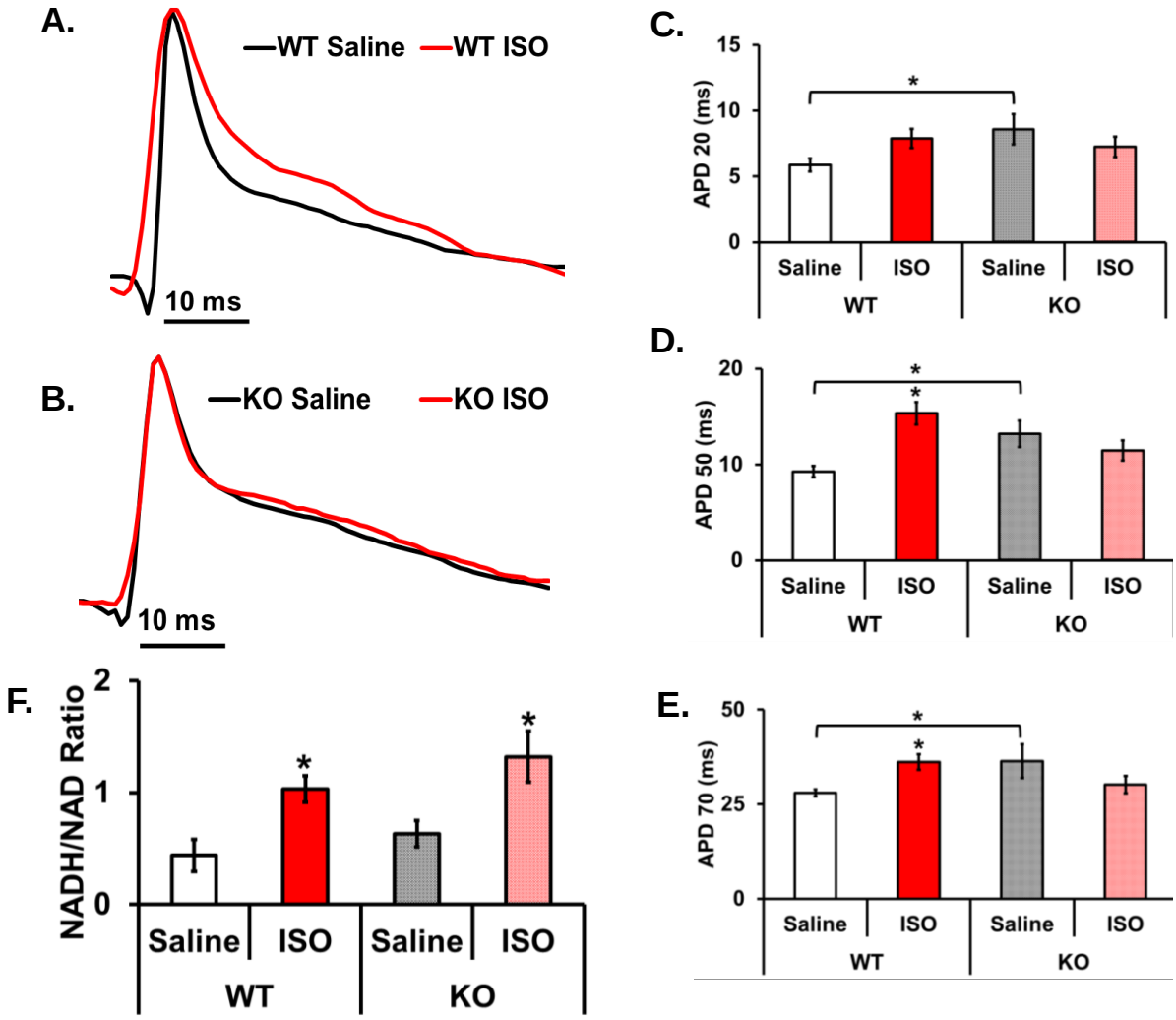

Figure 17: Monophasic Action Potential (MAPs) changes in isoproterenol treated mouse hearts: **A.** Representative MAP traces from a WT mouse heart infused (osmotic mini pumps) with saline (black line) and Isoproterenol (red line). **B.** Representative MAP traces from a KO mouse heart infused (osmotic mini pumps) with saline (black line) and Isoproterenol (red line). **C.** LV surface MAPs at 20% repolarization (APD 20) in WT ISO demonstrated a significant increase in duration, while KO-ISO MAPs were indistinguishable from KO-Saline. **D.** LV surface MAP at 50% repolarization (APD 50) in WT ISO demonstrated a significant increase in duration, while KO-ISO MAPS were indistinguishable from KO-Saline. **E.** LV surface MAPs at 70% repolarization (APD 70) in WT ISO demonstrated a significant increase in duration, while KO-ISO action potentials were indistinguishable from KO-Saline. The data represented are mean ± SEM (n=7), * represents $p \leq 0.05$ ISO vs. saline. **F.** NADH/NAD ratio of WT and KO hearts from saline or ISO. Both WT and KO-ISO hearts showed a significant increase in NADH/NAD ratios. Bars represent mean ± SEM (n=4), *$p \leq 0.05$ ISO vs. saline and WT saline vs. KO saline.

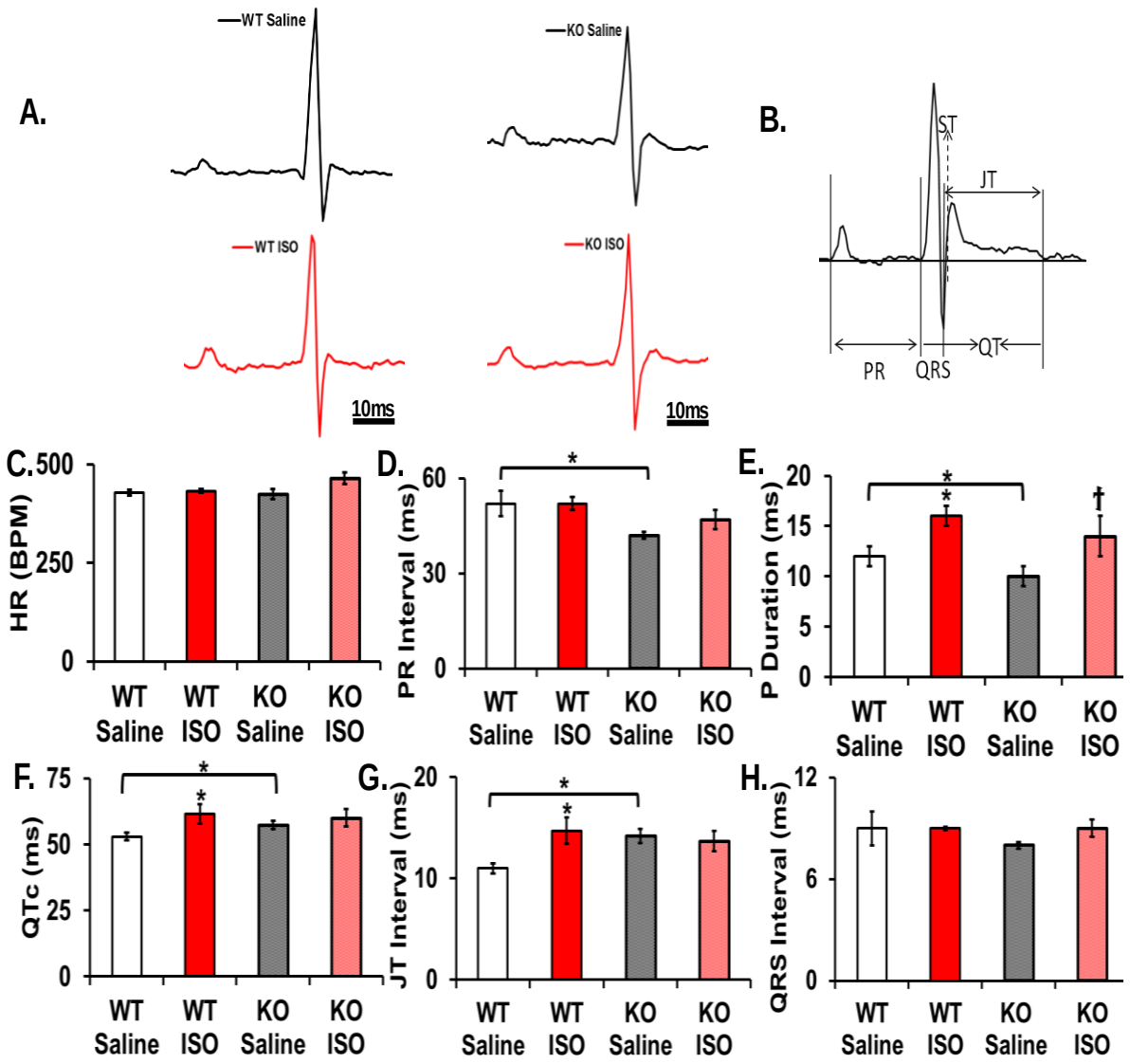

Figure 18: ECG Parameters. A. Representative lead II ECG traces from anesthetized mice after saline or ISO infusion of WT (Saline (black line) and ISO (red line)) and KO (Saline (black line) and ISO (red line)) scale bar represents 10ms. **B.** A representative mouse ECG diagram on different ECG parameters measured. **C.** Heart rates in WT and KO groups, the data represented are mean ± SEM (n=10-12). **D.** PR interval durations in WT and KO groups. The data represented are mean ± SEM (n=10-12), *p<0.05 WT saline vs. KO saline. **E.** P durations in WT and KO groups. The data represented are mean ± SEM (n=10-12), *p<0.05 ISO vs. saline as well as KO vs. WT saline's. **F.** QTc interval durations in WT and KO groups. The data represented are mean ± SEM (n=10-12), *p<0.05 ISO vs. saline as well as KO vs. WT saline's. **G.** JT interval durations in WT and KO groups. The data represented are mean ± SEM (n=10-12), *p<0.05 ISO vs. saline as well as KO vs. WT saline's. **H.** QRS interval durations in WT and KO groups. The data represented are mean ± SEM (n=10-12).

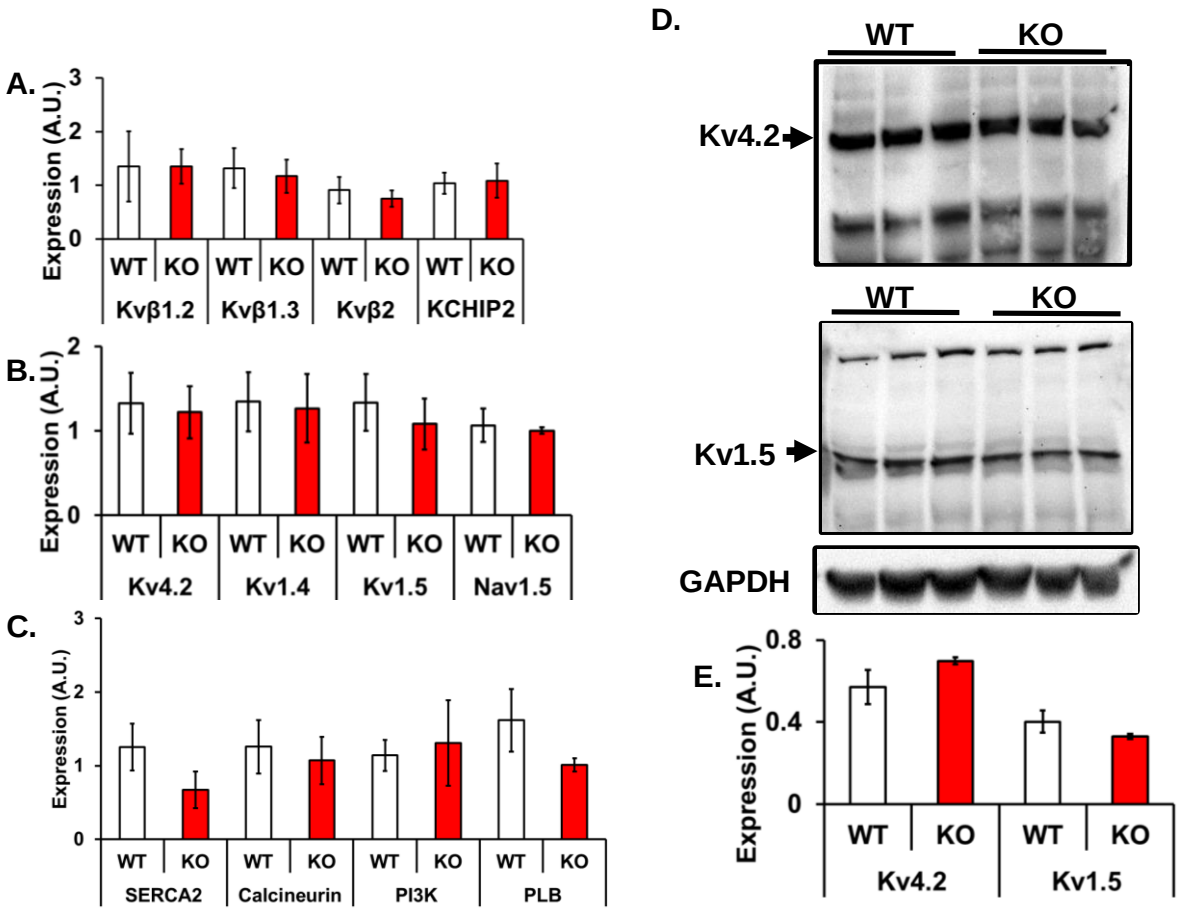

Figure 19: Gene expression. **A.** mRNAexpression of auxiliary subunits including Kvβ1.2 Kvβ1.3, Kvβ2, KCHIP2 the data represented are mean ± SEM (n=3). **B.** Gene expression of key cardiac channels including Kv4.2 Kv1.4, Kv1.5, Nav1.5 the data represented are mean ± SEM (n=3). **C.** Gene expression of key calcium regulators SERCA2, Calcineurin, PI3K, PLB (Phospholambin) the data represented are mean ± SEM (n=3). **D.** Protein expression of key Kv channels in the heart; Kv4.2 and Kv1.5 demonstrating no significant difference in membrane expression between wildtype (WT) and knockout (KO). **E.** The data represented are mean ± SEM (n=3).

CHAPTER FOUR:

Conclusion

Discussion

The Kvβ1.1 subunit demonstrates a unique ability to impart modulation on multiple Kv channels, this regulation on Kv channels particularly those found within the cardiovascular system impart profound physiological changes. In the absence of the Kvβ1.1 subunit both male and female mice demonstrate a significant increase in QTc duration as well as in action potential durations measured by monophasic action potential recordings of surface potential. These electrical measurements of the heart are equivalent to the measuring of the "repolarization reserve" a term given to emphasize the redundancy of multiple K^+ channels working to return the membrane potential to its resting rate a key component in the cardiac action potential (118). Often when this reserve is shortened significantly consequences can occur which include but are not limited to arrhythmias, early after depolarization's (EAD's) and, sudden cardiac death as well as exacerbating drug-induced arrhythmias. The Kvβ1.1 subunit in this work not only plays a significant role in the heart, its strong presence is also noted within the vascular system including the aorta (28). Fergus et al. found that the overall expression of Kvβ1.1 in the bovine aorta was almost double the amount when compared to other Kvβ subunits and other Kv channel chaperones. Indeed, one of the key repolarizing Kv currents found in the aorta, Kv1.5 an α-subunit demonstrated to interact and bind with Kvβ1.1 (137). These electrical changes noted in

the absence of Kvβ1.1 showed no alterations in key Kv channels thus demonstrating the change is solely from Kvβ1.1. (**Figure 7 & 16**) These alterations may be caused by Kv channel dysfunction and or gating abnormalities but this is due solely to the Kvβ1.1 absence.

While Kvβ1.1 is found in both male and female mice a significant increase in RNA was noted in females compared with males (**Figure 9**). This large increase in overall expression levels of Kvβ1.1 in WT females may be one explanation as to why vascular changes such as the significant increase in systolic and diastolic blood pressure were only noted in female mice. While blood pressure increased in KO male mice compared with their WT controls it was only KO female mice which demonstrated significant increases as well as increased aortic flow rates and an overall size increase in the heart. This physiological alteration in heart size may be in part due to the altered vascular parameters including increased blood pressure along with increased aortic flow rates. In addition, this work also demonstrated the interaction of Kvβ1.1 to MHCα or MYH6 the myosin heavy chain 6 protein one of the key myosin's found within the heart. These findings are in similar line with a previous study that highlighted the binding of Kvβ1 to actin and α-actinin (88). Recently, Kvβ2 protein was demonstrated to interact with ProSAP2 and Shank3 two proteins responsible for the neuronal structure of neurons thus highlighting that Kvβ proteins may play a role cell structure or the placement of ion channels (114). During pathophysiological forms of cardiac hypertrophy it is often demonstrated that a significant decrease is noted in MHCα with a significant increase in MHCβ (MYH7) (6). While no such trend was observed in these female mice it is plausible that a physiological form of cardiac hypertrophy is occurring however, more evidence is needed. In the absence of Kvβ1.1 a unique ability to impart physiological change within murine models is presented. Lack of Kvβ1.1 resulted in altered cardiac physiology including the prolongation of action potentials and the

overall shortening of the repolarization reserve as well as prolonged QTc durations. In addition, the vascular system was altered including increases in the aortic flow rate as well as blood pressure seen exclusively in female mice only.

Kvβ1.1 demonstrates not only an effect on the cardiovascular physiology when genetically deleted but can also impart electrical modulation by the manipulation of pyridine nucleotides including NAD and NADH. Kvβ1.1 belongs to the aldo-keto reductase family (AKR6A1) with the ability to bind pyridine nucleotides with high affinity. Indeed, as discussed earlier the first crystal structure of the Kvβ(2) subunits presented with an NADP molecule still bound. The modulation that occurs on the α-subunit by Kvβ is altered by which nucleotides are bound; the reduced forms (NADH/NADPH) or the oxidized forms (NAD/NADP). Previously demonstrated literature shows that when reduced forms are bound (NADH/NADPH) Kv channel inactivation is heavily favored. This was clearly demonstrated by Tipparaju et al in when Kv1.5 was expressed with and without Kvβ1.3 (human-mouse Kvβ1.1) in the presence of varying concentrations of NADH and NAD (137, 138). The injection of NADH into the cell transfected with Kv1.5 a normally non-inactivating current demonstrated greater inactivation including a significant decrease in tau values. While, the addition of NAD caused the Kv1.5 channel to remain open, thus abolishing inactivation. This gating phenomenon has been documented in multiple heterologous examples involving different Kv channels including Kv1.1 and Kv1.4 (98, 99). Pyridine nucleotide changes in the form of physiologically relevant concentrations continued the Kv channel modulation in the presence of a hypoxic nucleotide mix (favoring NADH/NADPH) which demonstrated again faster inactivation to otherwise non-inactivating channels (Kv1.5) (137).

While heterologous models provided the fundamental understanding of how Kvβ1.1 can impart modulation on multiple Kv channels a physiological or in vivo example still remained unknown. Many cardiac diseases including cardiac hypertrophy, myocardial ischemia, and the failing heart all demonstrate different etiologies however, one common trend in all was the significant increase in NADH levels within cardiac tissue(43, 70). One possible explanation is the metabolic switch from a fatty acid oxidation energy process to favoring a glycolytic requirement in cardiomyoctes. Traditionally in healthy cardiomyocytes fatty acid oxidation provides the overall energy requirements for the cell, however during times of great stress (such as myocardial ischemia) the myocytes begin to switch to rely more heavily upon the glycolytic pathway (69). This switch ultimately leads to an increase in pyruvate and subsequently an increase in cytosolic NADH levels. In addition, cardiac stress also leads to increased mitochondrial stress which can increase NADH levels (70). Therefore, cardiac stress leads to an accumulation of NADH and it is this increase that the Kvβ1.1 subunit senses and thus modulates subsequent α-subunits.

The addition of sodium lactate to the isolated heart has been one accepted model to increase intracellular concentrations of NADH, with the accumulation of lactate in the cardiomyocytes. The conversion of pyruvate to lactate and thus the formation of NAD molecules is significantly reduced and the NADH continues to increase. The exposure to 15 minutes of 10-20mM lactate in the murine heart was significant to increase the levels of NADH (FIG. 6) and thus alter the electrical properties significantly increasing monophasic potential durations in wildtype mice with Kvβ1.1 subunit present and capable of sensing to the NADH increase. The same experiment in knockout Kvβ1.1 hearts lead to no significant prolongation in monophasic action potential after the addition of lactate (FIG. 6). Similar trends were observed in adult

isolated cardiomyocytes which underwent lactate exposure; again WT myocytes demonstrated prolonged action potential durations at APD20 and APD50 while no increase was noted in KO myocytes. This prolongation in both monophasic and cellular action potentials is likely due to the Kvβ1.1 subunit sensing the increase in NADH (via lactate) and leading to faster inactivation of Kv channels (including Kv4.2 and Kv1.5). One molecular theory is faster inactivation allows for less time spent in activation therefore reducing the amount of K^+ ions leaving the cell thus taking addition time for the membrane potential to repolarize resulting in action potential prolongation. While lactate could contribute to other metabolic changes addition of sodium pyruvate restoring the NAD levels after lactate exposure demonstrated electrical alterations (MAP) are rather immediate. After 10 minutes of lactate exposure and significant prolongation, pyruvate when added for 10 minutes significantly restored the MAP signal to its initial value (FIG. 6G). This experiment demonstrated that the intracellular redox balance between NAD/NADH can be sensed by Kvβ1.1 and regulate selective Kv channels.

Indeed Kvβ1.1 has been demonstrated to bind to multiple Kv channels in this work in particular it is the first documentation of Kvβ1.1 interacting with and altering Kv4.2 current. The Kv4.2 current (Kv4.3 in humans) is one of the key repolarizing currents in cardiac action potentials and one of the first voltage-gated potassium channels to be activated which makes it of key importance. COS-7 cells transfected with Kv4.2 as well as Kvβ1.1 demonstrated a significant hyperpolarizing shift within the inactivation protocol after the introduction of lactate and subsequent increase in intracellular NADH. Kv4.2 alone showed no significant alterations with the addition of lactate once again demonstrating the importance of Kvβ1.1 to sense NAD/NADH alterations. These findings highlight the importance Kvβ1.1 plays during many cardiac diseases which can alter the NAD/NADH ratios.

While more research is needed on understanding how the Kvβ1.1 affects the overall cardiac repolarization reserve at different physiological states a greater understanding of how Kvβ1.1 affects other key organs is also important. Many initial reports have highlighted the importance Kvβ's play within the brain including learning and memory (32, 85, 89). Recently, with more and more genetic testing being conducting on large sample sizes a greater understanding of genetic mutations is coming into play. Such reports have demonstrated a correlation in epilepsy and schizophrenia with the Kvβ subunits (15, 62, 112, 161). Another rather important area of research yet to be explored is the role Kvβ1.1 plays in the uterus and during pregnancy. Previous research demonstrated that Kvβ1.1 was present in pregnant rats and altered concentrations (130). Further this work recently demonstrated that there is a significant increase in Kvβ1.1 in females compared with males. Taken together the absence of Kvβ1.1 during pregnancy could lead to altered uterine electrical activity which could alter overall muscle contractions and or overall structure as demonstrated in KO female mice presenting with enlarged hearts.

REFERENCES

1. **Accili EA, Kiehn J, Yang Q, Wang Z, Brown AM, and Wible BA**. Separable Kvbeta subunit domains alter expression and gating of potassium channels. *The Journal of biological chemistry* 272: 25824-25831, 1997.
2. **Aimond F, Kwak SP, Rhodes KJ, and Nerbonne JM**. Accessory Kvβ1 Subunits Differentially Modulate the Functional Expression of Voltage-Gated K+ Channels in Mouse Ventricular Myocytes. *Circulation Research* 96: 451-458, 2005.
3. **Bahring R, Vardanyan V, and Pongs O**. Differential modulation of Kv1 channel-mediated currents by co-expression of Kvbeta3 subunit in a mammalian cell-line. *Molecular membrane biology* 21: 19-25, 2004.
4. **Banerjee B, Peiris DN, Koo SH, Chui P, Lee EJ, and Hande MP**. Genomic imbalances in key ion channel genes and telomere shortening in sudden cardiac death victims. *Cytogenetic and genome research* 122: 350-355, 2008.
5. **Barry DM, Xu H, Schuessler RB, and Nerbonne JM**. Functional knockout of the transient outward current, long-QT syndrome, and cardiac remodeling in mice expressing a dominant-negative Kv4 alpha subunit. *Circ Res* 83: 560-567, 1998.
6. **Barry SP, Davidson SM, and Townsend PA**. Molecular regulation of cardiac hypertrophy. *The international journal of biochemistry & cell biology* 40: 2023-2039, 2008.
7. **Benjamin EJ, Levy D, Vaziri SM, D'Agostino RB, Belanger AJ, and Wolf PA**. Independent risk factors for atrial fibrillation in a population-based cohort. The Framingham Heart Study. *Jama* 271: 840-844, 1994.
8. **Berul CI, Aronovitz MJ, Wang PJ, and Mendelsohn ME**. In vivo cardiac electrophysiology studies in the mouse. *Circulation* 94: 2641-2648, 1996.
9. **Bonnet S, and Archer SL**. Potassium channel diversity in the pulmonary arteries and pulmonary veins: implications for regulation of the pulmonary vasculature in health and during pulmonary hypertension. *Pharmacology & therapeutics* 115: 56-69, 2007.
10. **Calloe K, Cordeiro JM, Di Diego JM, Hansen RS, Grunnet M, Olesen SP, and Antzelevitch C**. A transient outward potassium current activator recapitulates the electrocardiographic manifestations of Brugada syndrome. *Cardiovasc Res* 81: 686-694, 2009.
11. **Campomanes CR, Carroll KI, Manganas LN, Hershberger ME, Gong B, Antonucci DE, Rhodes KJ, and Trimmer JS**. Kv beta subunit oxidoreductase activity and Kv1 potassium channel trafficking. *The Journal of biological chemistry* 277: 8298-8305, 2002.
12. **Ceconi C, Bernocchi P, Boraso A, Cargnoni A, Pepi P, Curello S, and Ferrari R**. New insights on myocardial pyridine nucleotides and thiol redox state in ischemia and reperfusion damage. *Cardiovasc Res* 47: 586-594, 2000.
13. **Chapalamadugu KC, Panguluri SK, Bennett ES, Kolliputi N, and Tipparaju SM**. High level of oxygen treatment causes cardiotoxicity with arrhythmias and redox modulation. *Toxicology and applied pharmacology* 282: 100-107, 2015.
14. **Chiu YF, Chung RH, Lee CY, Kao HY, Hou L, and Hsu FC**. Identification of rare variants for hypertension with incorporation of linkage information. *BMC Proc* 8: S109, 2014.

15. **Connor JX, McCormack K, Pletsch A, Gaeta S, Ganetzky B, Chiu SY, and Messing A**. Genetic modifiers of the Kv beta2-null phenotype in mice. *Genes, brain, and behavior* 4: 77-88, 2005.
16. **Coppock EA, and Tamkun MM**. Differential expression of K(V) channel alpha- and beta-subunits in the bovine pulmonary arterial circulation. *American journal of physiology Lung cellular and molecular physiology* 281: L1350-1360, 2001.
17. **Crea F, Battipaglia I, and Andreotti F**. Sex differences in mechanisms, presentation and management of ischaemic heart disease. *Atherosclerosis* 241: 157-168, 2015.
18. **Daniels LB, and Maisel AS**. Cardiovascular biomarkers and sex: the case for women. *Nature reviews Cardiology* 2015.
19. **David M, Macias A, Moreno C, Prieto A, Martinez-Marmol R, Vicente R, Gonzalez T, Felipe A, Tamkun MM, and Valenzuela C**. Protein kinase C (PKC) activity regulates functional effects of Kvbeta1.3 subunit on KV1.5 channels: identification of a cardiac Kv1.5 channelosome. *The Journal of biological chemistry* 287: 21416-21428, 2012.
20. **Deschenes I, DiSilvestre D, Juang GJ, Wu RC, An WF, and Tomaselli GF**. Regulation of Kv4.3 current by KChIP2 splice variants: a component of native cardiac I(to)? *Circulation* 106: 423-429, 2002.
21. **Deschênes I, and Tomaselli GF**. Modulation of Kv4.3 current by accessory subunits. *FEBS Letters* 528: 183-188, 2002.
22. **Drazner MH**. The progression of hypertensive heart disease. *Circulation* 123: 327-334, 2011.
23. **Du XJ, Gao XM, Wang B, Jennings GL, Woodcock EA, and Dart AM**. Age-dependent cardiomyopathy and heart failure phenotype in mice overexpressing beta(2)-adrenergic receptors in the heart. *Cardiovasc Res* 48: 448-454, 2000.
24. **Ebert SN, Liu XK, and Woosley RL**. Female gender as a risk factor for drug-induced cardiac arrhythmias: evaluation of clinical and experimental evidence. *Journal of women's health / the official publication of the Society for the Advancement of Women's Health Research* 7: 547-557, 1998.
25. **El Gebeily G, El Khoury N, Mathieu S, Brouillette J, and Fiset C**. Estrogen regulation of the transient outward K current involves estrogen receptor alpha in mouse heart. *Journal of molecular and cellular cardiology* 86: 85-94, 2015.
26. **England SK, Uebele VN, Shear H, Kodali J, Bennett PB, and Tamkun MM**. Characterization of a voltage-gated K+ channel beta subunit expressed in human heart. *Proceedings of the National Academy of Sciences of the United States of America* 92: 6309-6313, 1995.
27. **Feinberg WM, Blackshear JL, Laupacis A, Kronmal R, and Hart RG**. Prevalence, age distribution, and gender of patients with atrial fibrillation. Analysis and implications. *Archives of internal medicine* 155: 469-473, 1995.
28. **Fergus DJ, Martens JR, and England SK**. Kv channel subunits that contribute to voltage-gated K+ current in renal vascular smooth muscle. *Pflugers Archiv : European journal of physiology* 445: 697-704, 2003.
29. **Fink M, Duprat F, Lesage F, Heurteaux C, Romey G, Barhanin J, and Lazdunski M**. A new K+ channel beta subunit to specifically enhance Kv2.2 (CDRK) expression. *The Journal of biological chemistry* 271: 26341-26348, 1996.
30. **Fischer F, Vonderlin N, Seyler C, Zitron E, Korkmaz S, Szabo G, Thomas D, Katus HA, and Scholz EP**. Isoenzyme-specific regulation of cardiac Kv1.5/Kvbeta1.2 ion channel

complex by protein kinase C: central role of PKCbetaII. *Naunyn-Schmiedeberg's archives of pharmacology* 387: 469-476, 2014.
31. **Ganfornina MD, Perez-Garcia MT, Gutierrez G, Miguel-Velado E, Lopez-Lopez JR, Marin A, Sanchez D, and Gonzalez C**. Comparative gene expression profile of mouse carotid body and adrenal medulla under physiological hypoxia. *The Journal of physiology* 566: 491-503, 2005.
32. **Giese KP, Storm JF, Reuter D, Fedorov NB, Shao LR, Leicher T, Pongs O, and Silva AJ**. Reduced K+ channel inactivation, spike broadening, and after-hyperpolarization in Kvbeta1.1-deficient mice with impaired learning. *Learning & memory* 5: 257-273, 1998.
33. **Gillis AM, Mathison HJ, Patel C, and Lester WM**. Quinidine pharmacodynamics in normal and isoproterenol-induced hypertrophied blood-perfused working rabbit hearts. *Journal of cardiovascular pharmacology* 27: 916-926, 1996.
34. **Go AS, Mozaffarian D, Roger VL, Benjamin EJ, Berry JD, Borden WB, Bravata DM, Dai S, Ford ES, Fox CS, Franco S, Fullerton HJ, Gillespie C, Hailpern SM, Heit JA, Howard VJ, Huffman MD, Kissela BM, Kittner SJ, Lackland DT, Lichtman JH, Lisabeth LD, Magid D, Marcus GM, Marelli A, Matchar DB, McGuire DK, Mohler ER, Moy CS, Mussolino ME, Nichol G, Paynter NP, Schreiner PJ, Sorlie PD, Stein J, Turan TN, Virani SS, Wong ND, Woo D, and Turner MB**. Executive summary: heart disease and stroke statistics--2013 update: a report from the American Heart Association. *Circulation* 127: 143-152, 2013.
35. **Goldman AM, Behr ER, Semsarian C, Bagnall RD, Sisodiya S, and Cooper PN**. Sudden unexpected death in epilepsy genetics: Molecular diagnostics and prevention. *Epilepsia* 57 Suppl 1: 17-25, 2016.
36. **Gowd BM, and Thompson PD**. Effect of female sex on cardiac arrhythmias. *Cardiology in review* 20: 297-303, 2012.
37. **Grande M, Suarez E, Vicente R, Canto C, Coma M, Tamkun MM, Zorzano A, Guma A, and Felipe A**. Voltage-dependent K+ channel beta subunits in muscle: differential regulation during postnatal development and myogenesis. *Journal of cellular physiology* 195: 187-193, 2003.
38. **Grant AO**. Cardiac ion channels. *Circulation Arrhythmia and electrophysiology* 2: 185-194, 2009.
39. **Grubb S, Aistrup GL, Koivumaki JT, Speerschneider T, Gottlieb LA, Mutsaers NA, Olesen SP, Calloe K, and Thomsen MB**. Preservation of cardiac function by prolonged action potentials in mice deficient of KChIP2. *American journal of physiology Heart and circulatory physiology* 309: H481-489, 2015.
40. **Gulbis JM, Mann S, and MacKinnon R**. Structure of a voltage-dependent K+ channel beta subunit. *Cell* 97: 943-952, 1999.
41. **Gutman GA, Chandy KG, Grissmer S, Lazdunski M, McKinnon D, Pardo LA, Robertson GA, Rudy B, Sanguinetti MC, Stuhmer W, and Wang X**. International Union of Pharmacology. LIII. Nomenclature and molecular relationships of voltage-gated potassium channels. *Pharmacological reviews* 57: 473-508, 2005.
42. **Hayama E, Imamura S, Wu C, Nakazawa M, Matsuoka R, and Nakanishi T**. Analysis of voltage-gated potassium channel beta1 subunits in the porcine neonatal ductus arteriosus. *Pediatric research* 59: 167-174, 2006.
43. **He Q, Feng Y, and Wang Y**. Transient outward potassium channel: a heart failure mediator. *Heart failure reviews* 20: 349-362, 2015.

44. **Heinemann SH, Rettig J, Wunder F, and Pongs O**. Molecular and functional characterization of a rat brain Kv beta 3 potassium channel subunit. *FEBS Lett* 377: 383-389, 1995.
45. **Hlavac V, Brynychova V, Vaclavikova R, Ehrlichova M, Vrana D, Pecha V, Trnkova M, Kodet R, Mrhalova M, Kubackova K, Gatek J, Vazan P, and Soucek P**. The role of cytochromes p450 and aldo-keto reductases in prognosis of breast carcinoma patients. *Medicine* 93: e255, 2014.
46. **Hsu CP, Oka S, Shao D, Hariharan N, and Sadoshima J**. Nicotinamide phosphoribosyltransferase regulates cell survival through NAD+ synthesis in cardiac myocytes. *Circ Res* 105: 481-491, 2009.
47. **Hu DL, Chen FK, Liu YQ, Sheng YH, Yang R, Kong XQ, Cao KJ, Gu HT, and Qian LM**. GATA-4 promotes the differentiation of P19 cells into cardiac myocytes. *International journal of molecular medicine* 26: 365-372, 2010.
48. **Jehle J, Schweizer PA, Katus HA, and Thomas D**. Novel roles for hERG K(+) channels in cell proliferation and apoptosis. *Cell death & disease* 2: e193, 2011.
49. **Jez JM, Bennett MJ, Schlegel BP, Lewis M, and Penning TM**. Comparative anatomy of the aldo-keto reductase superfamily. *The Biochemical journal* 326 (Pt 3): 625-636, 1997.
50. **Jones JM, Bentley E, Meisler MH, and Darling SM**. Genetic mapping of the voltage-gated shaker potassium channel beta subunit Kcnab1 to mouse chromosome 3. *Mammalian genome : official journal of the International Mammalian Genome Society* 9: 260, 1998.
51. **Jow F, Zhang ZH, Kopsco DC, Carroll KC, and Wang K**. Functional coupling of intracellular calcium and inactivation of voltage-gated Kv1.1/Kvbeta1.1 A-type K+ channels. *Proceedings of the National Academy of Sciences of the United States of America* 101: 15535-15540, 2004.
52. **Kay M, Swift L, Martell B, Arutunyan A, and Sarvazyan N**. Locations of ectopic beats coincide with spatial gradients of NADH in a regional model of low-flow reperfusion. *American journal of physiology Heart and circulatory physiology* 294: H2400-2405, 2008.
53. **Kilfoil PJ, Tipparaju SM, Barski OA, and Bhatnagar A**. Regulation of ion channels by pyridine nucleotides. *Circ Res* 112: 721-741, 2013.
54. **Kim DM, and Nimigean CM**. Voltage-Gated Potassium Channels: A Structural Examination of Selectivity and Gating. *Cold Spring Harbor perspectives in biology* 8: 2016.
55. **Kinoshita K, Takahashi H, Hata Y, Nishide K, Kato M, Fujita H, Yoshida S, Murai K, Mizumaki K, Nishida K, Yamaguchi Y, Kano M, Tabata T, and Nishida N**. SCN5A(K817E), a novel Brugada syndrome-associated mutation that alters the activation gating of NaV1.5 channel. *Heart rhythm : the official journal of the Heart Rhythm Society* 13: 1113-1120, 2016.
56. **Kleiman RB, and Houser SR**. Calcium currents in normal and hypertrophied isolated feline ventricular myocytes. *The American journal of physiology* 255: H1434-1442, 1988.
57. **Kobayashi K, and Neely JR**. Effects of ischemia and reperfusion on pyruvate dehydrogenase activity in isolated rat hearts. *Journal of molecular and cellular cardiology* 15: 359-367, 1983.
58. **Kong W, Po S, Yamagishi T, Ashen MD, Stetten G, and Tomaselli GF**. Isolation and characterization of the human gene encoding Ito: further diversity by alternative mRNA splicing. *The American journal of physiology* 275: H1963-1970, 1998.
59. **Kuo HC, Cheng CF, Clark RB, Lin JJ, Lin JL, Hoshijima M, Nguyen-Tran VT, Gu Y, Ikeda Y, Chu PH, Ross J, Giles WR, and Chien KR**. A defect in the Kv channel-

interacting protein 2 (KChIP2) gene leads to a complete loss of I(to) and confers susceptibility to ventricular tachycardia. *Cell* 107: 801-813, 2001.
60. **Kuryshev YA, Wible BA, Gudz TI, Ramirez AN, and Brown AM**. KChAP/Kvbeta1.2 interactions and their effects on cardiac Kv channel expression. *American journal of physiology Cell physiology* 281: C290-299, 2001.
61. **Kwak Y-G, Hu N, Wei J, George AL, Grobaski TD, Tamkun MM, and Murray KT**. Protein Kinase A Phosphorylation Alters Kvβ1.3 Subunit-mediated Inactivation of the Kv1.5 Potassium Channel. *Journal of Biological Chemistry* 274: 13928-13932, 1999.
62. **Lee YH, Kim JH, and Song GG**. Pathway analysis of a genome-wide association study in schizophrenia. *Gene* 525: 107-115, 2013.
63. **Lehmann MH, Hardy S, Archibald D, quart B, and MacNeil DJ**. Sex difference in risk of torsade de pointes with d,l-sotalol. *Circulation* 94: 2535-2541, 1996.
64. **Leicher T, Bahring R, Isbrandt D, and Pongs O**. Coexpression of the KCNA3B gene product with Kv1.5 leads to a novel A-type potassium channel. *The Journal of biological chemistry* 273: 35095-35101, 1998.
65. **Leicher T, Roeper J, Weber K, Wang X, and Pongs O**. Structural and functional characterization of human potassium channel subunit beta 1 (KCNA1B). *Neuropharmacology* 35: 787-795, 1996.
66. **Li G, Cheng G, Wu J, Zhou X, Liu P, and Sun C**. Drug-induced long QT syndrome in women. *Advances in therapy* 30: 793-802, 2013.
67. **Liao J, Su X, Chen P, Wang X, Xu L, Li X, Thean L, Tan C, Tan AG, Tay WT, Jun G, Zheng Y, Chew M, Wang YX, Tan QS, Barathi VA, Klein BE, Saw SM, Vithana EN, Tai ES, Iyengar SK, Mitchell P, Khor CC, Aung T, Wang JJ, Jonas JB, Teo YY, Wong TY, and Cheng CY**. Meta-analysis of genome-wide association studies in multiethnic Asians identifies two loci for age-related nuclear cataract. *Human molecular genetics* 23: 6119-6128, 2014.
68. **Lim WW, Baumert M, Neo M, Kuklik P, Ganesan AN, Lau DH, Tsoutsman T, Semsarian C, Sanders P, and Saint DA**. Slowed atrial and atrioventricular conduction and depressed HRV in a murine model of hypertrophic cardiomyopathy. *Clinical and experimental pharmacology & physiology* 43: 95-101, 2016.
69. **Lionetti V, Stanley WC, and Recchia FA**. Modulating fatty acid oxidation in heart failure. *Cardiovasc Res* 90: 202-209, 2011.
70. **Liu M, Gu L, Sulkin MS, Liu H, Jeong EM, Greener I, Xie A, Efimov IR, and Dudley SC, Jr.** Mitochondrial dysfunction causing cardiac sodium channel downregulation in cardiomyopathy. *J Mol Cell Cardiol* 54: 25-34, 2013.
71. **Liu M, Sanyal S, Gao G, Gurung IS, Zhu X, Gaconnet G, Kerchner LJ, Shang LL, Huang CL, Grace A, London B, and Dudley SC, Jr.** Cardiac Na+ current regulation by pyridine nucleotides. *Circulation research* 105: 737-745, 2009.
72. **Liu SQ, Jin H, Zacarias A, Srivastava S, and Bhatnagar A**. Binding of pyridine nucleotide coenzymes to the beta-subunit of the voltage-sensitive K+ channel. *The Journal of biological chemistry* 276: 11812-11820, 2001.
73. **Liu T, and O'Rourke B**. Regulation of the Na+/Ca2+ exchanger by pyridine nucleotide redox potential in ventricular myocytes. *The Journal of biological chemistry* 288: 31984-31992, 2013.
74. **Long SB, Campbell EB, and Mackinnon R**. Crystal structure of a mammalian voltage-dependent Shaker family K+ channel. *Science (New York, NY)* 309: 897-903, 2005.

75. **Lu Q, Peevey J, Jow F, Monaghan MM, Mendoza G, Zhang H, Wu J, Kim CY, Bicksler J, Greenblatt L, Lin SS, Childers W, and Bowlby MR**. Disruption of Kv1.1 N-type inactivation by novel small molecule inhibitors (disinactivators). *Bioorganic & medicinal chemistry* 16: 3067-3075, 2008.
76. **Lue WM, and Boyden PA**. Abnormal electrical properties of myocytes from chronically infarcted canine heart. Alterations in Vmax and the transient outward current. *Circulation* 85: 1175-1188, 1992.
77. **Maitra M, Schluterman MK, Nichols HA, Richardson JA, Lo CW, Srivastava D, and Garg V**. Interaction of Gata4 and Gata6 with Tbx5 is critical for normal cardiac development. *Developmental biology* 326: 368-377, 2009.
78. **Major P, Baczko I, Hiripi L, Odening KE, Juhasz V, Kohajda Z, Horvath A, Seprenyi G, Kovacs M, Virag L, Jost N, Prorok J, Ordog B, Doleschall Z, Nattel S, Varro A, and Bosze Z**. A novel transgenic rabbit model with reduced repolarization reserve: long QT syndrome caused by a dominant-negative mutation of the KCNE1 gene. *British journal of pharmacology* 173: 2046-2061, 2016.
79. **Makkar RR, Fromm BS, Steinman RT, Meissner MD, and Lehmann MH**. Female gender as a risk factor for torsades de pointes associated with cardiovascular drugs. *Jama* 270: 2590-2597, 1993.
80. **McCarthy NS, Vangjeli C, Cavalleri GL, Delanty N, Shianna KV, Surendran P, O'Brien E, Munroe PB, Masca N, Tomaszewski M, Samani NJ, and Stanton AV**. Two further blood pressure loci identified in ion channel genes with a gene-centric approach. *Circ Cardiovasc Genet* 7: 873-879, 2014.
81. **McCormack T, and McCormack K**. Shaker K+ channel beta subunits belong to an NAD(P)H-dependent oxidoreductase superfamily. *Cell* 79: 1133-1135, 1994.
82. **Mitchell GF, Jeron A, and Koren G**. Measurement of heart rate and Q-T interval in the conscious mouse. *The American journal of physiology* 274: H747-751, 1998.
83. **Molkentin JD, Kalvakolanu DV, and Markham BE**. Transcription factor GATA-4 regulates cardiac muscle-specific expression of the alpha-myosin heavy-chain gene. *Molecular and cellular biology* 14: 4947-4957, 1994.
84. **Moudgil R, Michelakis ED, and Archer SL**. The role of k+ channels in determining pulmonary vascular tone, oxygen sensing, cell proliferation, and apoptosis: implications in hypoxic pulmonary vasoconstriction and pulmonary arterial hypertension. *Microcirculation (New York, NY : 1994)* 13: 615-632, 2006.
85. **Murphy GG, Fedorov NB, Giese KP, Ohno M, Friedman E, Chen R, and Silva AJ**. Increased Neuronal Excitability, Synaptic Plasticity, and Learning in Aged Kvβ1.1 Knockout Mice. *Current Biology* 14: 1907-1915, 2004.
86. **Nabauer M, Beuckelmann DJ, Uberfuhr P, and Steinbeck G**. Regional differences in current density and rate-dependent properties of the transient outward current in subepicardial and subendocardial myocytes of human left ventricle. *Circulation* 93: 168-177, 1996.
87. **Nagaya N, and Papazian DM**. Potassium Channel α and β Subunits Assemble in the Endoplasmic Reticulum. *Journal of Biological Chemistry* 272: 3022-3027, 1997.
88. **Nakahira K, Matos MF, and Trimmer JS**. Differential interaction of voltage-gated K+ channel beta-subunits with cytoskeleton is mediated by unique amino terminal domains. *Journal of molecular neuroscience : MN* 11: 199-208, 1998.

89. **Need AC, Irvine EE, and Giese KP**. Learning and memory impairments in Kvβ1.1-null mutants are rescued by environmental enrichment or ageing. *European Journal of Neuroscience* 18: 1640-1644, 2003.
90. **Nerbonne JM**. Mouse models of arrhythmogenic cardiovascular disease: challenges and opportunities. *Current opinion in pharmacology* 15: 107-114, 2014.
91. **Nerbonne JM, and Kass RS**. Molecular Physiology of Cardiac Repolarization. *Physiological reviews* 85: 1205-1253, 2005.
92. **Nielsen JB, Bentzen BH, Olesen MS, David JP, Olesen SP, Haunso S, Svendsen JH, and Schmitt N**. Gain-of-function mutations in potassium channel subunit KCNE2 associated with early-onset lone atrial fibrillation. *Biomarkers in medicine* 8: 557-570, 2014.
93. **Nielsen NH, Winkel BG, Kanters JK, Schmitt N, Hofman-Bang J, Jensen HS, Bentzen BH, Sigurd B, Larsen LA, Andersen PS, Haunso S, Kjeldsen K, Grunnet M, Christiansen M, and Olesen SP**. Mutations in the Kv1.5 channel gene KCNA5 in cardiac arrest patients. *Biochem Biophys Res Commun* 354: 776-782, 2007.
94. **Odening KE, Choi BR, Liu GX, Hartmann K, Ziv O, Chaves L, Schofield L, Centracchio J, Zehender M, Peng X, Brunner M, and Koren G**. Estradiol promotes sudden cardiac death in transgenic long QT type 2 rabbits while progesterone is protective. *Heart rhythm : the official journal of the Heart Rhythm Society* 9: 823-832, 2012.
95. **Odening KE, Nerbonne JM, Bode C, Zehender M, and Brunner M**. In vivo effect of a dominant negative Kv4.2 loss-of-function mutation eliminating I(to,f) on atrial refractoriness and atrial fibrillation in mice. *Circulation journal : official journal of the Japanese Circulation Society* 73: 461-467, 2009.
96. **Ohanyan V, Yin L, Bardakjian R, Kolz C, Enrick M, Hakobyan T, Kmetz JG, Bratz I, Luli J, Nagane M, Khan N, Hou H, Kuppusamy P, Graham J, Fu FS, Janota D, Oyewumi MO, Logan SJ, Lindner JR, and Chilian WM**. Requisite Role of Kv1.5 Channels in Coronary Metabolic Dilation. *Circ Res* 2015.
97. **Olson TM, Alekseev AE, Liu XK, Park S, Zingman LV, Bienengraeber M, Sattiraju S, Ballew JD, Jahangir A, and Terzic A**. Kv1.5 channelopathy due to KCNA5 loss-of-function mutation causes human atrial fibrillation. *Human molecular genetics* 15: 2185-2191, 2006.
98. **Pan Y, Weng J, Cao Y, Bhosle RC, and Zhou M**. Functional coupling between the Kv1.1 channel and aldoketoreductase Kvbeta1. *The Journal of biological chemistry* 283: 8634-8642, 2008.
99. **Pan Y, Weng J, Levin EJ, and Zhou M**. Oxidation of NADPH on Kvbeta1 inhibits ball-and-chain type inactivation by restraining the chain. *Proceedings of the National Academy of Sciences of the United States of America* 108: 5885-5890, 2011.
100. **Panama BK, Korogyi AS, Aschar-Sobbi R, Oh Y, Gray CB, Gang H, Brown JH, Kirshenbaum LA, and Backx PH**. Reductions in the Cardiac Transient Outward K+ Current Ito Caused by Chronic beta-Adrenergic Receptor Stimulation Are Partly Rescued by Inhibition of Nuclear Factor kappaB. *The Journal of biological chemistry* 291: 4156-4165, 2016.
101. **Panama BK, Latour-Villamil D, Farman GP, Zhao D, Bolz SS, Kirshenbaum LA, and Backx PH**. Nuclear factor kappaB downregulates the transient outward potassium current I(to,f) through control of KChIP2 expression. *Circ Res* 108: 537-543, 2011.
102. **Panguluri SK, Tur J, Chapalamadugu KC, Katnik C, Cuevas J, and Tipparaju SM**. MicroRNA-301a mediated regulation of Kv4.2 in diabetes: identification of key modulators. *PloS one* 8: e60545, 2013.

103. **Panguluri SK, Tur J, Fukomoto J, Deng W, Sneed KB, Kolliputi N, Bennett ES, and Tipparaju SM**. Hyperoxia Induced Hypertrophy and Ion Channel Remodeling in Left Ventricle. *American Journal of Physiology - Heart and Circulatory Physiology* 2013.
104. **Panguluri SK, Tur J, Fukumoto J, Deng W, Sneed KB, Kolliputi N, Bennett ES, and Tipparaju SM**. Hyperoxia-induced hypertrophy and ion channel remodeling in left ventricle. *American journal of physiology Heart and circulatory physiology* 304: H1651-1661, 2013.
105. **Parcej DN, and Dolly JO**. Dendrotoxin acceptor from bovine synaptic plasma membranes. Binding properties, purification and subunit composition of a putative constituent of certain voltage-activated K+ channels. *The Biochemical journal* 257: 899-903, 1989.
106. **Patel SP, and Campbell DL**. Transient outward potassium current, 'Ito', phenotypes in the mammalian left ventricle: underlying molecular, cellular and biophysical mechanisms. *The Journal of physiology* 569: 7-39, 2005.
107. **Penning TM**. The aldo-keto reductases (AKRs): Overview. *Chemico-biological interactions* 234: 236-246, 2015.
108. **Perez-Garcia MT, Lopez-Lopez JR, and Gonzalez C**. Kvbeta1.2 subunit coexpression in HEK293 cells confers O2 sensitivity to kv4.2 but not to Shaker channels. *The Journal of general physiology* 113: 897-907, 1999.
109. **Pham TV, Sosunov EA, Gainullin RZ, Danilo P, Jr., and Rosen MR**. Impact of sex and gonadal steroids on prolongation of ventricular repolarization and arrhythmias induced by I(K)-blocking drugs. *Circulation* 103: 2207-2212, 2001.
110. **Pillai JB, Isbatan A, Imai S-i, and Gupta MP**. Poly(ADP-ribose) Polymerase-1-dependent Cardiac Myocyte Cell Death during Heart Failure Is Mediated by NAD+ Depletion and Reduced Sir2α Deacetylase Activity. *Journal of Biological Chemistry* 280: 43121-43130, 2005.
111. **Pillai VB, Sundaresan NR, Kim G, Gupta M, Rajamohan SB, Pillai JB, Samant S, Ravindra PV, Isbatan A, and Gupta MP**. Exogenous NAD Blocks Cardiac Hypertrophic Response via Activation of the SIRT3-LKB1-AMP-activated Kinase Pathway. *Journal of Biological Chemistry* 285: 3133-3144, 2010.
112. **Pongs O, and Schwarz JR**. Ancillary subunits associated with voltage-dependent K+ channels. *Physiol Rev* 90: 755-796, 2010.
113. **Postema PG, and Wilde AA**. The measurement of the QT interval. *Current cardiology reviews* 10: 287-294, 2014.
114. **Proepper C, Putz S, Russell R, Boeckers TM, and Liebau S**. The Kvbeta2 subunit of voltage-gated potassium channels is interacting with ProSAP2/Shank3 in the PSD. *Neuroscience* 261: 133-143, 2014.
115. **Rasmusson RL, Morales MJ, Wang S, Liu S, Campbell DL, Brahmajothi MV, and Strauss HC**. Inactivation of voltage-gated cardiac K+ channels. *Circ Res* 82: 739-750, 1998.
116. **Rehm H, and Lazdunski M**. Purification and subunit structure of a putative K+-channel protein identified by its binding properties for dendrotoxin I. *Proceedings of the National Academy of Sciences of the United States of America* 85: 4919-4923, 1988.
117. **Rettig J, Heinemann SH, Wunder F, Lorra C, Parcej DN, Oliver Dolly J, and Pongs O**. Inactivation properties of voltage-gated K+ channels altered by presence of [beta]-subunit. *Nature* 369: 289-294, 1994.
118. **Roden DM**. Taking the "idio" out of "idiosyncratic": predicting torsades de pointes. *Pacing and clinical electrophysiology : PACE* 21: 1029-1034, 1998.

119. **Roepke TK, Kontogeorgis A, Ovanez C, Xu X, Young JB, Purtell K, Goldstein PA, Christini DJ, Peters NS, Akar FG, Gutstein DE, Lerner DJ, and Abbott GW**. Targeted deletion of kcne2 impairs ventricular repolarization via disruption of I(K,slow1) and I(to,f). *FASEB journal : official publication of the Federation of American Societies for Experimental Biology* 22: 3648-3660, 2008.
120. **Rosenberg MA, Das S, Pinzon PQ, Knight AC, Sosnovik DE, Ellinor PT, and Rosenzweig A**. A Novel Transgenic Mouse Model of Cardiac Hypertrophy and Atrial Fibrillation. *Journal of atrial fibrillation* 2: 1-15, 2012.
121. **Rossow CF, Dilly KW, Yuan C, Nieves-Cintron M, Cabarrus JL, and Santana LF**. NFATc3-dependent loss of I(to) gradient across the left ventricular wall during chronic beta adrenergic stimulation. *J Mol Cell Cardiol* 46: 249-256, 2009.
122. **Ryge J, Winther O, Wienecke J, Sandelin A, Westerdahl AC, Hultborn H, and Kiehn O**. Transcriptional regulation of gene expression clusters in motor neurons following spinal cord injury. *BMC genomics* 11: 365, 2010.
123. **Sah R, Ramirez RJ, and Backx PH**. Modulation of Ca(2+) release in cardiac myocytes by changes in repolarization rate: role of phase-1 action potential repolarization in excitation-contraction coupling. *Circ Res* 90: 165-173, 2002.
124. **Sah R, Ramirez RJ, Oudit GY, Gidrewicz D, Trivieri MG, Zobel C, and Backx PH**. Regulation of cardiac excitation-contraction coupling by action potential repolarization: role of the transient outward potassium current (I(to)). *The Journal of physiology* 546: 5-18, 2003.
125. **Schmitt N, Grunnet M, and Olesen SP**. Cardiac potassium channel subtypes: new roles in repolarization and arrhythmia. *Physiol Rev* 94: 609-653, 2014.
126. **Scicluna BP, Tanck MW, Remme CA, Beekman L, Coronel R, Wilde AA, and Bezzina CR**. Quantitative trait loci for electrocardiographic parameters and arrhythmia in the mouse. *J Mol Cell Cardiol* 50: 380-389, 2011.
127. **Sewing S, Roeper J, and Pongs O**. Kv beta 1 subunit binding specific for shaker-related potassium channel alpha subunits. *Neuron* 16: 455-463, 1996.
128. **Sharma A, Masri J, Jo OD, Bernath A, Martin J, Funk A, and Gera J**. Protein kinase C regulates internal initiation of translation of the GATA-4 mRNA following vasopressin-induced hypertrophy of cardiac myocytes. *The Journal of biological chemistry* 282: 9505-9516, 2007.
129. **Speerschneider T, and Thomsen MB**. Physiology and analysis of the electrocardiographic T wave in mice. *Acta physiologica (Oxford, England)* 209: 262-271, 2013.
130. **Suzuki T, and Takimoto K**. Differential expression of Kv4 pore-forming and KChIP auxiliary subunits in rat uterus during pregnancy. *American journal of physiology Endocrinology and metabolism* 288: E335-341, 2005.
131. **Swain SM, Sahoo N, Dennhardt S, Schonherr R, and Heinemann SH**. Ca(2+)/calmodulin regulates Kvbeta1.1-mediated inactivation of voltage-gated K(+) channels. *Scientific reports* 5: 15509, 2015.
132. **Sysa-Shah P, Sorensen LL, Abraham MR, and Gabrielson KL**. Electrocardiographic Characterization of Cardiac Hypertrophy in Mice that Overexpress the ErbB2 Receptor Tyrosine Kinase. *Comparative medicine* 65: 295-307, 2015.
133. **Szabo I, Zoratti M, and Gulbins E**. Contribution of voltage-gated potassium channels to the regulation of apoptosis. *FEBS Lett* 584: 2049-2056, 2010.

134. **Tadros R, Ton AT, Fiset C, and Nattel S**. Sex differences in cardiac electrophysiology and clinical arrhythmias: epidemiology, therapeutics, and mechanisms. *The Canadian journal of cardiology* 30: 783-792, 2014.
135. **Tang T, Lai NC, Wright AT, Gao MH, Lee P, Guo T, Tang R, McCulloch AD, and Hammond HK**. Adenylyl cyclase 6 deletion increases mortality during sustained β-adrenergic receptor stimulation. *Journal of molecular and cellular cardiology* 60: 60-67, 2013.
136. **Thomsen MB, Sosunov EA, Anyukhovsky EP, Ozgen N, Boyden PA, and Rosen MR**. Deleting the accessory subunit KChIP2 results in loss of I(to,f) and increased I(K,slow) that maintains normal action potential configuration. *Heart rhythm : the official journal of the Heart Rhythm Society* 6: 370-377, 2009.
137. **Tipparaju SM, Li XP, Kilfoil PJ, Xue B, Uversky VN, Bhatnagar A, and Barski OA**. Interactions between the C-terminus of Kv1.5 and Kvbeta regulate pyridine nucleotide-dependent changes in channel gating. *Pflugers Arch* 463: 799-818, 2012.
138. **Tipparaju SM, Liu S-Q, Barski OA, and Bhatnagar A**. NADPH binding to β-subunit regulates inactivation of voltage-gated K+ channels. *Biochemical and Biophysical Research Communications* 359: 269-276, 2007.
139. **Tipparaju SM, Saxena N, Liu SQ, Kumar R, and Bhatnagar A**. Differential regulation of voltage-gated K+ channels by oxidized and reduced pyridine nucleotide coenzymes. *American journal of physiology Cell physiology* 288: C366-376, 2005.
140. **Tozakidou M, Goltz D, Hagenstrom T, Budack MK, Vitzthum H, Szlachta K, Bahring R, and Ehmke H**. Molecular and functional remodeling of I(to) by angiotensin II in the mouse left ventricle. *J Mol Cell Cardiol* 48: 140-151, 2010.
141. **Tur J, Chapalamadugu KC, Padawer T, Badole SL, Kilfoil PJ, Bhatnagar A, and Tipparaju SM**. Deletion of Kvβ1.1 subunit leads to electrical and haemodynamic changes causing cardiac hypertrophy in female murine hearts. *Experimental Physiology* n/a-n/a, 2016.
142. **Vidal M, Wieland T, Lohse MJ, and Lorenz K**. beta-Adrenergic receptor stimulation causes cardiac hypertrophy via a Gbetagamma/Erk-dependent pathway. *Cardiovasc Res* 96: 255-264, 2012.
143. **Villa C, and Combi R**. Potassium Channels and Human Epileptic Phenotypes: An Updated Overview. *Frontiers in cellular neuroscience* 10: 81, 2016.
144. **Voudris KV, Apostolakis S, Karyofillis P, Doukas K, Zaravinos A, Androutsopoulos VP, Michalis A, Voudris V, and Spandidos DA**. Genetic diversity of the KCNE1 gene and susceptibility to postoperative atrial fibrillation. *American heart journal* 167: 274-280 e271, 2014.
145. **Wang J, Paradis P, Aries A, Komati H, Lefebvre C, Wang H, and Nemer M**. Convergence of protein kinase C and JAK-STAT signaling on transcription factor GATA-4. *Molecular and cellular biology* 25: 9829-9844, 2005.
146. **Wang Z, Kiehn J, Yang Q, Brown AM, and Wible BA**. Comparison of binding and block produced by alternatively spliced Kvbeta1 subunits. *The Journal of biological chemistry* 271: 28311-28317, 1996.
147. **Webb IG, Nishino Y, Clark JE, Murdoch C, Walker SJ, Makowski MR, Botnar RM, Redwood SR, Shah AM, and Marber MS**. Constitutive glycogen synthase kinase-3α/β activity protects against chronic β-adrenergic remodelling of the heart. *Cardiovascular Research* 87: 494-503, 2010.

148. **Weng J, Cao Y, Moss N, and Zhou M**. Modulation of voltage-dependent Shaker family potassium channels by an aldo-keto reductase. *The Journal of biological chemistry* 281: 15194-15200, 2006.
149. **Wettwer E, Amos GJ, Posival H, and Ravens U**. Transient outward current in human ventricular myocytes of subepicardial and subendocardial origin. *Circ Res* 75: 473-482, 1994.
150. **Wickenden AD, Kaprielian R, Kassiri Z, Tsoporis JN, Tsushima R, Fishman GI, and Backx PH**. The role of action potential prolongation and altered intracellular calcium handling in the pathogenesis of heart failure. *Cardiovasc Res* 37: 312-323, 1998.
151. **Wickenden AD, Lee P, Sah R, Huang Q, Fishman GI, and Backx PH**. Targeted expression of a dominant-negative K(v)4.2 K(+) channel subunit in the mouse heart. *Circ Res* 85: 1067-1076, 1999.
152. **Xiong Q, Cao Q, Zhou Q, Xie J, Shen Y, Wan R, Yu J, Yan S, Marian AJ, and Hong K**. Arrhythmogenic cardiomyopathy in a patient with a rare loss-of-function KCNQ1 mutation. *Journal of the American Heart Association* 4: e001526, 2015.
153. **Xu J, Yu W, Wright JM, Raab RW, and Li M**. Distinct functional stoichiometry of potassium channel beta subunits. *Proceedings of the National Academy of Sciences of the United States of America* 95: 1846-1851, 1998.
154. **Yahagi K, Davis HR, Arbustini E, and Virmani R**. Sex differences in coronary artery disease: pathological observations. *Atherosclerosis* 239: 260-267, 2015.
155. **Yamamoto T, Byun J, Zhai P, Ikeda Y, Oka S, and Sadoshima J**. Nicotinamide mononucleotide, an intermediate of NAD+ synthesis, protects the heart from ischemia and reperfusion. *PLoS One* 9: e98972, 2014.
156. **Yang EK, Alvira MR, Levitan ES, and Takimoto K**. Kvbeta subunits increase expression of Kv4.3 channels by interacting with their C termini. *The Journal of biological chemistry* 276: 4839-4844, 2001.
157. **Yang H, Elko P, Fromm BS, Baga JJ, Pires LA, Schuger CD, Steinman RT, and Lehmann MH**. Maximal ascending and descending slopes of the T wave in men and women. *Journal of electrocardiology* 30: 267-276, 1997.
158. **Yang T, Yang P, Roden DM, and Darbar D**. Novel KCNA5 mutation implicates tyrosine kinase signaling in human atrial fibrillation. *Heart rhythm : the official journal of the Heart Rhythm Society* 7: 1246-1252, 2010.
159. **Yu W, Xu J, and Li M**. NAB domain is essential for the subunit assembly of both alpha-alpha and alpha-beta complexes of shaker-like potassium channels. *Neuron* 16: 441-453, 1996.
160. **Zaklyazminskaya E, and Dzemeshkevich S**. The role of mutations in the SCN5A gene in cardiomyopathies. *Biochimica et biophysica acta* 1863: 1799-1805, 2016.
161. **Zhang Y, Kong W, Gao Y, Liu X, Gao K, Xie H, Wu Y, Wang J, Gao F, Wu X, and Jiang Y**. Gene Mutation Analysis in 253 Chinese Children with Unexplained Epilepsy and Intellectual/Developmental Disabilities. *PLoS ONE* 10: e0141782, 2015.
162. **Zhu Z, Zhu S, Liu D, Yu Z, Yang Y, van der Giet M, and Tepel M**. GATA4-mediated cardiac hypertrophy induced by d-myo-inositol 1,4,5-tris-phosphate. *Biochemical and biophysical research communications* 338: 1236-1240, 2005.

APPENDIX:
Reprint Permissions

JOHN WILEY AND SONS LICENSE
TERMS AND CONDITIONS

Aug 26, 2016

This Agreement between Jared Tur ("You") and John Wiley and Sons ("John Wiley and Sons") consists of your license details and the terms and conditions provided by John Wiley and Sons and Copyright Clearance Center.

License Number	3880330472584
License date	Jun 01, 2016
Licensed Content Publisher	John Wiley and Sons
Licensed Content Publication	Experimental Physiology
Licensed Content Title	Deletion of Kvβ1.1 subunit leads to electrical and haemodynamic changes causing cardiac hypertrophy in female murine hearts
Licensed Content Author	Jared Tur,Kalyan C. Chapalamadugu,Timothy Padawer,Sachin L. Badole,Peter J. Kilfoil,Aruni Bhatnagar,Srinivas M. Tipparaju
Licensed Content Date	Feb 25, 2016
Licensed Content Pages	15
Type of use	Dissertation/Thesis
Requestor type	Author of this Wiley article
Format	Print and electronic
Portion	Full article
Will you be translating?	No

Title of your thesis / dissertation	Redox Regulation of the Kvβ1.1 Subunit within the Heart
Expected completion date	Dec 2016
Expected size (number of pages)	200
Requestor Location	Jared Tur 12901 Bruce B downs Blvd TAMPA, FL 33612 United States Attn: Jared Tur
Publisher Tax ID	EU826007151
Billing Type	Invoice
Billing Address	Jared Tur 12901 Bruce B downs Blvd TAMPA, FL 33612 United States Attn: Jared Tur
Total	0.00 USD
Terms and Conditions	

TERMS AND CONDITIONS

This copyrighted material is owned by or exclusively licensed to John Wiley & Sons, Inc. or one of its group companies (each a"Wiley Company") or handled on behalf of a society with which a Wiley Company has exclusive publishing rights in relation to a particular work (collectively "WILEY"). By clicking "accept" in connection with completing this licensing transaction, you agree that the following terms and conditions apply to this transaction (along with the billing and payment terms and conditions established by the Copyright Clearance Center Inc., ("CCC's Billing and Payment terms and conditions"), at the time that you opened your RightsLink account (these are available at any time at http://myaccount.copyright.com).

Terms and Conditions

- The materials you have requested permission to reproduce or reuse (the "Wiley Materials") are protected by copyright.

- You are hereby granted a personal, non-exclusive, non-sub licensable (on a stand-alone basis), non-transferable, worldwide, limited license to reproduce the Wiley Materials for the purpose specified in the licensing process. This license, **and any CONTENT (PDF or image file) purchased as part of your order,** is for a one-time use only and limited to any maximum distribution number specified in the license. The first instance of republication or reuse granted by this license must be completed within two years of the date of the grant of this license (although copies prepared before the end date may be distributed thereafter). The Wiley Materials shall not be used in any other manner or for any other purpose, beyond what is granted in the license. Permission is granted subject to an appropriate acknowledgement given to the author, title of the material/book/journal and the publisher. You shall also duplicate the copyright notice that appears in the Wiley publication in your use of the Wiley Material. Permission is also granted on the understanding that nowhere in the text is a previously published source acknowledged for all or part of this Wiley Material. Any third party content is expressly excluded from this permission.

- With respect to the Wiley Materials, all rights are reserved. Except as expressly granted by the terms of the license, no part of the Wiley Materials may be copied, modified, adapted (except for minor reformatting required by the new Publication), translated, reproduced, transferred or distributed, in any form or by any means, and no derivative works may be made based on the Wiley Materials without the prior permission of the respective copyright owner.**For STM Signatory Publishers clearing permission under the terms of the STM Permissions Guidelines only, the terms of the license are extended to include subsequent editions and for editions in other languages, provided such editions are for the work as a whole in situ and does not involve the separate exploitation of the permitted figures or extracts,** You may not alter, remove or suppress in any manner any copyright, trademark or other notices displayed by the Wiley Materials. You may not license, rent, sell, loan, lease, pledge, offer as security, transfer or assign the Wiley Materials on a stand-alone basis, or any of the rights granted to you hereunder to any other person.

- The Wiley Materials and all of the intellectual property rights therein shall at all times remain the exclusive property of John Wiley & Sons Inc, the Wiley Companies, or their respective licensors, and your interest therein is only that of having possession of and the right to reproduce the Wiley Materials pursuant to Section 2 herein during the continuance of this Agreement. You agree that you own no right, title or interest in or to the Wiley Materials or any of the intellectual property rights therein. You shall have no rights hereunder other than the license as provided for above in Section 2. No right, license or interest to any trademark, trade name, service mark or other branding ("Marks") of WILEY or its licensors is granted hereunder, and you agree that you shall not assert any such right, license or interest with respect thereto

- NEITHER WILEY NOR ITS LICENSORS MAKES ANY WARRANTY OR REPRESENTATION OF ANY KIND TO YOU OR ANY THIRD PARTY, EXPRESS, IMPLIED OR STATUTORY, WITH RESPECT TO THE MATERIALS OR THE ACCURACY OF ANY INFORMATION CONTAINED IN THE MATERIALS, INCLUDING, WITHOUT LIMITATION, ANY IMPLIED WARRANTY OF MERCHANTABILITY, ACCURACY, SATISFACTORY QUALITY, FITNESS FOR A PARTICULAR PURPOSE, USABILITY, INTEGRATION OR NON-INFRINGEMENT AND ALL SUCH

WARRANTIES ARE HEREBY EXCLUDED BY WILEY AND ITS LICENSORS AND WAIVED BY YOU.

- WILEY shall have the right to terminate this Agreement immediately upon breach of this Agreement by you.

- You shall indemnify, defend and hold harmless WILEY, its Licensors and their respective directors, officers, agents and employees, from and against any actual or threatened claims, demands, causes of action or proceedings arising from any breach of this Agreement by you.

- IN NO EVENT SHALL WILEY OR ITS LICENSORS BE LIABLE TO YOU OR ANY OTHER PARTY OR ANY OTHER PERSON OR ENTITY FOR ANY SPECIAL, CONSEQUENTIAL, INCIDENTAL, INDIRECT, EXEMPLARY OR PUNITIVE DAMAGES, HOWEVER CAUSED, ARISING OUT OF OR IN CONNECTION WITH THE DOWNLOADING, PROVISIONING, VIEWING OR USE OF THE MATERIALS REGARDLESS OF THE FORM OF ACTION, WHETHER FOR BREACH OF CONTRACT, BREACH OF WARRANTY, TORT, NEGLIGENCE, INFRINGEMENT OR OTHERWISE (INCLUDING, WITHOUT LIMITATION, DAMAGES BASED ON LOSS OF PROFITS, DATA, FILES, USE, BUSINESS OPPORTUNITY OR CLAIMS OF THIRD PARTIES), AND WHETHER OR NOT THE PARTY HAS BEEN ADVISED OF THE POSSIBILITY OF SUCH DAMAGES. THIS LIMITATION SHALL APPLY NOTWITHSTANDING ANY FAILURE OF ESSENTIAL PURPOSE OF ANY LIMITED REMEDY PROVIDED HEREIN.

- Should any provision of this Agreement be held by a court of competent jurisdiction to be illegal, invalid, or unenforceable, that provision shall be deemed amended to achieve as nearly as possible the same economic effect as the original provision, and the legality, validity and enforceability of the remaining provisions of this Agreement shall not be affected or impaired thereby.

- The failure of either party to enforce any term or condition of this Agreement shall not constitute a waiver of either party's right to enforce each and every term and condition of this Agreement. No breach under this agreement shall be deemed waived or excused by either party unless such waiver or consent is in writing signed by the party granting such waiver or consent. The waiver by or consent of a party to a breach of any provision of this Agreement shall not operate or be construed as a waiver of or consent to any other or subsequent breach by such other party.

- This Agreement may not be assigned (including by operation of law or otherwise) by you without WILEY's prior written consent.

- Any fee required for this permission shall be non-refundable after thirty (30) days from receipt by the CCC.

- These terms and conditions together with CCC's Billing and Payment terms and conditions (which are incorporated herein) form the entire agreement between you and WILEY concerning this licensing transaction and (in the absence of fraud) supersedes all prior agreements and representations of the parties, oral or written. This Agreement may not be amended except in writing signed by both parties. This Agreement shall be binding upon and inure to the benefit of the parties' successors, legal representatives, and

authorized assigns.

- In the event of any conflict between your obligations established by these terms and conditions and those established by CCC's Billing and Payment terms and conditions, these terms and conditions shall prevail.

- WILEY expressly reserves all rights not specifically granted in the combination of (i) the license details provided by you and accepted in the course of this licensing transaction, (ii) these terms and conditions and (iii) CCC's Billing and Payment terms and conditions.

- This Agreement will be void if the Type of Use, Format, Circulation, or Requestor Type was misrepresented during the licensing process.

- This Agreement shall be governed by and construed in accordance with the laws of the State of New York, USA, without regards to such state's conflict of law rules. Any legal action, suit or proceeding arising out of or relating to these Terms and Conditions or the breach thereof shall be instituted in a court of competent jurisdiction in New York County in the State of New York in the United States of America and each party hereby consents and submits to the personal jurisdiction of such court, waives any objection to venue in such court and consents to service of process by registered or certified mail, return receipt requested, at the last known address of such party.

WILEY OPEN ACCESS TERMS AND CONDITIONS

Wiley Publishes Open Access Articles in fully Open Access Journals and in Subscription journals offering Online Open. Although most of the fully Open Access journals publish open access articles under the terms of the Creative Commons Attribution (CC BY) License only, the subscription journals and a few of the Open Access Journals offer a choice of Creative Commons Licenses. The license type is clearly identified on the article.

The Creative Commons Attribution License

The Creative Commons Attribution License (CC-BY) allows users to copy, distribute and transmit an article, adapt the article and make commercial use of the article. The CC-BY license permits commercial and non-

Creative Commons Attribution Non-Commercial License

The Creative Commons Attribution Non-Commercial (CC-BY-NC)License permits use, distribution and reproduction in any medium, provided the original work is properly cited and is not used for commercial purposes.(see below)

Creative Commons Attribution-Non-Commercial-NoDerivs License

The Creative Commons Attribution Non-Commercial-NoDerivs License (CC-BY-NC-ND) permits use, distribution and reproduction in any medium, provided the original work is properly cited, is not used for commercial purposes and no modifications or adaptations are

made. (see below)

Use by commercial "for-profit" organizations

Use of Wiley Open Access articles for commercial, promotional, or marketing purposes requires further explicit permission from Wiley and will be subject to a fee.

Further details can be found on Wiley Online Library
http://olabout.wiley.com/WileyCDA/Section/id-410895.html

Other Terms and Conditions:

v1.10 Last updated September 2015

Questions? customercare@copyright.com or +1-855-239-3415 (toll free in the US) or +1-978-646-2777.

Dear Jared Tur,

Thank you very much for your request and for your interest in our content.

Please feel free to include the figure in your thesis or dissertation subject to the guidelines listed on our website. I've copied them below:

http://www.sciencemag.org/site/about/permissions.xhtml#thesis

(NOTE: If you are the Original Author of the AAAS article being reproduced, please refer to your License to Publish for rules on reproducing your paper in a dissertation or thesis.)

Reproducing AAAS Material in your Thesis or Dissertation

AAAS permits the use of content published in its journals *Science*, *Science Technical Medicine*, and *Science Signaling*, but only provided the following criteria are met.

1. If you are using figure(s)/table(s), permission is granted for use in print and electronic versions of your dissertation or thesis.
2. A full text article may be used only in print versions of a dissertation or thesis. AAAS does not permit the reproduction of full text articles in electronic versions of theses or dissertations.
3. The following credit line must be printed along with the AAAS material: "From [Full Reference Citation]. Reprinted with permission from AAAS."
4. All required credit lines and notices must be visible any time a user accesses any part of the AAAS material and must appear on any printed copies that an authorized user might make.
5. The AAAS material may not be modified or altered except that figures and tables may be modified with permission from the author. Author permission for any such changes must be secured prior to your use.
6. AAAS must publish the full paper prior to your use of any of its text or figures.

7. If the AAAS material covered by this permission was published in *Science* during the years 1974–1994, you must also obtain permission from the author, who may grant or withhold permission, and who may or may not charge a fee if permission is granted. See original article for author's address. This condition does not apply to news articles.

8. If you are an Original Author on the AAAS article being reproduced, please refer to your License to Publish for rules on reproducing your paper in a dissertation or thesis.

Permission covers the distribution of your dissertation or thesis on demand by a third party distributor (e.g. ProQuest / UMI), provided the AAAS material covered by this permission remains in situ and is not distributed by that third party outside of the context of your Thesis/Dissertation.

Permission does not apply to figures/photos/artwork or any other content or materials included in your work that are credited to non-AAAS sources.

If the requested material is sourced to or references non-AAAS sources, you must obtain authorization from that source as well before using that material.

You agree to hold harmless and indemnify AAAS against any claims arising from your use of any content in your work that is credited to non-AAAS sources.

By using the AAAS Material identified in your request, you agree to abide by all the terms and conditions herein.

AAAS makes no representations or warranties as to the accuracy of any information contained in the AAAS material covered by this permission, including any warranties of merchantability or fitness for a particular purpose.

If how you wish to use our content falls outside of these guidelines or if you have any questions please just let me know.

Best regards,

Alexander Lee

Rights & Permissions Assistant

Science/AAAS, Office of Publishing

1200 New York Avenue NW

Washington, DC 20005

202-326-6673

alee@aaas.org